ISBN 978-82-326-4486-5 (printed version)
ISBN 978-82-326-4487-2 (electronic version)
ISSN 1503-8181

Diana Gonzalez

Doctoral Thesis

Doctoral theses at NTNU, 2020:67

Diana Gonzalez

Methodologies to determine cost-effective development strategies for offshore fields during early-phase studies using proxy models and optimization

NTNU
Norwegian University of
Science and Technology
Faculty of Engineering
Department of Geoscienceand Petroleum

NTNU
Norwegian University of
Science and Technology

Doctoral theses at NTNU, 2020:67

NTNU

NTNU
Norwegian University of
Science and Technology

Diana Gonzalez

Methodologies to determine cost-effective development strategies for offshore fields during early-phase studies using proxy models and optimization

Thesis for the degree of Philosophiae Doctor

Trondheim, February 2020

Norwegian University of Science and Technology
Faculty of Engineering
Department of Geoscienceand Petroleum

NTNU
Norwegian University of
Science and Technology

NTNU
Norwegian University of Science and Technology

Thesis for the degree of Philosophiae Doctor

Faculty of Engineering
Department of Geoscienceand Petroleum

ISBN 978-82-326-4486-5 (printed version)
ISBN 978-82-326-4487-2 (electronic version)
ISSN 1503-8181

Doctoral theses at NTNU, 2020:67

Printed by Skipnes Kommunikasjon as

Abstract

This thesis summarizes research efforts for developing a structured methodology for decision support in feasibility studies and concept planning phases of oil and gas field development. The objective in developing the methodology was to provide an easy-to-use facility to integrate the production-governing elements of oil and gas fields that capture the integrated production and economic performance of the system. This in a modular and scalable manner that includes numerical optimization and uncertainty analyses needed to support engineering decisions. The novelty of the methodology stems from a variety of measures to integrate field architecture, reservoir extraction and production facilities performance in a proxy model, shorten the running time, simplifying the input demands and making an efficient optimization scheme.

To represent the production performance of the integrated production system, a collection of value tables were used, computed from coupled models that included a tank reservoir, wellbore and network. This allowed to estimate production profiles without having to run the coupled model each time target rates are varied. Furthermore, it allowed to capture the effect well and flowline pressure drops have on field performance. Additionally, a proxy model for capital, drilling and operational expenditures was obtained by applying linear regression to data points extracted from a commercial cost estimation software. An optimization problem was then formulated to find production and drilling schedule that maximize NPV. The problem was formulated as a mixed-integer linear problem using SOS2 variables, which allowed low running times. The effect of uncertainty of reservoir size, well productivity, production system layout and costs was evaluated using probability trees.

The methodology was tested on field scale data from the Barents Sea Wisting field, which is currently under predevelopment study phase. The public domain data of the field was sufficient to employ and test the methodology. With regards to production, the Wisting field has distinct characteristics that includes remote location with non-existing infrastructure, low reservoir pressure and temperature and wax deposit tendency.

The results at the end of the study and the testing of the results provide a template and an input for developing a commercial software package for performing structured feasibility studies and concept planning during the engineering design of oil and gas fields.

In order to establish a wider variety of field development scenarios for the particular Wisting field, the research encompassed also a feasibility study of two known flow assurance concepts for control of wax deposition, cold flow and electrical heat tracing. The first study confirmed the feasibility of the cold flow approach for transportation of Wisting-like oil. The second study quantified the economic and technical performance of several configurations of heat tracing element along the pipe and heating schedule when transporting waxy crude oil in the pipeline. Subsequently, the model of the Wisting field case was modified to include the cold flow technology and the methodology for field development decision support was executed. The results of this new analysis confirm that the implementation of cold flow could lead to a modest improvement in the economic outcome of the field.

Acknowledgements

I am deeply grateful to my supervisor Professor Milan Stanko, for giving me this opportunity. I appreciate all you have done to help me reach this goal, all the support, guidance, and friendly disposition. Milan is a wonderful person and professional. It has been an enriching experience to work with him.

I would like to thank my co-supervisor Professor Michal Golan, for his willingness to guide me through the realization of this thesis and for been a source of inspiration. Thank you for your friendship.

I want to thank my co-supervisor Professor Sigbjørn Sangesland for his support during the realization of this thesis.

To SUBPRO for giving me the opportunity to work with this project and providing the financial support.

Within SUBPRO I want to especially thank the Field Architecture group for accompany me during all the stages of this project.

I thank Arnaud Hoffmann and Thiago Lima Silva, for sharing their knowledge on mathematical optimization with me. This thesis is possible thanks to you.

To my colleagues at the Department of Geoscience and Petroleum, thank you for improving my working environment with nice lunch times, interesting talks and social experiences.

Thanks to the Department of Geoscience and Petroleum, for providing an excellent working atmosphere.

Sincere thanks to my friends in Norway for making easier and funnier my time here.

To Gilberto Núñez, thank you for making the long working hours more enjoyable with good laughs and “sjokolade kake”. I also want to thank you for your disposition to lend me a hand when I needed it.

To my family and friends for their presence and unconditional support and love.

I finally want to thank you, Abraham. I am lucky to have you in my life.

Content

Abstract i
Acknowledgements iii
Content v
List of Figures ix
List of Tables xv
Abbreviations xix
Chapter 1 21
Introduction 21
1.1. Problem Background 21
1.2. Thesis objectives 25
1.3. Thesis overview 25
1.4. List of publications 26
Chapter 2 27
Study Case – Wisting Field 27
Chapter 3 31
Development of the proxy model to compute the production performance of the integrated production system (reservoir, well and surface pipe network) 31
3.1. Background 31
3.2. Generation of production system's proxy models 34
3.2.1. Production potential 34
3.2.2. Generation of production potential curves -Wisting field case 36
3.2.3. Using the production potential curve to plan the production scheduling of a field 41
3.2.4. Validation of the production potential proxy model 41
3.2.5. Validation of the production potential proxy model approach in the Gullfaks Statfjord oil reservoir 45
Chapter 4 52
Development of the proxy models of the cost and estimation of net present value 52
4.1. Background 52
4.2. Proxy model for cost data 53
4.2.1. Generation of proxy models for estimation of cost – Case Wisting field 54
4.3. NPV Estimation 60
Chapter 5 62

The NPV optimization problem for early field development planning 62
5.1. Background 62
5.2. Optimization formulation 63
5.2.1. Linear reformulation 67
5.2.2. Application of the optimization formulation to a Wisting field case 69
5.2.3. Validation of optimization 71
Chapter 6 77
Uncertainty analysis specifications for early field development planning 77
6.1. Background 77
6.2. Uncertainty analysis specifications 79
6.3. Application of uncertainty analysis 80
Chapter 7 83
Applying the decision-support methodology on the Wisting field case 83
7.1. Evaluation of the method on Wisting field case 83
7.1.1. Step 1: Identification and selection of feasible field development strategies 84
7.1.2. Step 2: Generation of proxy model of production potential 84
7.1.3. Step 3: Cost estimation 87
7.1.4. Step 4: Optimization 88
7.1.5. Step 5: Analysis of uncertainties 91
7.2. General observations 95
Chapter 8 97
Applicability of cold flow and heat tracing for handling wax deposition in subsea pipelines of remote offshore, low pressure and temperature oil reservoirs 97
8.1. Background 98
8.2. Flow assurance issues: Wax deposition 99
8.2.1. Molecular diffusion 100
8.2.2. Shear dispersion 100
8.3. Wax Deposition Modelling in OLGA 100
8.3.1. RRR (Rygg, Rydahl and Rønningsen) Model 100
8.3.2. Matzain Model 102
8.3.3. Heat Analogy 102
8.4. Flow assurance technologies 102
8.4.1. Cold Flow 102
8.4.2. Electrical Heat Tracing (EHT) 103
8.5. Cold Flow study 103
8.5.1. Cold Flow Concepts for Wax Flow Assurance 104
8.5.2. Non-Insulated Pipe Section 104

8.5.3. Passive Cooler with a Bundle of Parallel pipes 104
8.5.4. Active Cooler 105
8.5.5. Cases 105
8.5.6. Case 1: Non-Insulated Pipe Section 106
8.5.7. Case 2: Passive Cooler with a Bundle of Parallel Pipes 107
8.5.8. Case 3: Active Cooler 108
8.5.9. Results of Cold Flow study 108
8.6. Electrical Heat Tracing study 111
8.6.1. Study Case 112
8.6.2. Results and Discussion 113
8.7. Observations 116
8.7.1. About Cold Flow 116
8.7.2. About Electric Heat Tracing 116
Chapter 9 119
Effect of cold flow wax control method on Wisting study case 119
9.1. Cold flow system 119
9.2. Generation of production potential proxy models 120
9.3. Generation of cost models 121
9.4. Optimization to estimate production and drilling scheduling 121
9.5. Uncertainty analysis 123
9.6. General Observations 125
Chapter 10 127
Conclusions and recommendations 127
10.1. Recommendations for future works 130
References 133
Appendix A 139
Input data for material balance model 139
Appendix B 141
Input data for surface network model 141
Appendix C 147
Black oil tables 147
Appendix D 149
Proxy models used for validation of production potential approach 149
Appendix E 153
MILP formulation 153
Appendix F 159
Proxy model for Study Case based on Wisting (used in chapter 7) 159

Appendix G 165
Water injection table used in optimization 165
Appendix H 167
Result from optimization: Optimum production rate for study case 167
Appendix I 173
AMPL's input files 173

List of Figures

List of figures for Chapter 1

Figure 1.1. Field development process 22
Figure 1.2. Value chain model for feasibility study and conceptual planning 23

List of figures for Chapter 2

Figure 2.1. Wisting Field [3] 27
Figure 2.2. Wisting Field located in the Barents Sea 28

List of figures for Chapter 3

Figure 3.1. Production Profile 32
Figure 3.2. Coupling between a material balance model and a model of the production system [8] 34
Figure 3.3. Production potential vs. cumulative production for a dry gas reservoir 36
Figure 3.4. Production system layout 37
Figure 3.5. Coupling process used 38
Figure 3.6. Production potential oil rate for case with 1 well and maximum choke opening .. 39
Figure 3.7. GOR and WC for case with 1 well and maximum choke opening 39
Figure 3.8. Potential oil rate for different number of wells 40
Figure 3.9. GOR for different number of wells 40
Figure 3.10. WC for different number of wells 40
Figure 3.11. Gas lift performance curves for generic production system 42
Figure 3.12. Proxy model validation for Case 1. Oil production profile and cumulative oil production 43
Figure 3.13. Proxy model validation for Case 1. GOR and WC 43
Figure 3.14. Proxy model validation for Case 2. . Oil production profile and cumulative oil production 43
Figure 3.15. Proxy model validation for Case 2. GOR and WC 44
Figure 3.16. Proxy model validation for Case 3. Oil production profile and cumulative oil production 44
Figure 3.17. Proxy model validation for Case 3. GOR and WC 44
Figure 3.18. Gullfaks Statfjord reservoir model (property: porosity) 46
Figure 3.19. Gullfaks Statfjord's actual oil production profile 46
Figure 3.20. Gullfaks Statfjord's production potential curve: Oil rate 47
Figure 3.21. Gullfaks Statfjord's production potential curves: Gas oil ratio and water cut 47
Figure 3.22. Production potential approach validation using Gullfaks Statfjord's reservoir model. Oil rate and cumulative oil production. Plateau rate: 10 000 Sm^3/d (62 898.27 stb/d) 48
Figure 3.23. Production potential approach validation using Gullfaks Statfjord's reservoir model. GOR and WC. Plateau rate: 10 000 Sm^3/d (62 898.27 stb/d) 48

Figure 3.24. Production potential approach validation using Gullfaks Statfjord's reservoir model. Oil rate and cumulative oil production. Plateau rate: 8 000 Sm^3/d (50 318.62 stb/d).. 48
Figure 3.25. Production potential approach validation using Gullfaks Statfjord's reservoir model. GOR and WC. Plateau rate: 8 000 Sm^3/d (50 318.62 stb/d) 49
Figure 3.26. Production potential approach validation using Gullfaks Statfjord's reservoir model. Oil rate and cumulative oil production. Plateau rate: 6 000 Sm3/d (37 738.96 stb/d) . 49
Figure 3.27. Production potential approach validation using Gullfaks Statfjord's reservoir model. GOR and WC. Plateau rate: 6 000 Sm3/d (37 738.96 stb/d) 49
Figure 3.28. Production potential approach validation using Gullfaks Statfjord's reservoir model. Oil rate and cumulative oil production. Plateau rate: 4 000 Sm3/d (25 159.31 stb/d) . 50
Figure 3.29. Production potential approach validation using Gullfaks Statfjord's reservoir model. GOR and WC. Plateau rate: 4 000 Sm3/d (25 159.31 stb/d) 50

List of figures for Chapter 4

Figure 4.1. Annual net cash flow 52
Figure 4.2. Production system layout used for cost estimation..... 55
Figure 4.3. Comparison of CAPEX between cost data and cost proxy models for TLP concept 58
Figure 4.4. Comparison of OPEX between cost data and cost proxy models for TLP concept 58
Figure 4.5. Comparison of CAPEX between cost data and cost proxy models for FPSO concept 58
Figure 4.6. Comparison of OPEX between cost data and cost proxy models for FPSO concept 59
Figure 4.7. Comparison of CAPEX between cost data and cost proxy models for Tie-Back concept 59
Figure 4.8. Comparison of OPEX between cost data and cost proxy models for Tie-Back concept 59
Figure 4.9. Comparison between DRILLEX cost data and cost proxy models for all concepts 60
Figure 4.10. Typical NPV curve 61

List of figures for Chapter 5

Figure 5.1. Excel spreadsheet representing calculation of NPV during five years of production 65
Figure 5.2. Solver setup to find maximum NPV..... 66
Figure 5.3. Optimum oil production profile and oil production potential for strategy TLP with GL + WI 70
Figure 5.4. Profit obtained from optimization..... 71
Figure 5.5. Comparison of production profile obtained with optimization formulation and brute-force optimization (Plateau rate 70 000 stb/d) 72
Figure 5.6. Comparison of production profile obtained with optimization formulation and brute-force optimization (Plateau rate 75 000 stb/d) 72
Figure 5.7. Comparison of production profile obtained with optimization formulation and brute-force optimization (Plateau rate 80 000 stb/d) 72

Figure 5.8. Comparison of production profile obtained with optimization formulation and brute-force optimization (Plateau rate 85 000 stb/d) 73
Figure 5.9. Comparison of production profile obtained with optimization formulation and brute-force optimization (Plateau rate 90 000 stb/d) 73
Figure 5.10. Comparison of production profile obtained with optimization formulation and brute-force optimization (Plateau rate 95 000 stb/d) 73
Figure 5.11. Production profile obtained with optimal plateau rate 74
Figure 5.12. Comparison of optimal production profile obtained with the optimization formulation (without restriction on the maximum number of wells that can be drilled in a year) and the brute force optimization with plateau rate of 86 996 stb/d 75

List of figures for Chapter 6

Figure 6.1. Decision tree for the uncertainty variables that affect the production performance of the field 80
Figure 6.2. NPV probability 81

List of figures for Chapter 7

Figure 7.1. Potential oil rate for all the recovery scenarios 86
Figure 7.2. Potential GOR for all recovery scenarios 86
Figure 7.3. Potential water cut for all recovery scenarios 87
Figure 7.4. Optimum oil production profile and oil production potential for strategy TLP with Gas Lifted wells 89
Figure 7.5. Optimum oil production profile and oil production potential for strategy TLP with GL + WI 89
Figure 7.6. Optimum oil production profile and oil production potential for strategy TLP with MPB + WI 89
Figure 7.7. Uncertainty in production system layout 91
Figure 7.8. Decision Tree diagram for potential curves uncertainty 92
Figure 7.9. Decision tree diagram for costs uncertainty 92
Figure 7.10. NPV's cumulative density function. All uncertainty cases 93
Figure 7.11. Comparison of NPV's cumulative density function for all recovery scenarios 94
Figure 7.12. Comparison of NPV's cumulative density function for all topside facilities 94

List of figures for Chapter 8

Figure 8.1. Electrical Heat Trace [65] 103
Figure 8.2. Non-insulated pipe section concept 104
Figure 8.3. Passive cooler with a bundle of parallel pipes. (a) 3D isometric of a parallel pipe heat exchanger with natural cooling, (b) modelling approximation 105
Figure 8.4. Schematic flowline diagram used in OLGA 105
Figure 8.5. Equivalent one-dimensional loop used in OLGA simulations 107
Figure 8.6. Schematic diagram of Case 2 used in OLGA 107
Figure 8.7. Schematic diagram of Case 3 used in OLGA 108
Figure 8.8. Required cooling length for Case 1 after 90 days of production 108
Figure 8.9. Added pressure drop for Case 1 after 90 days of production 109
Figure 8.10. Wax thickness profile for Case 1 after 90 days of production 109

Figure 8.11. Results for Case 2 after 90 days of production. (a) required cooling length. (b) added pressure drop 110
Figure 8.12. Wax thickness profile for Case 2 after 90 days of production 110
Figure 8.13. Wax thickness profile for Case 3 after 90 days of production 111
Figure 8.14. Required power consumption per meter of pipeline with insulation for both pipeline lengths, 8 km and 50 km 113
Figure 8.15. Required power consumption per meter of pipeline without insulation for both pipeline lengths, 8 km and 50 km 114
Figure 8.16. Total power required for pipelines with insulation 115
Figure 8.17. Total power required. For pipeline without insulation 115

List of figures for Chapter 9

Figure 9.1. Proxy model of oil production potential. Comparison between the base study case and the case with Cold Flow 121
Figure 9.2. Production potential comparison between the original study case and the case with Cold Flow 122
Figure 9.3. Decision tree diagram for uncertainty in production potential (study case with cold flow) 123
Figure 9.4. Decision tree diagram for cost uncertainty (study case with cold flow) 124
Figure 9.5. NPV's cumulative distribution function (study case with cold flow) 124

List of figures for Appendix A

Figure A.1. Oil to Gas relative permeability 140
Figure A.2. Oil to Water relative permeability 140

List of figures for Appendix B

Figure B.1. Tubing layout 142

List of figures for Appendix H

Figure H.1. Optimum oil production profile and oil production potential for strategy TLP with GL 167
Figure H.2. Optimum oil production profile and oil production potential for strategy FPSO with GL 167
Figure H.3. Optimum oil production profile and oil production potential for strategy Tie-back with GL 168
Figure H.4. Optimum oil production profile and oil production potential for strategy TLP with GL + WI 168
Figure H.5. Optimum oil production profile and oil production potential for strategy FPSO with GL + WI 169
Figure H.6. Optimum oil production profile and oil production potential for strategy Tie-back with GL + WI injection 169
Figure H.7. Optimum oil production profile and oil production potential for strategy TLP with MPB + WI 170

Figure H.8. Optimum oil production profile and oil production potential for strategy FPSO with MPB + WI 170
Figure H.9. Optimum oil production profile and oil production potential for strategy Tie-back with MPB + WI 171

List of Tables

List of tables for Chapter 2

Table 2.1. Estimation of Wisting reserves 28
Table 2.2. Wisting reservoir properties 29

List of tables for Chapter 3

Table 3.1. Results of reservoir model with natural depletion 37
Table 3.2. Cases for validation of production potential proxy models 42
Table 3.3. Differences in results between proxy model of production potential approach and coupled model MBAL/PipeSim for all cases 45
Table 3.4. Gullfaks Statfjord oil properties 45
Table 3.5. Differences in results between production potential approach and Gullfaks Statfjord's reservoir model 50

List of tables for Chapter 4

Table 4.1. Data used for costs sensitivity analysis 55
Table 4.2. Linear regression statistics for costs equations 57

List of tables for Chapter 5

Table 5.1. Optimum drilling schedule example case 70
Table 5.2. Plateau rates and number of wells used in brute-force optimization 71
Table 5.3. Maximum NPV obtained for validation of optimization formulation 74

List of tables for Chapter 7

Table 7.1. Optimum drilling schedule for all strategies 90
Table 7.2. Maximum NPV obtained for each development strategy 90
Table 7.3. NPV's probabilities 93
Table 7.4. NPV probabilities. Recovery scenarios and topside facilities 94

List of tables for Chapter 8

Table 8.1. Wall material properties 106
Table 8.2. Sensitivity variables values used for Case 1 106
Table 8.3. Parameter used for Study Case 112

List of tables for Chapter 9

Table 9.1. Cost estimation of SINTEF-BP Cold Flow Technology 120
Table 9.2. Drilling schedule comparison between the original study case and the case with Cold Flow 122
Table 9.3. NPV comparison between the original study case and the case with Cold Flow . 122
Table 9.4. NPV's probabilities, comparison between original study case and case with cold flow 124

List of tables for Appendix A

Table A.1. Tool Options 139
Table A.2. Tank parameters 139
Table A.3. Water influx 139
Table A.4. Relative permeability 139
Table A.5. Black oil model 140
Table A.6. Tank prediction data 140

List of tables for Appendix B

Table B.1. Reservoir data 141
Table B.2. IPR model 141
Table B.3. Geothermal survey 142
Table B.4. Tubing configuration 143
Table B.5. Properties 143
Table B.6. Heat transfer 143
Table B.7. Properties 144
Table B.8. Heat transfer 144
Table B.9. Properties 144
Table B.10. Heat transfer 144
Table B.11. Properties 145
Table B.12. Heat transfer 145
Table B.13. Data used for black oil model 145

List of tables for Appendix C

Table C.1. Black oil table 1 147
Table C.2. Black oil table 2 148

List of tables for Appendix D

Table D.1. Validation case 1 characteristics 149
Table D.2. Proxy model for validation case 1 149
Table D.3. Validation case 2 characteristics 149
Table D.4. Proxy model for validation case 2 149
Table D.5. Validation case 3 characteristics 150

Table D.6. Proxy model for validation case 3 150

List of tables for Appendix E

Table E.1. Set of time steps 153
Table E.2. Optimization parameters 153
Table E.3. Field variables 153
Table E.4. Economic variables 154
Table E.5. Set of breakpoints used in the MILP formulation 154
Table E. 6. Auxiliary variables used in the MILP formulation 154
Table E.7. Piecewise linear functions used in MILP 154

List of tables for Appendix F

Table F.1. Potential oil rate for gas lifted wells concept 159
Table F.2. Gas oil ratio for gas lifted wells concept 159
Table F.3. Water cut for gas lifted wells concept 159
Table F.4. Potential oil rate for gas lifted wells + water injection concept 160
Table F.5. Gas oil ratio for gas lifted wells + water injection concept 160
Table F.6. Water cut for gas lifted wells + water injection concept 161
Table F.7. Potential oil rate for multiphase boosting + water injection concept 162
Table F.8. Gas oil ratio for multiphase boosting + water injection concept 162
Table F. 9. Water cut for multiphase boosting + water injection concept 163

List of tables for Appendix G

Table G.1. Cumulative water injection table as function of cumulative oil production used in optimization routine 165

Abbreviations

1D	One dimensional
3D	Three dimensions
API	American Petroleum Institute
Bo	Oil formation volume factor
CAPEX	Capital expenditures (MM NOK)
CDF	Cumulative distribution function
DEH	Direct electric heating
DG	Decision gate
DRILLEX	Drilling expenditures (MM NOK)
EHT	Electric heat tracing
EOR	Enhance oil recovery
ESP	Electric submersible pump
FDP	Field development planning
FPSO	Floating production storage and offloading
GL	Gas lift
GOR	Gas-oil ratio (scf/stb)
GVF	Gas volume fraction
ID	Interior diameter
IOIP	Initial oil in place (MM stb)
IPR	Inflow performance relationship
IRR	Internal rate of return
IT	Information technology
kh	Horizontal permeability (mD)
kv	Vertical permeability (mD)
LP	Linear programming
MILP	Mixed integer lineal programming
MM	Millions
MPB	Multiphase boosting
MW	Mega watts
NOK	Norwegian crown (currency)
Np	Cumulative oil production
NPV	Net present value (MM NOK)
Nw	Number of wells
OPEX	Operating expenditures (MM NOK)
P	Probability
Pb	Pressure at bubble point
PI	Productivity index
PiP	Pipe-in-Pipe
P_R	Reservoir pressure

PVT	Pressure, volume, temperature
Pwf	Flowing bottom-hole pressure
PWL	Piecewise linear
RRR	Rygg, Rydahl and Rønnigsen
Rs	Solution gas-oil ratio
SOS	Special ordered set
SOS2	Special ordered set of type 2
stb	Stock tank barrel
STOIIP	Stock tank oil initially in place
TLP	Tension leg platform
USD	United State dollar
WAT	Wax appearance temperature (oC)
WC	Water cut
WI	Water injection (stb/d)

Chapter 1

Introduction

1.1. Problem Background

Once a new reservoir has been discovered and its potential for exploitation assessed, begins the phase of field development planning (FDP). Regarding engineering efforts, this is the most important and challenging phase in the life of an oil/gas field, particularly in offshore fields and remote or isolated land-based fields. In such cases, most important decisions on how the field will be produced and operated take place in this stage. Additionally, since the number of uncertainties related to the reservoir characteristics and the cost of the project is high, the task of finding the best production strategy becomes highly complex.

The purpose of field development planning is to identify the best strategy to exploit an asset by finding concepts that are technically feasible and provide the best economic performance. To do so, a multidisciplinary team is required. The disciplines typically involved are geoscience, reservoir, production and facilities engineering, petroleum economics, and project and operations management.

Methodologies to provide decision support to field development have evolved over time from a simple intuitive “poke and hope” approach at the early stage of the petroleum era to a more sophisticated, modeling and engineering-based approach, nowadays. The global nature of the petroleum upstream industry drives the decision-support methodologies to converge gradually to a universal global pattern satisfying all stockholders.

The need to refine the methodology has been enhanced in the current era of the petroleum industry where newly discovered reservoirs and the associated development schemes become more challenging. Typical challenges encountered nowadays are related to deep and ultra-deep waters fields, longer offset and tiebacks of satellite fields and well clusters, arctic environments, high pressure and high temperature reservoirs, heavy oils, low-energy reservoirs, unstable oil and gas market (demands and processes).

Universal developments of IT capabilities with quick computational algorithms, quick data management (storage, transfer, analysis, visualization), and better data acquisition and transfer allow great improvement of the decision working processes during field development.

Furthermore, the current transformation of the global upstream industry with many new, small and lean entities entering the role of field developers and field operators creates the need to provide simple, structured, and transparent decision methodologies.

An overview of a typical field development process is provided in Figure 1.1. It is typically divided in three main phases: identification of business case, project planning, and project execution. Additionally, there are typically five major decision gates (DG) along the process to decide if to go further with the next phase, wait, or redo a phase.

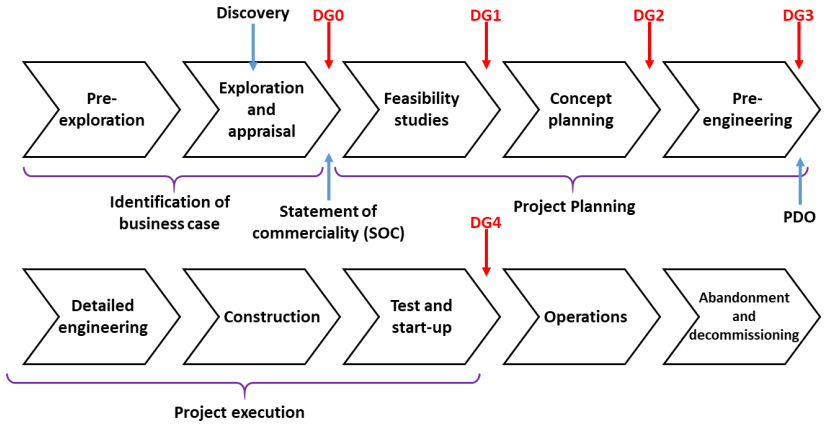

Figure 1.1. Field development process

This thesis focuses on the technical evaluations that occurs during the early phases of project planning, in particular the stages between DG0 and DG2 i.e. “feasibility studies” and “concept planning”. The main goal of the stage feasibility studies is to find one or more field development strategies that are technically, commercially and organizationally feasible. The main goal of concept planning is to compare the field development strategies flagged earlier and select the most attractive.

To perform these tasks, typically a value chain model is established by the field design team (Figure 1.2). The value chain model includes all information available about the system, but it also includes all the main design features of the field that are considered, such as:

- Well type
- Reservoir pressure support strategy
- Production scheduling
- Platform type
- Production system layout

The evaluation of each field development strategy is done considering a variety of issues ranging from geopolitics, corporate strategy, technical constraints, project cost, operational flexibility and scalability, operating and financial risks, among others. However, one of the main factors that is often used to compare alternatives is the project cost, often represented by indicators such as Net Present Value (NPV) or Internal Rate of Return (IRR). The project cost is affected by most elements of the value chain model; e.g. the production profile, oil price, type of surface facilities, platform type, tax regime, etc.

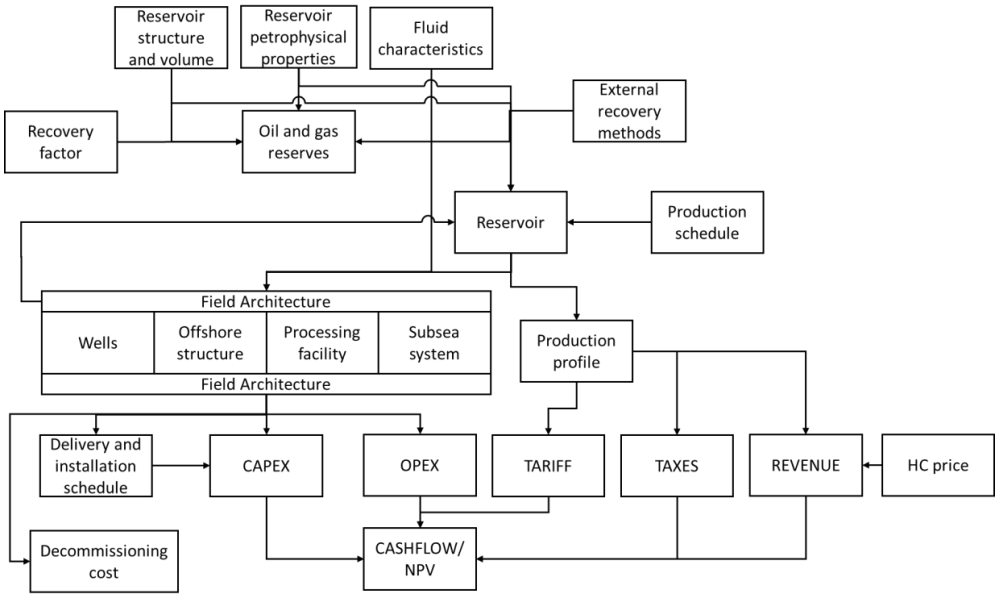

Figure 1.2. Value chain model for feasibility study and conceptual planning

The main objective of the field design team is to find the best development strategy that provides maximum profit and fulfills the technical constraints. This, however, is challenging because the value chain model is often not fully integrated on a digital platform, thus information transfer between disciplines is performed manually, it is time consuming and consistency is often not achieved. There are also working processes that are not easily automated and require performing labor-intensive tasks if input is modified. Moreover, the time frame allocated for feasibility studies and concept planning is typically short. Therefore, an exhaustive evaluation of all development alternatives and a proper analysis of the effect of uncertainties is seldom performed, which might lead to poor decision making and subsequently to a suboptimal field development strategy.

This is the industrial and research problem of interest for the present PhD work. Specifically, this research will look into developing a method to provide decision-support to field planners during the early phases of feasibility studies and concept planning when defining the field production profile, drilling schedule, type of offshore structure, pressure support method and selection of artificial lift. The method should have a low running time suitable to perform exhaustive evaluations and probabilistic analyses during the field planning process. This is performed by the following steps:

- Creating an efficient (low running time) integrated proxy model of the value chain model that contains all relevant field design features and computation of most relevant performance indicators to consider in the evaluation. The proxy model is intended to capture the first order of magnitude effects and not being a high-fidelity proxy.

- Perform efficient (low running time) numerical optimization on the proxy model of the value chain to find optimal development strategies that provide the most cost-effective solution.

- Evaluate the effect of uncertainties on the results of the numerical optimization using probabilistic methods.

This research has made special emphasis on capturing the interaction between the subsurface (reservoir) system and the well and surface piping transportation system to the offshore structure when computing the field production profiles. The de-coupling between reservoir models and production system models has been flagged by previous research and by oil and gas companies as a deficiency existing in current working processes in the industry. This can add up to the inability to study more field development strategies during the field development process.

There has been extensive research into this topic in the past, with a varying degree of model complexity, model execution and optimization methods to quantify uncertainty and variables of interest, such as well control, drilling schedule, well placement, reservoir realizations, economic model, etc. However, the differentiating characteristics and contributions of the present research are as follow:

- Extension of the well potential concept used in reservoir engineering to an integrated production system including reservoir, inflow, flow in wellbore and well in gathering network, and considering the presence of adjustable equipment such as chokes and artificial lift equipment. This concept allows to build a proxy model to estimate field production profiles suitable for systems where the reservoir is represented by a tank and the wells in the network are producing from a single reservoir unit.

- Formulation of the NPV optimization as a mixed-integer linear problem by using SOS2 variables. This allows for the optimization problem to be solved with low running times, suitable for extensive sensitivity studies and it guarantees global optimality.

- Development of a method to advice field planners during early-phase development that has low running time and average computing power requirements. The method is suitable for extensive probabilistic evaluations that consider first-order interactions between elements in the field value chain and captures the interdependency between reservoir and production system.

- The method is intended for the field development phases where the information about the subsurface is scarce and uncertain, and complex subsurface models are under development.

The methodology will be tested on a synthetic case based on publicly available data of the Wisting field, which is currently under development. The business case has been suggested by the industry partners in the SUBPRO research program of which this project is a part of. Additionally, a master thesis [1] [2] has successfully applied the methodology developed in this PhD research work to another synthetic field named “Safari” proposed by AkerSolutions.

The Wisting field has low pressure, low temperature and low GOR and it is in a remote location in the Barents Sea, 400 km from shore. Because of the low temperature and low GOR, flow assurance, in particular wax deposition is a big concern in this field. Because of this, this research project has also evaluated the applicability of two wax control methods, cold flow and heat tracing, to overcome the problem. While the author does not claim ownership or rights on the development of the technologies analyzed, it hopes to provide a publicly available,

verifiable, and rigorous study case that could serve as an open-source reference for field development teams considering these solutions.

1.2. Thesis objectives

The objective of this research is to develop and test a methodology to provide decision support during early field development to estimate optimum field production profile, drilling schedule, platform type, pressure support mechanism and artificial lift type that maximize NPV. The methodology is based on:

- Development of an integrated proxy model of the value chain that captures the main interdependencies of the variables of interest for the analysis. The proxy model to estimate production profiles is based on an extension of the production potential concept used in reservoir engineering.

- Development of a numerical optimization problem to maximize NPV as a function of production and drilling schedule. The optimization is formulated as a mixed integer linear problem.

- Evaluation of the effect of uncertainties such as cost values, reservoir size, well productivity and layout of the production system, using probability trees.

Additionally, this research work analyzes the applicability of cold flow and heat tracing for the control of wax deposition on submarine pipelines of remote low energy oil reservoirs in a study case using a 1D mechanistic multiphase simulation tool.

1.3. Thesis overview

This thesis is structured as a monograph, and the content of each chapter is presented next.

Chapter 2 presents information of Wisting field. The Wisting field is an offshore oil reservoir located in the Barents Sea that, at the moment of writing this dissertation, is under development stage. This field is used as study case to evaluate the methodology developed.

Chapter 3 presents the development of the proxy models that represent the flow performance of the production system. These proxy models consist of curves of production potential of the reservoir, where oil rate, GOR and WC are expressed as function of cumulative oil production and number of wells. These proxy models are later used in the optimization to estimate the production profile of the system.

Chapter 4 presents the development of the proxy models to express the costs of the systems and explains how the net present value is estimated to compute the profit of project. The costs are represented by linear equations generated from cost data using data regression methods.

Chapter 5 describes the optimization formulation developed to determine the optimum production profile and drilling schedule that give maximum profit in the field for a specific development strategy.

Chapter 6 shows the techniques used to perform uncertainty analyses.

Chapter 7 presents the results of the decision-support methodology developed when applied on a synthetic field based on Wisting. Several technical concepts were compared using the methodology and the best strategy to apply on the field was identified.

Chapter 8 gives a feasibility study of two flow assurance technologies for the control of wax deposition in offshore oil production systems, Cold Flow and Electrical Heat Tracing. For Cold Flow, three concepts for installation at the upstream end of a production flowline were studied: a non-insulated pipe section, a parallel pipe heat exchanger with natural cooling and a heat exchanger with forced cooling. For Electrical Heat Tracing, a feasibility study of four strategies was performed. The required power consumption of each strategy was compared against each other and the most efficient strategies were determined. At the same time, the effect of having insulation in the pipeline was addressed. Both analyses were performed with a commercial 1D mechanistic multiphase flow simulator.

Chapter 9 presents the application of the decision support methodology in a model of the Wisting field that uses Cold Flow as wax control method. The implementation of Cold Flow resulted in reduction in costs and increase in the field profits.

Chapter 10 presents a summary of the results obtained, the relevant conclusion of the thesis and recommendations for future works.

1.4. List of publications

This research has generated the following direct publications:

Paper I: González, D., Stanko, M., Hoffmann, A. *Decision support method for early-phase design of offshore hydrocarbon fields using model-based optimization*. Journal of Petroleum Exploration and Production Technology (2019).
https://doi.org/10.1007/s13202-019-00817-z

Paper II: González, D., Stanko, M. and Golan, M. (2018). *Numerical Feasibility Study of a Wax Cold Flow Approach for Subsea Tie-In Flowlines Using a 1D Mechanistic Multiphase Flow Simulator*. Engineering, 10, 109-123.
https://doi.org/10.4236/eng.2018.103008

Paper III: González, D., Stanko, M. and Golan, M. (2018). *Numerical Feasibility Study of Electric Heating Strategies for Subsea Tie-In Flowlines Using a 1-D Mechanistic Multiphase Flow Simulator*. Engineering, 10, 561-571.
https://doi.org/10.4236/eng.2018.109040

In addition, an indirect publication was generated during the realization of this thesis:

Arnaud Hoffmann, Milan Stanko, Diana Gonzalez. (2019). *Optimization production profile using a coupled reservoir-network model*. Journal of Petroleum Exploration and Production Technology. Volume 9, Issue 3, pp 2123-2137.

Chapter 2

Study Case – Wisting Field

The method developed in this thesis was tested on a synthetic case based on publicly available data of the Wisting field, which is currently under development. The business case has been suggested by the industry partners in the SUBPRO research program of which this project is a part of. This chapter presents the main characteristics of Wisting field.

Wisting is a shallow oil reservoir discovered in 2013 by the company OMV. It is located in the Barents Sea at approximately 310 km north of Hammerfest and 170 km northeast of Johan Castberg field (Figure 2.1). Wisting production license is PL 537. It was granted in 2009, and is shared by four companies Equinor Energy AS (35%), OMV Norge AS (25%, operator), Idemitsu Petroleum Norge AS (25%) and Petoro AS (20%).

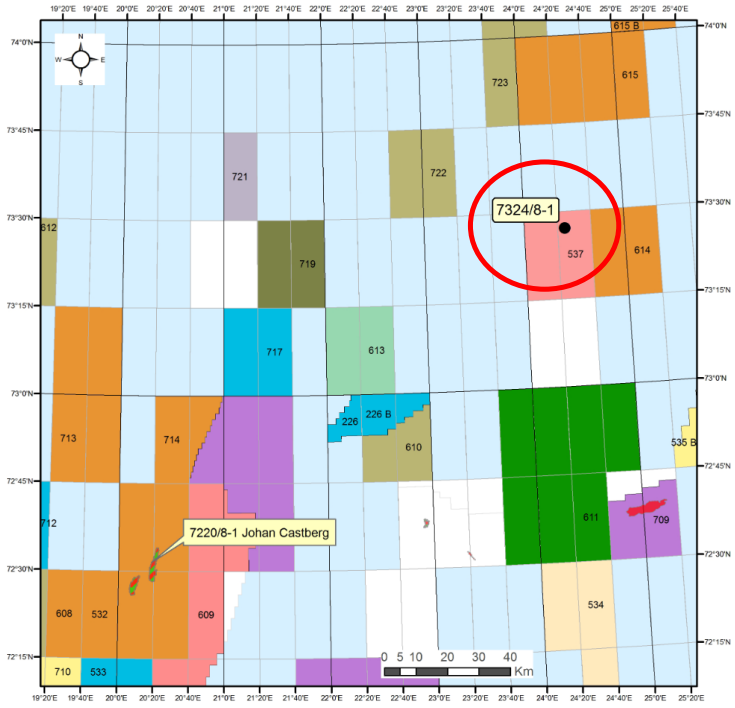

Figure 2.1. Wisting Field [3]

The field has several major segments (shown in Figure 2.2): Wisting Central, Wisting Central West, Wisting Central South, Hanssen, Bjaaland and Hassel. Six wells have been drilled in PL 537 license [3]:

- Exploration wells 7324/8-1 S and 7324/7-1, drilled in 2013.
- Exploration well 7324/7-2, drilled in Hanssen prospect in 2014 to prove hydrocarbons in the Realgrunnen Subgroup.
- Exploration well 7324/8-2, drilled in 2015 to test the Bjaaland prospect.
- Appraisal well 7324/7-3 S, drilled in 2016, it was the first horizontal well of so shallow depth drilled in the Barents Sea.
- Appraisal well 7324/8-3, drilled in 2017.

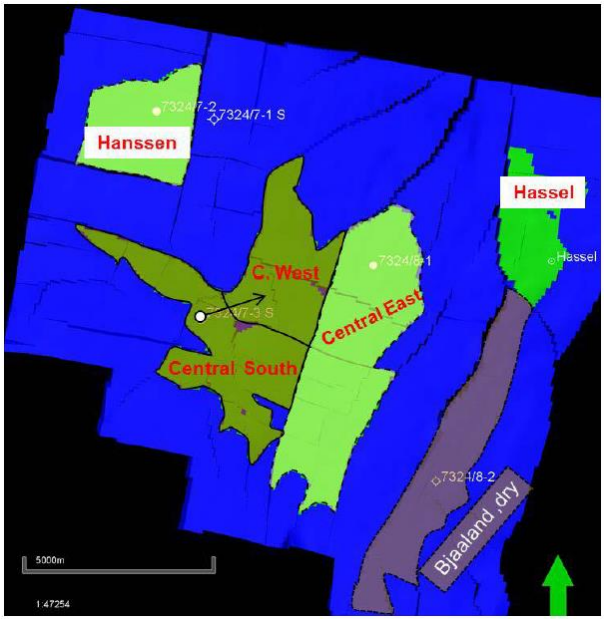

Figure 2.2. Wisting Field located in the Barents Sea

Wisting is a shallow reservoir located 250 m below the seabed, the water depth is 400 m and the oil column is of 50-60 m. It is a low energy reservoir with a reservoir pressure of approximately 70 bara and a temperature of 17 ^{o}C. The total in-place volume is estimated to range from 818 to 1264 MM bbl of oil, with an average of 1025 MM bbl as shown in Table 2.1.

Table 2.1. Estimation of Wisting reserves

	Low	**Base**	**High**
STOOIP [MM bbl]	818	1025	1264

Flow assurance issues can appear. The wax appearance temperature (WAT) of the oil in Wisting is 15 - 17 ºC, while the sea water temperature is 4 ºC. Wax control methods have to be considered during the development phase.

The reservoir properties are shown in Table 2.2.

Table 2.2. Wisting reservoir properties

Property	Value
Reservoir Temperature (ºC)	17.7
Reservoir Pressure (bara)	71.4
Bubble point pressure (bara)	64.4
Two stage GOR (Sm3/Sm3)	44.6
Bo @ Pb (m3/Sm3)	1.076
Oil API	39
Base IOIP (MM stb)	1025

Chapter 3

Development of the proxy model to compute the production performance of the integrated production system (reservoir, well and surface pipe network)

In this thesis, the production performance of the production system is represented by production potential curves (proxy models of production performance). The curves are tables of maximum oil production rates, producing GOR and WC as function of the cumulative oil production (Np) and number of wells (Nw). These proxy models are used here to estimate field production without needing to run the coupled models of reservoir and production network. To generate the production potential curves, a reservoir model and a production network model must be coupled and the simulation must be run to obtain the maximum production that the field can deliver. In the following section, more details about the generation of the production potential proxy models are presented.

3.1. Background

A hydrocarbon production system is composed by sub-surface elements, like reservoirs and wells, and surface components (pipelines, manifolds, valves, equipment, etc.). These elements allow the transportation of the production and injection streams between topside facilities and reservoir.

The production performance of the production system partly depends on the pressure losses of the fluids from the reservoir to the processing facilities. This means, flow in the reservoir, flow in the well, flow in the surface piping network and flow in the platform until the separator. The pressure at the separator is usually kept constant by a pressure and level control system and this typically decouples the processing facilities from the upstream part of the system (therefore, they can usually be modeled and simulated independently or considering a weak coupling).

The most important indicator of the performance of the production system is the production profile (production of oil and gas rate over time). The production profile is the source of revenue for a project, and forecasting of the production is key to assess the economic value of the development strategies.

A production profile typically has three phases (Figure 3.1): build-up phase, plateau phase and decline phase. The build-up phase begins after the first production, and is the phase in which the wells are been drilled and brought on stream. Once the plateau rate is reached, any extra production potential from the reservoir is choked. The plateau rate is decided during the FDP (field development planning) and, usually, the processing facilities are designed to work at that rate. Typical plateau rates varies between 2% and 5% of the STOIIP (stock tank oil initially in place) per year [4]. The last phase of the production profile takes place when the well potential cannot sustain any longer the plateau rate and the production declines. This decline continues until the end of the economic life of the field. The abandonment rate is decided by the petroleum economics, it is the rate at which the revenues from production becomes lower than the costs of producing the field.

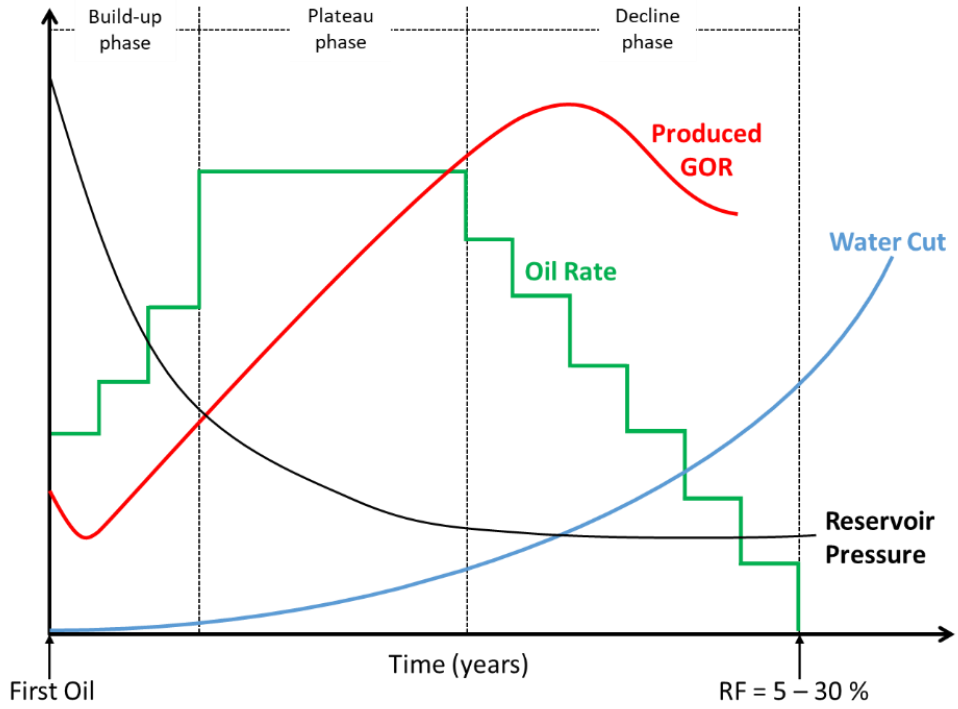

Figure 3.1. Production Profile

During early phases of field development, only reservoir models are typically used to forecast the production profile. Three types or models are commonly used:

- Material Balance (typically require some IPR equation to forecast the production profile)
- Decline Curves Analysis
- Reservoir simulation.

When using a reservoir model only, all these approaches models require some sort of pressure on the boundary (e.g. sand-face or wellhead) that represents the rest of the system. This pressure is the minimum pressure required to flow from reservoir to surface facilities and depends on the flow output from the reservoir, but it is often kept constant with respect to rate. This creates some inaccuracies when computing the production profile expected from the field.

These models require different amounts and levels of detail of input data. Material balance is using overall volumes, assuming homogeneous reservoir unit (no spatial variation), uniform saturation (i.e. all wells in a reservoir unit produce the same GOR and WC). Reservoir simulator requires information about the spatial distribution of reservoir properties, well location, etc. Decline curves analysis required historic production rate data to forecast future production by extrapolating this data and assuming that the production rate declines as function of time. For early phases of offshore field development, usually simple material balance models or simplified reservoir simulation models are used. A material balance model is used in the present study.

Reservoir models and models of the well and gathering network are often built in different modeling tools and are used, updated and maintained by different business units in the oil and gas companies. To capture the interdependencies between them and obtain more realistic production profiles typically Integrated Asset Models are built to couple both.

Reservoir models are transient in nature, while well and gathering network models are typically steady state. Various methods have been proposed [5] to couple reservoir and surface network models and they strongly depend on the type of reservoir model employed. For example, when using reservoir simulator, if the source code of both simulators is accessible, a method consists of including the network equations in the Newton iterations of the reservoir simulator.

Another way, often referred as loose coupling, is when the models exchange information through an interface software (sometimes custom-made or built using a third-party software [6] [7]). In this case, the coupling location has to be specified, this could be either at the bottom-hole, at the sand-face or at the wellhead. In this type of coupling, the near-well inflow from the formation is often represented in the network model by an IPR equation. The IPR equation is typically estimated using an analytical or empirical expression that uses input from the reservoir model. The rates estimated with the network model are then passed to the reservoir model, where produced volumes are estimated, and new values of pressure and saturation are computed. There are choices of explicit or implicit coupling depending if the time-step is re-calculated.

As an example, consider the coupling of a network model and a reservoir model using a tank material balance (Figure 3.2). Here, in each time step, the results from the material balance model (saturations, pressure, etc.) are transferred to the production system model. Since the production system model is steady state, the IPR is computed in every time step to account for the changes due to reservoir depletion. If there are adjustable elements, they are set and the production system model is then run. The results from the production system model are transferred back to the reservoir model to compute the cumulative oil production and solve the material balance equations for next time step.

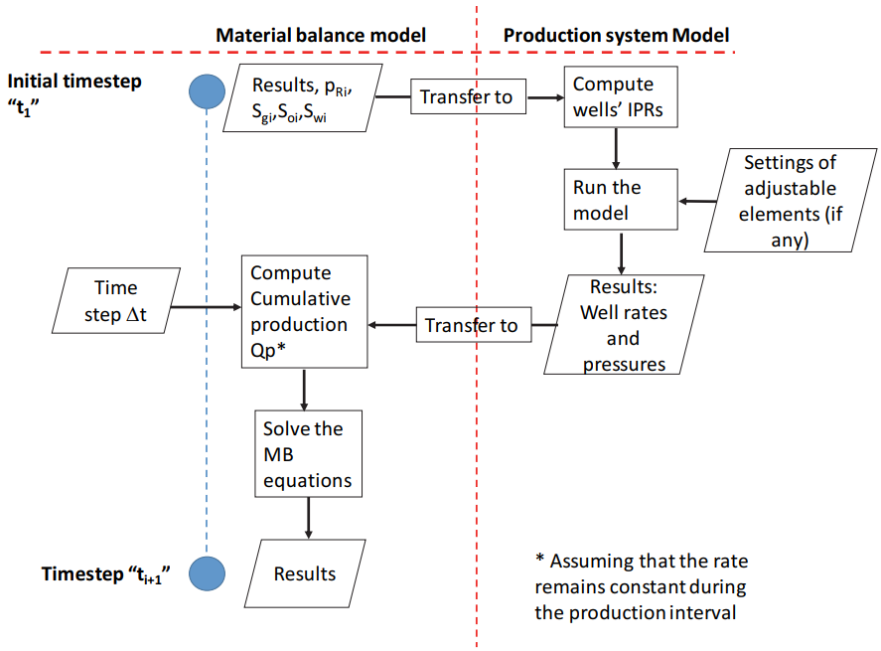

Figure 3.2. Coupling between a material balance model and a model of the production system [8]

3.2. Generation of production system's proxy models

This section presents the concept of production potential, used in this thesis as proxy model to represent the field production performance and the procedure to generate the production potential curves. These proxy models consists of maximum oil production, producing GOR and WC as function of cumulative oil production and number of wells Additionally, proxy models are built for several examples of synthetic field cases. The production profiles computed with the proxy models are compared against simulator models to verify their validity.

3.2.1. Production potential

This thesis uses the concept of production potential to build the proxy model of the integrated production system. In reservoir simulation, the well production potential at any given point in time is the well rate (oil if an oil producer or gas if a gas producer) obtained when the minimum bottom-hole pressure is imposed as a boundary condition. This defines the maximum rate that the well can produce. The field production potential is the sum of the well production potentials. These values are often reported in the output file of the reservoir simulator.

In this thesis the production potential will be defined as the maximum well (or field) rate that can be produced at a given point in time. This rate is obtained using a coupled model of reservoir and network. For example, if the system has wellhead chokes, then the well potential is often achieved when chokes are fully open. If the system has gas-lifted wells, then the well potential is found by finding the gas lift rate for which oil production is maximum.

When using material balance to model the reservoir, even though calculations are performed in time, fluid saturations and reservoir pressure are often a function of cumulative production only. Well and network models use IPR equations to represent the near wellbore inflow that use fluid saturations and reservoir pressure as input. Therefore, the production potential will also depend on cumulative production from the reservoir only.

As an example, let us consider a production system consisting of a single well producing from a dry gas reservoir. The material balance equation for a dry gas tank is expressed by:

$$p_R = \frac{Z_R \cdot p_i}{Z_i} \cdot \left(1 - \frac{G_p}{G}\right) \tag{3.1}$$

Where:

p_R : Reservoir pressure

Z_R : Gas compressibility factor at current reservoir conditions

p_i : Initial reservoir pressure

Z_i : Gas compressibility factor at initial reservoir conditions

G_p : Cumulative gas produced

G : Initial gas in place

The low-pressure back pressure equation can be used to express the production of a well:

$$q_w = C \cdot \left(p_R^2 - p_{wf}^2\right)^n \tag{3.2}$$

Finally, the tubing equation and the flow line equation (assuming horizontal flowline) are represented by the following expressions, respectively:

$$q_w = C_T \cdot \left(\frac{p_{wf}^2}{e^S} - p_{wh}^2\right)^{0.5} \tag{3.3}$$

$$q_w = C_{fl} \cdot \left(p_{wh}^2 - p_{sep}^2\right)^{0.5} \tag{3.4}$$

Here:

q_w : Well production rate (in this case gas)

C : Back pressure coefficient

C_T : Tubing coefficient

C_{fl} : Flowline coefficient

p_{wf} : Flowing bottom-hole pressure

p_{wh} : Well-head pressure

p_{sep} : Separator pressure

n : Backpressure exponent

Combining the four equations, an expression relating the gas production rate and the cumulative gas production is obtained:

$$\left(\left(\frac{q_w}{C}\right)^{\frac{1}{n}} + e^s \cdot \left(\frac{q_w}{C_T}\right)^2 + e^s \cdot \left(\frac{q_w}{C_{fl}}\right)^2 + e^s \cdot p_{sep}^2\right)^{0.5} = \frac{Z_R \cdot p_i}{Z_i} \cdot \left(1 - \frac{G_p}{G}\right) \tag{3.5}$$

Using equation (3.5), the behavior of the gas production potential can be represented as function of the cumulative gas production as shown in Figure 3.3.

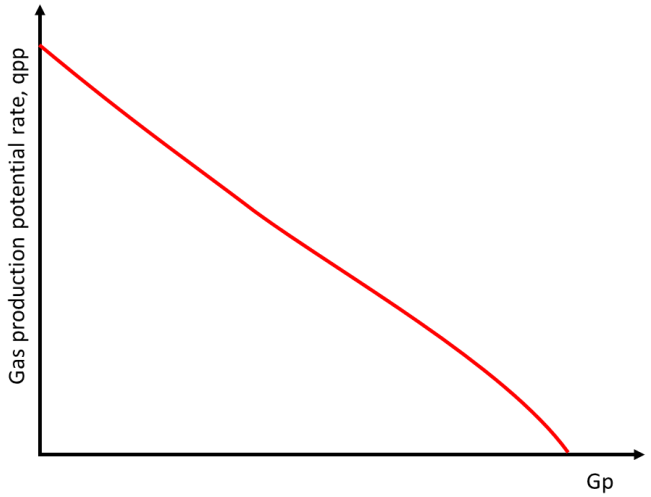

Figure 3.3. Production potential vs. cumulative production for a dry gas reservoir

3.2.2. Generation of production potential curves -Wisting field case

For this thesis, the simulators used to generate the production potential curves (maximum oil rate, producing GOR and WC) were MBAL [9], to model the reservoir, and PipeSim [10], to model the surface network. MBAL is a simulator that uses material balance to perform history matching and prediction runs of reservoir models. PipeSim is a steady state production network simulator that allows modelling the production system from bottom-hole (completion) to an endpoint or sink, defined by a constant pressure or flow rate. Tubing, chokes, pumps, separators, pipelines, risers, lifting methods are some of the elements that can be modeled in PipeSim. The models were built using the Wisting field (chapter 2) as study case.

The reservoir was modeled as a single oil tank. Black-oil PVT tables were used to model the fluid properties (shown in

Appendix C). For the tank's input data, an initial reservoir pressure of 71.4 bara, initial reservoir temperature of 17.7 ºC and IOIP of 1025 MMstb were used. The porosity and the connate water saturation were assumed to be 0.25 and 0.1 respectively, and no Gas Cap was considered. For the water influx, an aquifer was modeled with the Hurst-van Everdingen model with assumed permeability of 400mD. Further details about the input data used in the reservoir model are presented in Appendix A. An example of the results (p_R, N_p, WC, GOR) obtained with the reservoir model considering natural depletion (no water injection) are presented in Table 3.1.

Table 3.1. Results of reservoir model with natural depletion

Tank pressure	**Cum Oil Produced**	**Water cut**	**Producing GOR**
(bara)	(MMstb)	(percent)	(scf/stb)
71.4	0.00	0.00	0.00
64.37	40.15	0.00	244.81
61.08	80.41	0.00	230.42
57.97	120.56	0.00	216.83
55.01	160.71	0.00	205.89
52.04	200.86	0.00	220.90
48.87	241.12	0.00	260.65
45.13	281.27	0.00	359.99
40.12	321.42	0.00	548.45
33.21	361.57	0.00	790.73
24.95	401.83	0.00	909.41
14.02	441.98	0.00	1126.27
2.89	482.13	0.00	1011.54
1.42	492.17	0.00	483.17

For the surface network all wells were assumed identical. They were horizontal wells, with maximum choke opening in the wellheads. The layout of the surface network consisted of 3-well clusters followed by flowlines. All the flowlines commingled at the base of a riser. The riser has an elevation of 480 m and is followed by a sink, which represents the end of the production system (separator). Details of the pipelines and wells are shown in the Appendix B. Figure 3.4 shows a representation of the production system layout used.

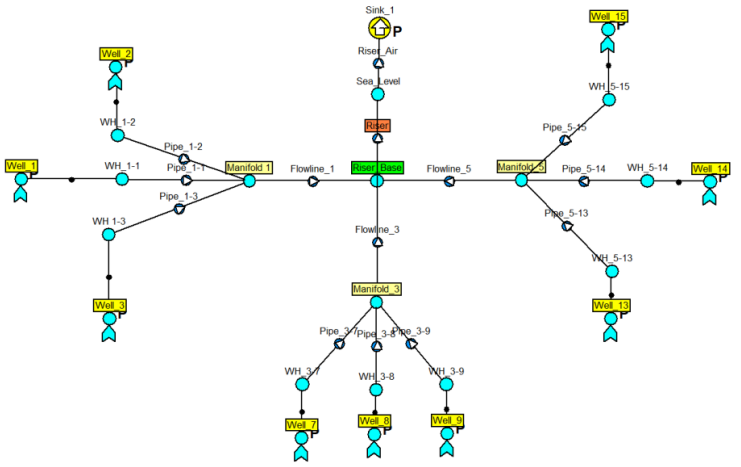

Figure 3.4. Production system layout

To compute the productivity index of the wells, Joshi's model for steady-state horizontal well productivity was used [11]. The fluid properties were calculated with a black-oil model, using the same black-oil tables used in the reservoir model. For the boundary conditions, a pressure of 15 bara was used for the first stage separator and the inlet static pressure in the completion was inputted from the reservoir pressure obtained in the material balance model.

The coupling between both simulators was performed through a third application, Excel, which served as interface software. The coupling process was semi-automated. The reservoir model in MBAL was first run standalone using as input a given field oil production profile. Reservoir pressure, water cut and gas-oil ratio values were extracted from the results and stored in a table versus time. These parameters were a function of cumulative production only and this function did not vary with the production profile imposed.

The results of the material balance model for the whole production horizon were then used as an input in Pipesim. A script was programmed in Excel to transfer the material balance results of a given time to a Pipesim model. The script uses an application programming interface of Pipesim, OpenLink [12]. The script then runs the network model, gets the flow rates and stores them in an Excel's Spreadsheet. The process is repeated for all time steps. A diagram of the process is presented in Figure 3.5.

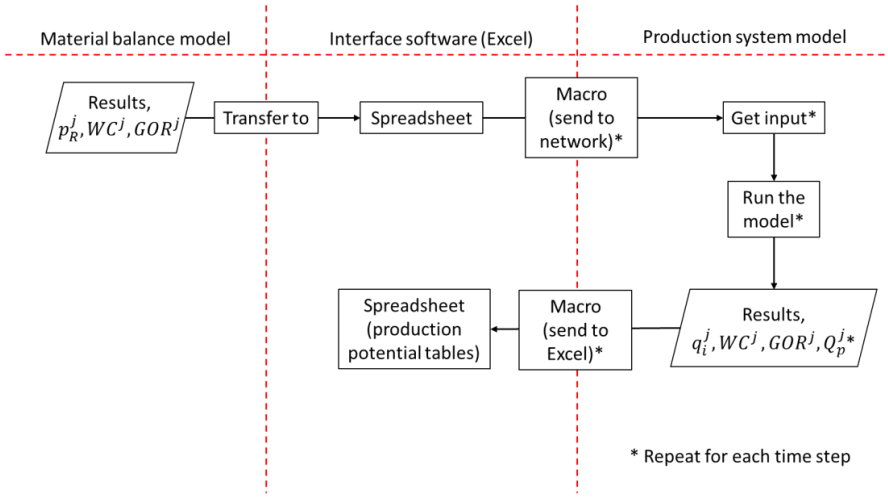

Figure 3.5. Coupling process used

The coupling location between the material balance model and the network model was at the bottom-hole. The results transferred from MBAL to PipeSim were reservoir pressure ($p_R{}^j$), producing gas-oil ratio (GOR^j) and water cut (WC^j). In both simulators, Black-Oil was used to model the PVT properties of the production fluids based on the information presented in Appendix A, B and C. In both models, the data from the PVT tables shown in appendix C was used to calibrate or match the black oil properties. Standing correlation was used to estimate the bubble point pressure (P_b), formation volume factor (B_o) and solution gas-oil ratio (Rs). For the oil viscosity, Beggs et al. correlation was used. The result of this coupling is a set of curves (proxy model) of maximum oil rate, producing GOR and WC as function of cumulative oil production and number of wells.

The production potential for a field with a single well equipped with a wellhead choke with maximum choke opening, are shown in Figure 3.6 and Figure 3.7. These results were obtained for a network model with a flowline of 3 km, a riser of 480 m and a separator pressure of 15bara. For the reservoir pressure, WC and GOR, the values shown in Table 3.1 were used. The values of the remaining parameter were taken from Appendix B.

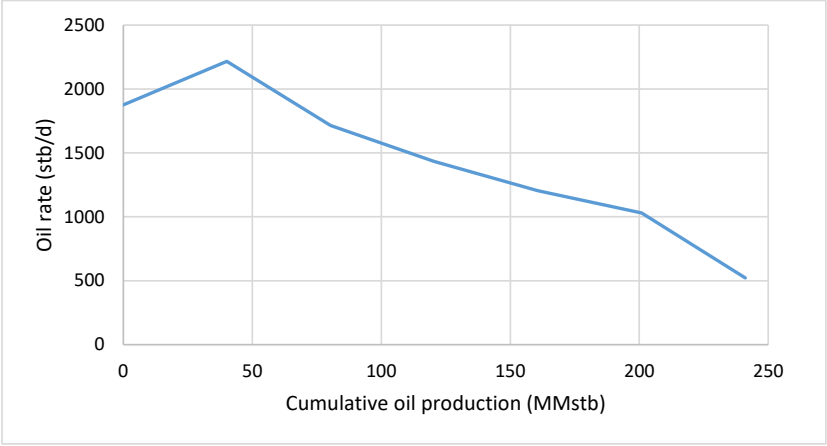

Figure 3.6. Production potential oil rate for case with 1 well and maximum choke opening

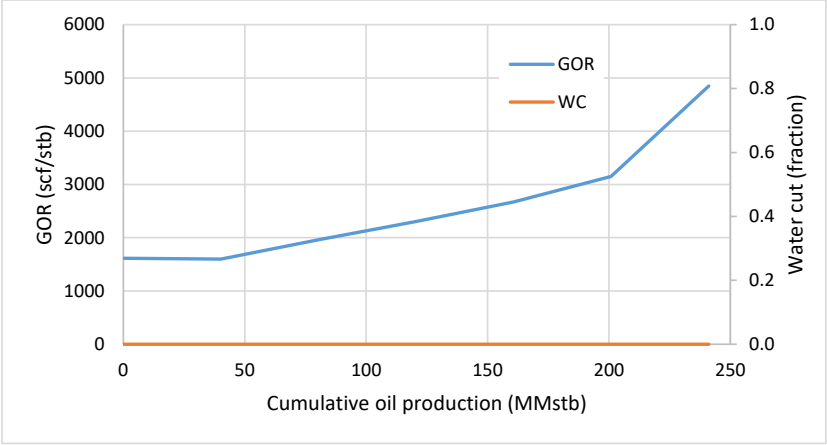

Figure 3.7. GOR and WC for case with 1 well and maximum choke opening

The production potential is mainly declining with cumulative production. This is because the reservoir pressure is declining (see Table 3.1) and thus the deliverability of the formation is reduced.

The network model was modified and the number of wells was varied in the range 1-15. All wells were considered identical. The results of the production potential are shown in Figure 3.8 to Figure 3.10. Here, it can be observed that the field production potential increases if more wells are included in the system.

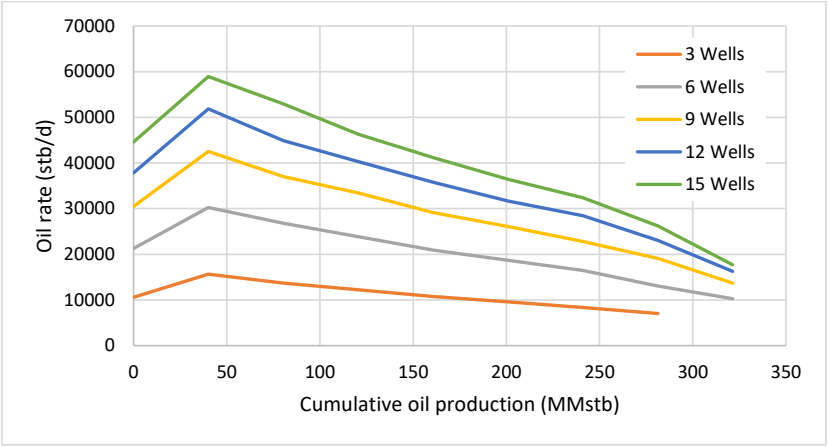

Figure 3.8. Potential oil rate for different number of wells

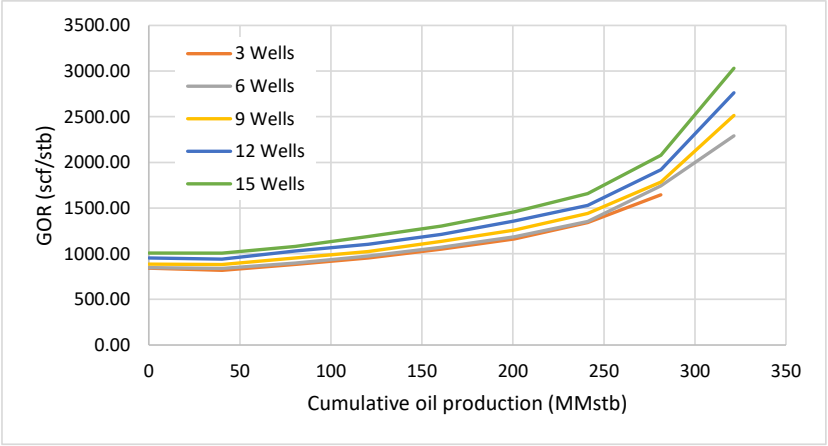

Figure 3.9. GOR for different number of wells

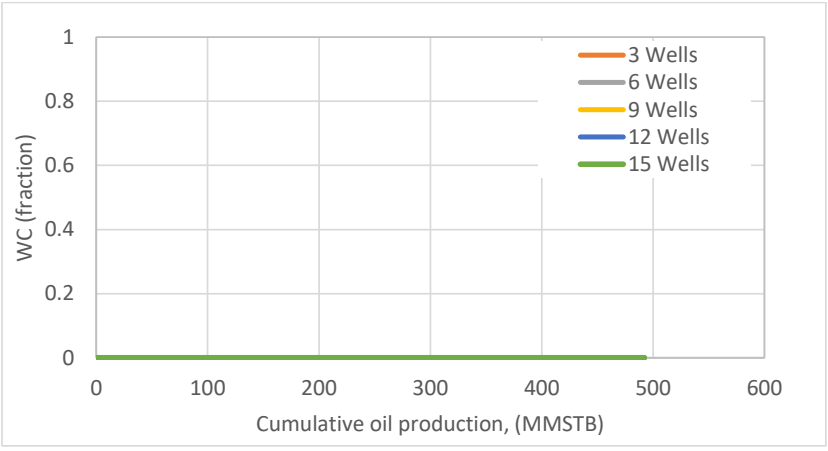

Figure 3.10. WC for different number of wells

3.2.3. Using the production potential curve to plan the production scheduling of a field

The curve of production potential vs. cumulative production can be used to plan the production scheduling of a field without the need to perform runs of integrated reservoir and network models. This is possible because the time dependency of the production potential is eliminated by expressing it as a function of the cumulative production.

A possible process to generate a production profile from production potential curves (production potential versus cumulative production) is as follows:

1. At any point in time, t^j, with the value of cumulative production, N_p^j, interpolate in the production potential curve to find the production potential. The field planner then decides on the value to produce on that time using the production potential as the upper bound.

2. A time step is chosen, and the production rate chosen in step 1 is assumed to remain constant during the time step.

3. In the subsequent point in time, t^{j+1}, the cumulative production is estimated using the production rate imposed in step 2. With the cumulative production, and the production potential curve, a new value of production potential is obtained. The field planner then decides on the rate to produce on that time.

4. The process is repeated until the end of field life is reached

For fields operated in constant production (plateau mode), the field planner usually chooses to produce at a rate that is below the field production potential. However, such fields will eventually enter in decline, a point at which the production potential becomes lower than the desired plateau rate. The field planner then decides to produce as much as possible (at production potential).

The estimation of cumulative production proposed in Step 2 could be inaccurate, especially when producing at production potential. Because the production potential usually declines with cumulative production, it is physically not possible to maintain the production rate constant during the interval between two times. A workaround is to use an implicit method, where the cumulative production in the interval is computed using the production potential at both ends of the interval (e.g. trapezoidal rule), or reducing the size of the time step.

3.2.4. Validation of the production potential proxy model

The objective of this section is to validate the production potential proxy model as an alternative to estimate the field production schedule. For this, the production schedule derived using the production potential curves where compared against the output of a coupled MBAL/PipeSim model. The models were coupled using the approach shown in Figure 3.5. Three cases where used for the validation (Table 3.2):

Table 3.2. Cases for validation of production potential proxy models

	Case 1	Case2	Case 3
Res. Size (stb)	1025	818	1264
Number of wells	9	15	6
Recovery mechanism	Gas Lift	Gas Lift + Water Injection	Multiphase Boosting + Water Injection
Plateau rate (stb/d)	35 000	50 000	90 000

To determine the optimal gas lift rate of case 1 and case 2, the Pipesim operation, "Artificial Lift Performance", was used. This operation allows analyzing the effect of artificial lift on a well. For the case of this thesis, the operation was used to determine the gas lift rate that gives highest production liquid rate. This rate was assumed the same for all wells and constant with time.

In reality, the gas lift injection rate will be affected by depletion. A sensitivity analysis was performed, where the "Artificial Lift Performance" operation of Pipesim was run for different reservoir pressures (to account for the effect of reservoir depletion). This gave as result curves of production liquid rate vs. gas lift rate for each reservoir pressure. Figure 3.11 shows an example of the variation of the gas lift performance curves with depletion.

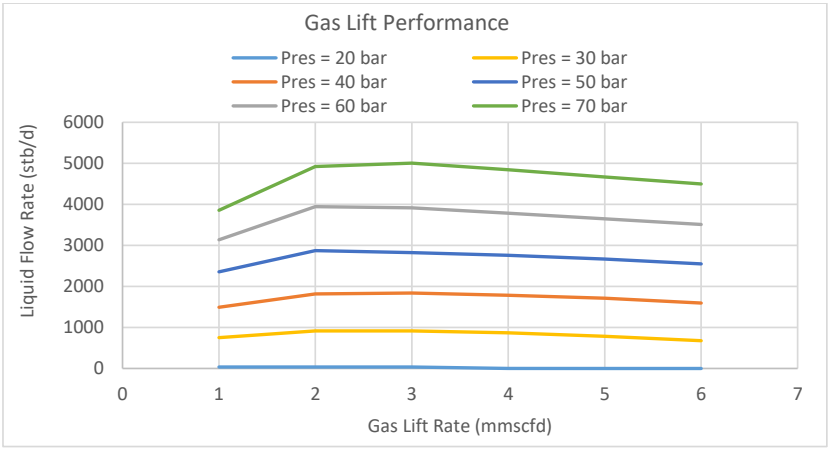

Figure 3.11. Gas lift performance curves for generic production system

The procedure to determine the production profile based on the production potential curve is explained in section 3.2.3. For each case, the plateau rates used are shown in Table 3.2. The proxy models (maximum oil rate, producing GOR and WC vs. cumulative oil production) used for each case are presented in Appendix D.

The oil production, cumulative oil production, GOR and WC profiles for each case are shown in Figure 3.12 to Figure 3.17. The figures compare the results obtained with the proxy model approach and with the coupled MBAL/PipeSim simulation. The difference between both approaches are summarized in Table 3.3.

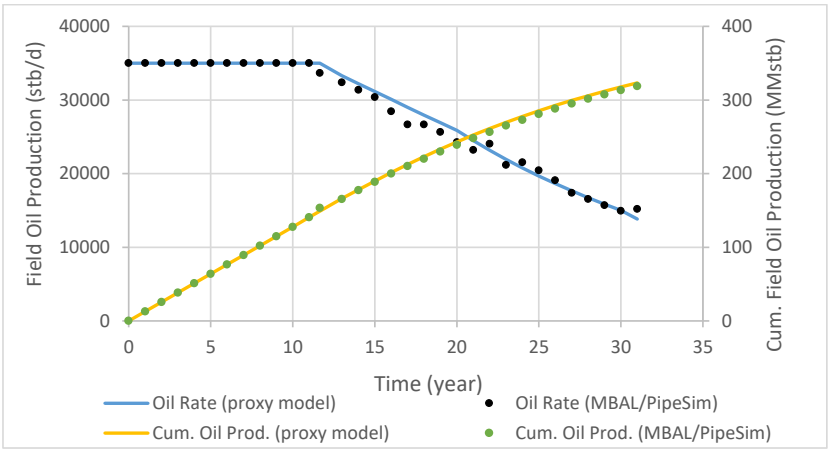

Figure 3.12. Proxy model validation for Case 1. Oil production profile and cumulative oil production

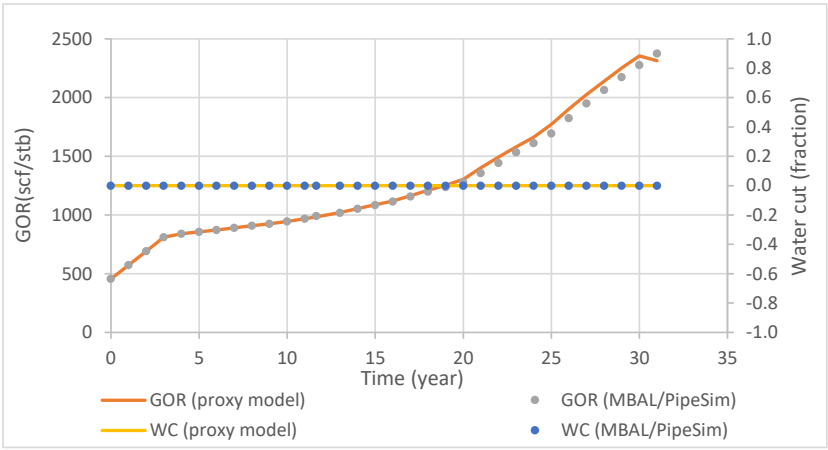

Figure 3.13. Proxy model validation for Case 1. GOR and WC

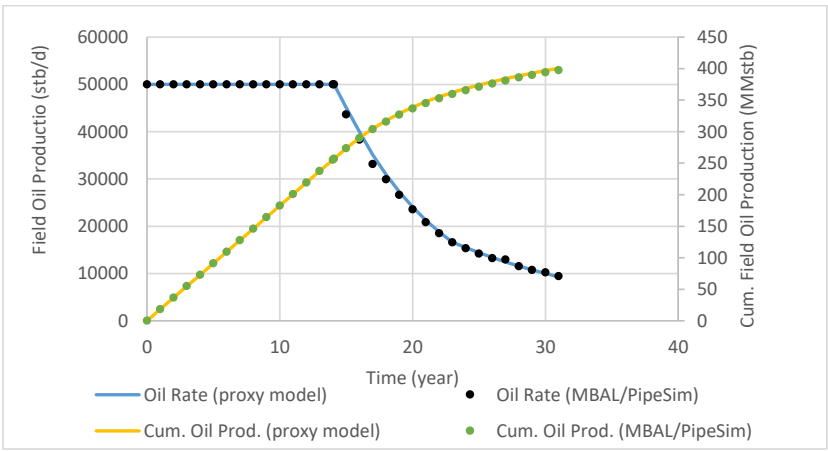

Figure 3.14. Proxy model validation for Case 2. . Oil production profile and cumulative oil production

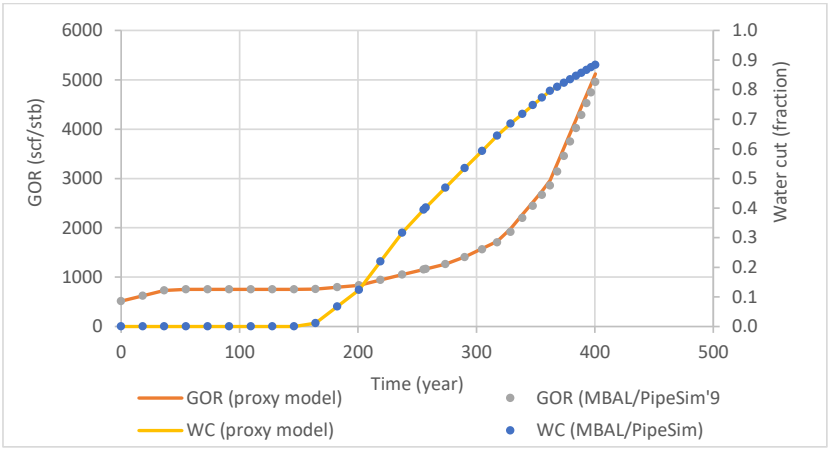

Figure 3.15. Proxy model validation for Case 2. GOR and WC

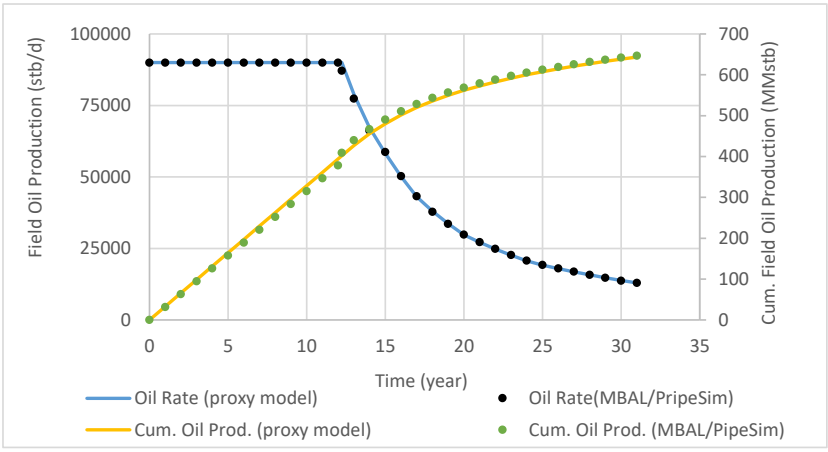

Figure 3.16. Proxy model validation for Case 3. Oil production profile and cumulative oil production

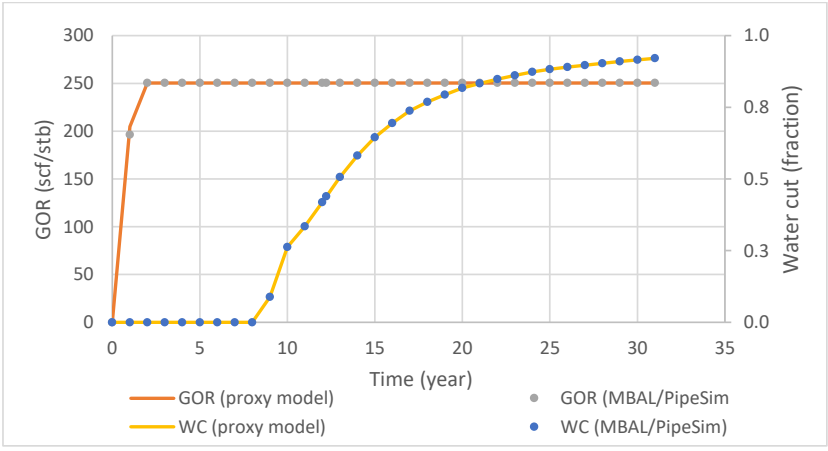

Figure 3.17. Proxy model validation for Case 3. GOR and WC

Table 3.3. Differences in results between proxy model of production potential approach and coupled model MBAL/PipeSim for all cases

Average Relative error (%)			
	Case 1	**Case 2**	**Case 3**
Prod. Profile	2.44	1.13	0.34
Cum. Prod	1.42	0.35	2.39
GOR	0.88	1.59	0.13
WC	0.00	0.01	0.01

Based on the results shown it can be observed that both, the proxy model and the coupled reservoir-network model, yield similar outcomes. A similar validation can be found on the work of Angga [1], who validated the production potential curves approach against a full GAP [13] simulation based on Safari field (a synthetic field). The field consists of three reservoirs: Løve, Nesehorn and Sebra. In his study, Angga compared the oil, gas and water production profiles and the gas and water injection rates obtained with the production potential approach and a GAP simulation. He found that, both approaches yield to almost identical outcomes with a maximum error of 5%.

3.2.5. Validation of the production potential proxy model approach in the Gullfaks Statfjord oil reservoir

The production potential approach is used to estimate the field production schedule of the Gullfaks Statfjord field, which is currently under production in the Norwegian Continental Shelf. For this, the production schedule obtained using the field's production potential curves are compared against the production schedule obtained from a 3D reservoir model of the field generated in Eclipse [14]. The Gullfaks Statfjord field has been use only for validation of the production potential approach and it was not used for any other purpose in this PhD work.

Gullfaks is an oil field located in the Tampen area of the North Sea. The field was discovered in 1978 and production started in 1986. Gullfaks produces oil from the Brent, Statfjord, Cook and Lunde Formations. The reservoir is located at depths of 1700 – 2000 m. The oil is produced through pressure support from water, gas and water alternating gas injection, been water flooding the main strategy. The oil is transported via loading buoys onto shuttle tankers and rich gas is transported by Statpipe to Kårstø terminal for processing [15]. The reservoir model used is a representation of Gullfaks Statfjord (Figure 3.18) and the field's main properties are [16]:

Table 3.4. Gullfaks Statfjord oil properties

Property	**Value**
Initial oil in place* (MM stb)	3283
Initial reservoir pressure (bara)	320
Temperature (^{o}C)	76
Average porosity (%)	26
Average permeability (md)	1000
API (^{o})	29
Bubble point pressure at 1850m TVD MSL (bara)	200 - 240
Initial GOR (scf/stb)	915
Oil viscosity at bubble point (cp)	0.43
* Value corresponding to Gullfaks field (all formations)	

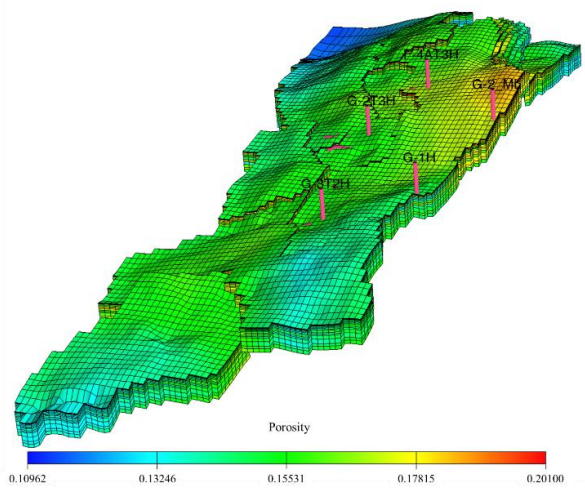

Figure 3.18. Gullfaks Statfjord reservoir model (property: porosity)

Gulffaks Statfjord reservoir model has five oil production wells and no injectors. The start date of the simulation was 13 April 1999 and the model was run for approx. five and half years (until 1 November 2004). The model doesn't include well tables nor the surface transport system to the processing facilities. A minimum flowing bottom-hole pressure has been defined that represent the minimum pressure required to flow to the processing facilities. The model has 64 cells in the x direction, 110 in the y direction and 15 cells is the z direction. The actual production profile obtained from performing history matching with the reservoir model is shown in Figure 3.19.

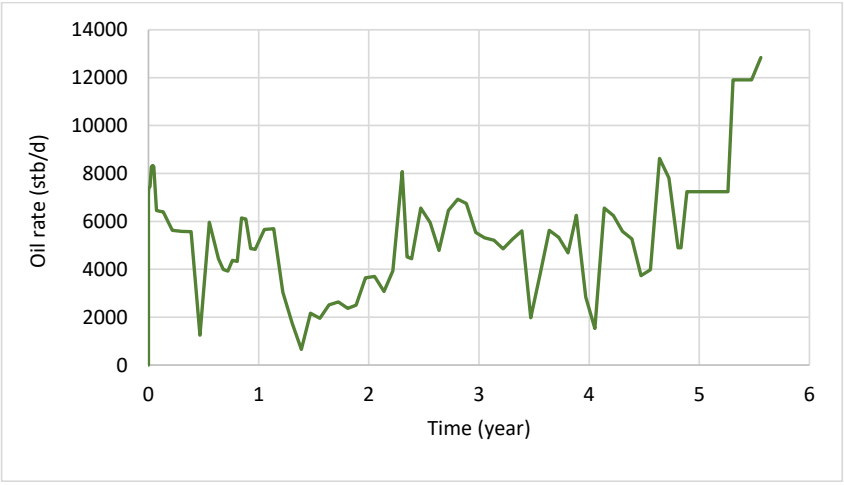

Figure 3.19. Gullfaks Statfjord's actual oil production profile

Generation of production potential curves with the reservoir model

The model was initially run without any rate restriction to obtain the production potential curves, which are shown in Figure 3.20 and Figure 3.21.

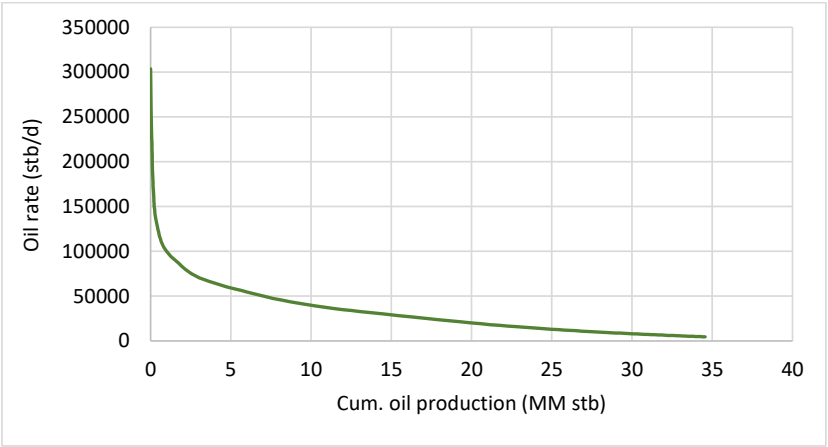

Figure 3.20. Gullfaks Statfjord's production potential curve: Oil rate

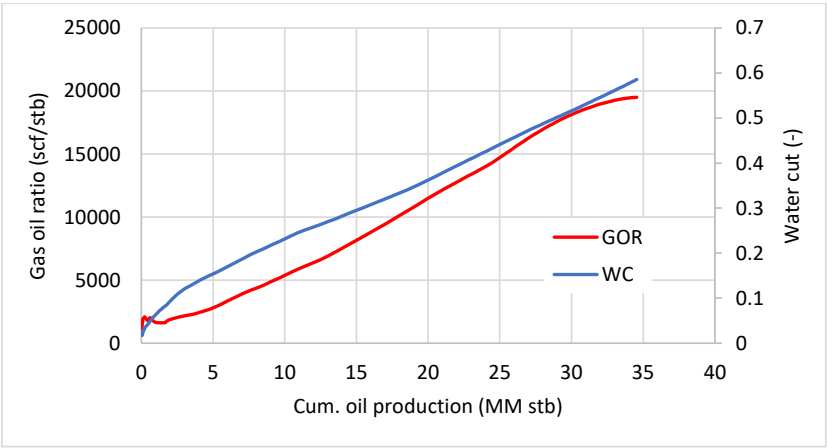

Figure 3.21. Gullfaks Statfjord's production potential curves: Gas oil ratio and water cut

The procedure explained in section 3.2.3 was used to determine the production scheduling of the field and compare it against the output of reservoir simulator. The field was produced in plateau mode with a fixed field target rate until it naturally started declining. Four different plateau rates were tested: 10 000 Sm^3/d (62 898.27 stb/d), 8 000 Sm^3/d (50 318.62 stb/d), 6 000 Sm^3/d (37 738.96 stb/d) and 4 000 Sm^3/d (25 159.31 stb/d). The plateau rate was imposed as a field constraint in Eclipse, meaning that the rate in each wells was allowed to change in order to maintain the constant plateau rate of the field. The optimization was run for approx. five and half years (from13 April 1999 to 1 November 2004).

The production schedule obtained for each plateau rate with the production potential approach and with the field's reservoir model is shown in Figure 3.22 to Figure 3.29. The difference between both approaches are summarized in Table 3.5. To calculate this difference, the production potential approach was applied using the same time steps generated by the reservoir model for each plateau rate.

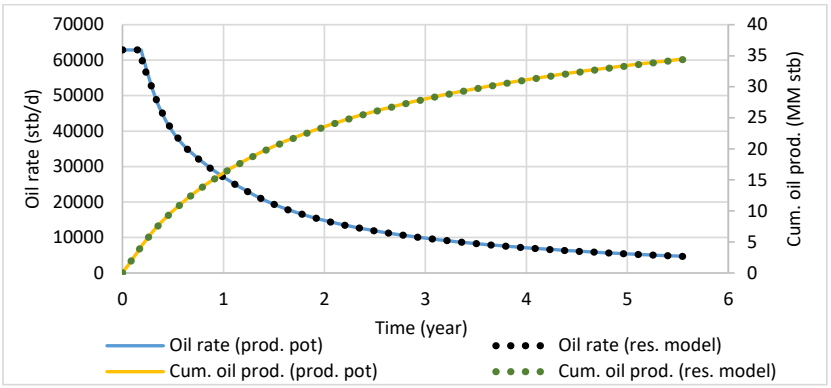

Figure 3.22. Production potential approach validation using Gullfaks Statfjord's reservoir model. Oil rate and cumulative oil production. Plateau rate: 10 000 Sm^3/d (62 898.27 stb/d)

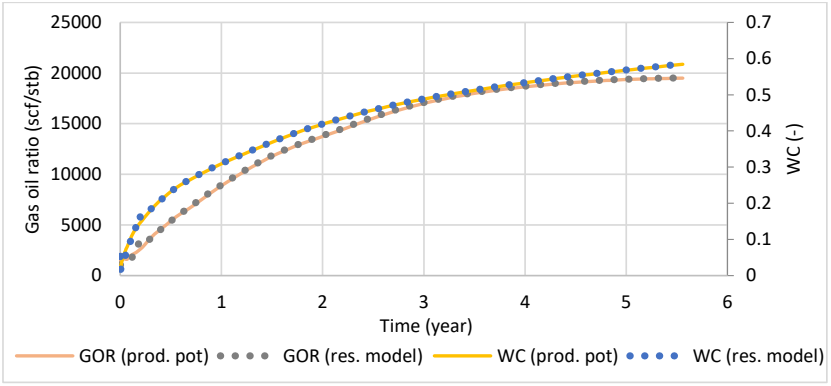

Figure 3.23. Production potential approach validation using Gullfaks Statfjord's reservoir model. GOR and WC. Plateau rate: 10 000 Sm^3/d (62 898.27 stb/d)

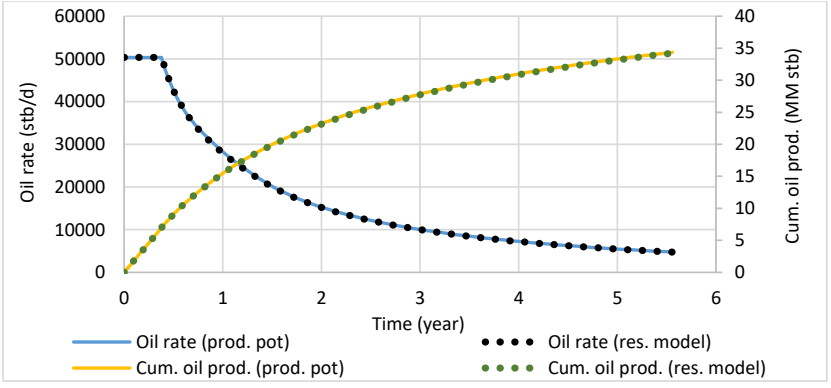

Figure 3.24. Production potential approach validation using Gullfaks Statfjord's reservoir model. Oil rate and cumulative oil production. Plateau rate: 8 000 Sm^3/d (50 318.62 stb/d)

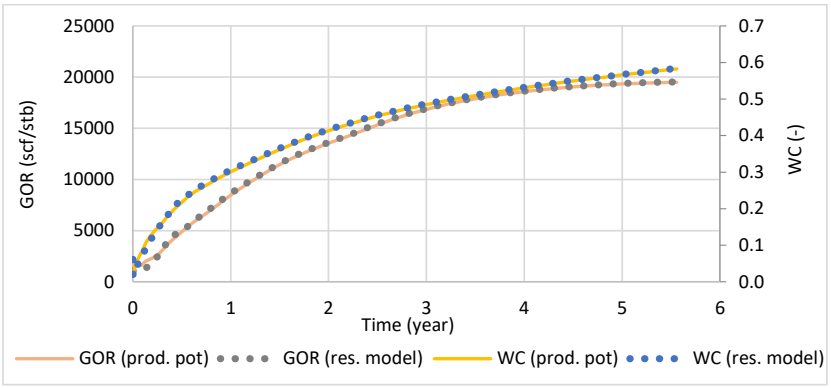

Figure 3.25. Production potential approach validation using Gullfaks Statfjord's reservoir model. GOR and WC. Plateau rate: 8 000 Sm^3/d (50 318.62 stb/d)

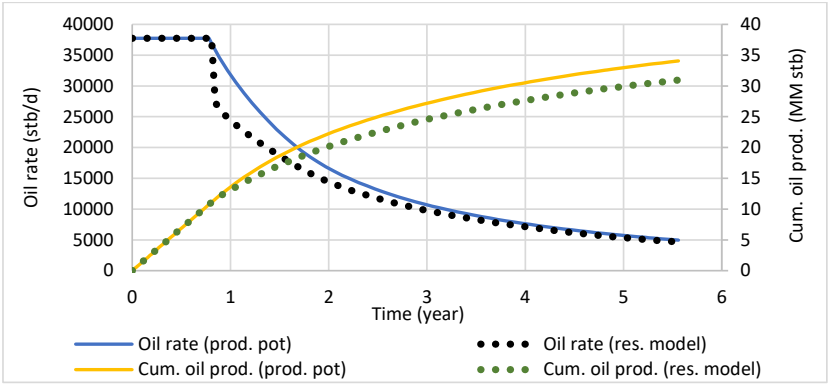

Figure 3.26. Production potential approach validation using Gullfaks Statfjord's reservoir model. Oil rate and cumulative oil production. Plateau rate: 6 000 Sm3/d (37 738.96 stb/d)

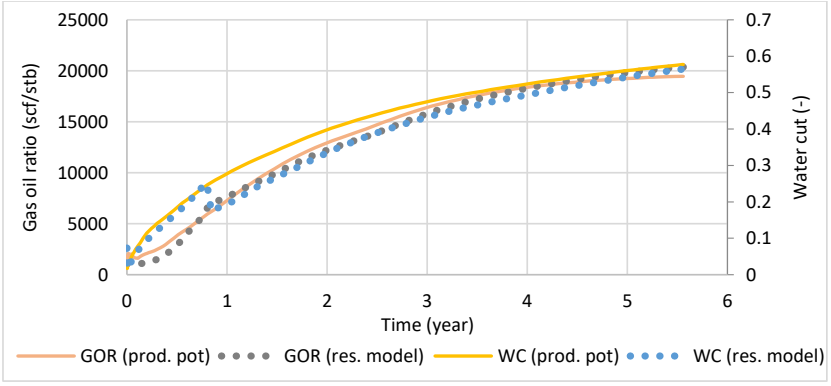

Figure 3.27. Production potential approach validation using Gullfaks Statfjord's reservoir model. GOR and WC. Plateau rate: 6 000 Sm3/d (37 738.96 stb/d)

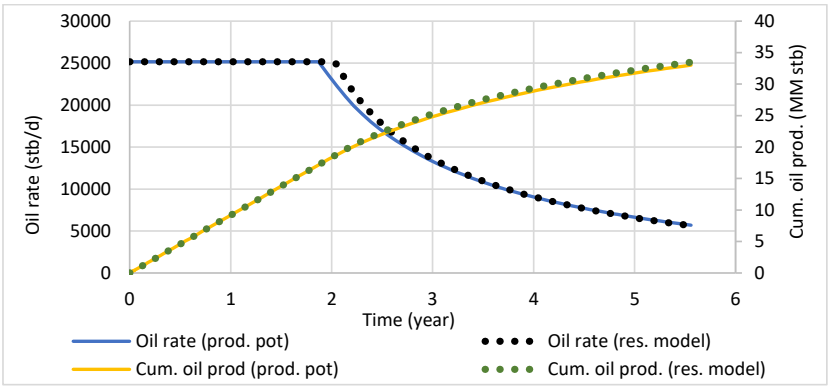

Figure 3.28. Production potential approach validation using Gullfaks Statfjord's reservoir model. Oil rate and cumulative oil production. Plateau rate: 4 000 Sm3/d (25 159.31 stb/d)

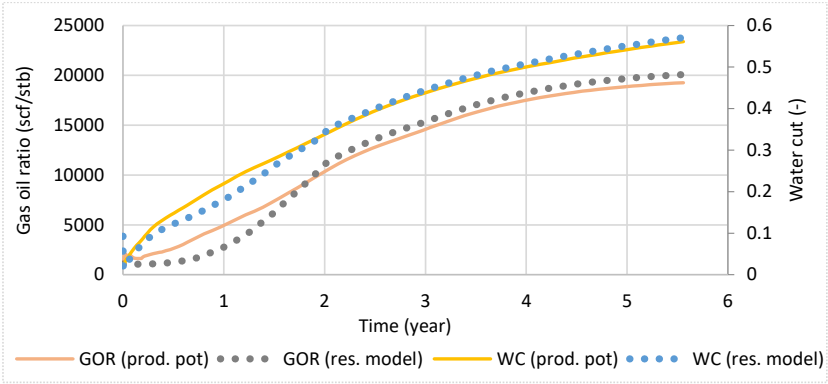

Figure 3.29. Production potential approach validation using Gullfaks Statfjord's reservoir model. GOR and WC. Plateau rate: 4 000 Sm3/d (25 159.31 stb/d)

Table 3.5. Differences in results between production potential approach and Gullfaks Statfjord's reservoir model

Average Relative error (%)				
	qp=62 898.27 (stb/d)	**qp=50 318.62 (stb/d)**	**qp=37 738.96 (stb/d)**	**qp=25 159.31 (stb/d)**
Prod. Profile	0.37	0.39	8.00	1.09
Cum. Prod	0.23	0.25	6.09	0.70
GOR	4.98	5.95	10.27	20.65
WC	3.04	3.75	11.89	8.22
Maximum Relative error (%)				
	qp=62 898.27 (stb/d)	**qp=50 318.62 (stb/d)**	**qp=37 738.96 (stb/d)**	**qp=25 159.31 (stb/d)**
Prod. Profile	4.71	1.19	24.06	12.35
Cum. Prod	0.74	0.38	9.65	1.61
GOR	48.65	49.67	47.82	66.86
WC	31.31	32.12	31.59	30.52

Minimum Relative error (%)				
	qp=62 898.27 (stb/d)	**qp=50 318.62 (stb/d)**	**qp=37 738.96 (stb/d)**	**qp=25 159.31 (stb/d)**
Prod. Profile	0.00	0.00	0.00	0.00
Cum. Prod	0.00	0.00	0.00	0.00
GOR	0.10	0.21	0.03	0.56
WC	0.03	0.20	0.22	0.07

The results obtained show that using the production potential curves to determine oil, water and gas production rates with time of the Gullfaks Statfjord field is a fair approximation when compared against the output of a detailed 3D reservoir model. The average relative error in the oil rate was 8% with a maximum of 24%. The average relative error was bigger for the GOR and WC when lower plateau rates were used, reaching 20% and 12%, with a maximum of 56% and 31% respectively. It seems that the production potential approach is more accurate when scheduling production with plateau rates closer to the production potential of the field at initial reservoir pressure.

Based on the validations presented in this section and the ones performed by Angga [1], it could be concluded that the production potential approach is a valid approach to compute field production profiles with low computing time when compared against the output against more complex models. Therefore, it is suitable to be employed in early field development studies and sensitivity analyses.

Chapter 4

Development of the proxy models of the cost and estimation of net present value

To determine the feasibility of a specific field development concept, an economic analysis could be performed where the profit of the concept can be estimated using the NPV. For this, information related to the revenues and costs associate with that concept is needed. This chapter focuses on the method used in this thesis to estimate those costs and considerations made to calculate the NPV.

4.1. Background

The development of an oil/gas reservoir involves high cost investments under an environment of high uncertainty. The necessary information for an economic analysis consists of capital costs, operating costs, estimated production profile, taxes and oil/gas price forecasts.

The attractiveness of a project strategy is often measured with the cash flow of the project, which forms the basis of the economic evaluation methods used in field development planning. The net cash flow is estimated by calculating the revenues and subtracting the expenditures of the project in each year. A typical representation of the annual net cash flow is presented in Figure 4.1.

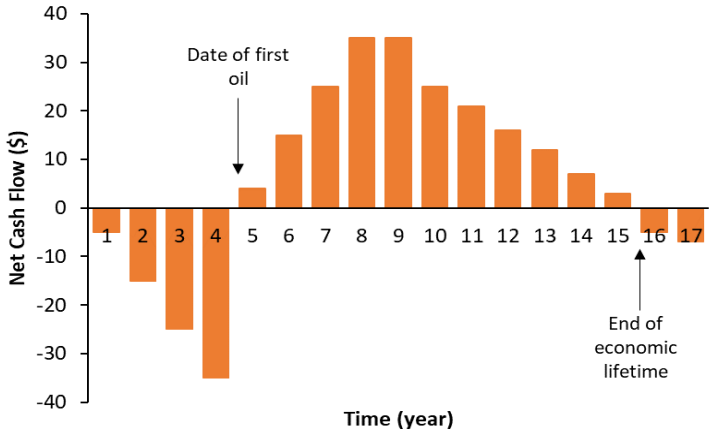

Figure 4.1. Annual net cash flow

The revenue comes from the sale of hydrocarbons. The expenditures from a project consists of capital expenditures (platform, facilities, wells), operational expenditures and abandonment costs. Other expenditures considered, when information is available, are the royalties and the taxes. These represent the host government claims from the income of the hydrocarbon sales.

It is necessary to consider the effect of time in the value of money to perform a proper economic analysis. Discounting is the technique used to compare the value of sums of money spent at different times. When applying discounting to the cumulative cash flow (sum of all annual cash flow), we get the discounted cash flow or net present value (NPV), which is often the most important indicator of the profitability of a project. The NPV is represented in equation (4.1).

$$NPV = \sum_j \frac{cash\ flow^j}{(1+DR)^j} \tag{4.1}$$

where

$DR =$ annual discount rate used to determine the present value,

$j =$ time expressed in years,

This chapter presents the method to estimate the costs used in this thesis and the equation used to estimate the Net Present Value of the field for a specific field development scenario.

4.2. Proxy model for cost data

The costs considered for the estimation of the net present value in this work are capital, drilling and operating expenditures (CAPEX, DRILLEX and OPEX). Neither the abandonment cost nor the taxes and royalties were taken into account. The CAPEX includes the cost of the production system (pipelines, valves, manifolds, equipment, umbilical, etc.) and the processing facilities (platforms, FPSO, etc.). DRILLEX represents the costs of the wells and X-mass trees (drilling rig, tubing, completion, etc.). OPEX considers the costs that takes place once the field is in operation (maintenance, inspections, offshore personnel, etc.).

In general, cost estimation requires a significant amount of input and is a labor and time intensive manual process. Furthermore, it is especially difficult to have an accurate cost estimation during early field development, since detailed specifications of the production system components is needed and this might not be available at this stage. Moreover, if the design conditions are changed, it takes considerable time and effort to compute the updated cost figures. A possible alternative, is to generate cost models based on previous projects and historical cost figures.

The strategy used in this research is to use simplified cost models based on equations that capture the first order effect of the field design features under study on the cost figures. This approach has been used in the past [17] [18] [19], for example, Nunes et al. [17] [18] used these type of equations for analysis of field development during the concept screening stage. This type of models is suitable for numerical optimization schemes or analyses of uncertainty where the input must be varied several times in an iterative process.

The following assumptions/simplifications are performed for estimating the cost:

- DRILLEX is affected by the number of injectors and producers. A lump sum has been used to estimate DRILLEX that includes all costs of drilling, testing, completing the wells, etc. The wells are subsea, distributed in 4-slope templates. Injectors and producers cost the same.

- CAPEX is typically split in several components: offshore structure, subsea system, processing facilities. In this work a unique cost figure is used to compound all. The factors that affect the CAPEX are: the type of offshore structure, subsea structures (pipelines, manifolds, equipment, umbilical, etc.), the maximum rate of oil, gas and water produced from the field, etc.

- OPEX is expressed as an annual average. This means that, every year has the same value of OPEX. This cost considers all the expenses that take place once the field starts operations. like maintenance of all elements of the production system, cost of supply and stand-by vessels, costs of interventions, reservoir area fee, insurance, tax, fuel consumption, offshore personnel, etc.

In this work, the costs are expressed as function of the capacity of the processing facility (this is, maximum oil, gas and water rates that can be processed) and the number of production and injection wells in the field. The proxy models consists of linear equations, created from a multivariable linear regression, of CAPEX, OPEX and DRILLEX as function of the mentioned variables ($q_o^{capacity}$, $q_g^{capacity}$, $q_w^{capacity}$, Nw^{field}, for CAPEX and OPEX, and $Nw_{d,p+i}^{j}$, for DRILLEX).

A commercial software for the estimation of costs in offshore production systems was used [20]. This research work did not question or verified the validity and accuracy of the cost data used, because of the limited information available in the literature to the general public and because the emphasis of the present research is on the method rather than on the results.

To generate the costs proxy models, a sensitivity analysis was perform where the CAPEX, OPEX and DRILLEX were estimated for different values of oil, gas and water rate capacities, and number of well in the field (producers and injectors). This gave as results a set of costs values (cost data). Then, a multivariable linear regression was performed. This resulted in equations of the form:

$$E_{capex} = a_{cap} \cdot q_o^{capacity} + b_{cap} \cdot q_g^{capacity} + c_{cap} \cdot q_w^{capacity} + d_{cap} \cdot Nw^{field} + e_{cap} \tag{4.2}$$

$$E_{opex} = a_{op} \cdot q_o^{capacity} + b_{op} \cdot q_g^{capacity} + c_{op} \cdot q_w^{capacity} + d_{op} \cdot Nw^{field} + e_{op} \tag{4.3}$$

$$E_{drillex} = a_{drill} \cdot Nw_{d,p+i}^{j} + b_{drill} \tag{4.4}$$

In equations (4.2) and (4.3) $q_o^{capacity}$ and $q_w^{capacity}$ are be expressed in units of stb/d and $q_g^{capacity}$ has units of MM scf/d.

4.2.1. Generation of proxy models for estimation of cost – Case Wisting field

This section presents generation of the proxy models for cost estimations. For the sensitivity analysis performed, three values of oil rate, gas rate and water rate capacities of the processing facilities were used, as well as thee different number of wells. In addition, three type of

processing facilities were considered: TLP, FPSO and Tie-Back to existing facility. The three costs used in this thesis were estimated, using a costs estimation commercial software, for a combination of all the sensitivity variables point. This gave 81 (3x3x3x3) values of CAPEX, OPEX and DRILLEX, estimated for each processing facility (i.e. 81 cost values for TLP, 81 for FPSO and 81 for Tie-Back). Table 4.1 gives the values used for the sensitivity analysis.

Table 4.1. Data used for costs sensitivity analysis

Oil Rate Sm^3/d (stb/d)	**Gas Rate MM Sm^3/d (MM scf/d)**	**Water rate Sm^3/d (stb/d)**	**N. wells (prod + inj)**
5 000 (31 449)	1.5 (53)	20 000 (125 796)	10 + 10
15 000 (94 347)	2.5 (88)	30 000 (188 694)	15 + 15
25 000 (15 7245)	3.5 (124)	40 000 (251 592)	20 + 20

The cost estimation software required some information to perform cost estimation and economic analysis (to determine NPV). For this thesis, only the cost estimation was considered. The results of the economic analysis were not used. A summary of the most relevant information required by the software is presented below.

- **General input:** the general input consist of information related to field location, currency, recoverable volumes, oil and gas prices, discount rate, insurance etc.

- **Wells and subsea system:** Same number of producer and injectors wells were used for the analysis. These are distributed using 4-slots templates. Some of the required data for wells are: number and type of wells, drilling method, well lengths, number of X-mass tree, number of 4-slots templates, number of satellite slots, etc.

- **Layout of production system:** The layout of the production system is shown in Table 4.2. The system consists of production flowlines, water injection flowlines, gas injection flowline (for gas lift), umbilical and power cables. Additionally, one oil export flowline and one gas export flowline are considered.

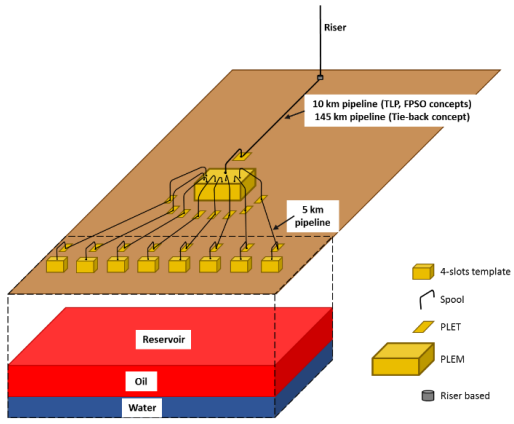

Figure 4.2. Production system layout used for cost estimation

- **Topside:** three topside concepts were used in this work: Tension Leg Platform, FPSO and Tie-back to existing facility (is this case a FPSO). For the topside the following information is required: platform concept, number of beds in living quarters, drilling package, storage volume of oil/condensate, number of inlet separators, oil production capacity, gas production capacity, inlet separator pressure, maximum liquid capacity, water capacity, gas capacity, etc.

- **Tie-Back additional specifications:** There are some additional specifications for the tie-back concept. They are related to the additional weights needed and some topside modification. The additional weight used in this work were those calculated by the software (default values). The topside modification used are the ones suggested by the software and they are listed below:

    - Drilling derrick
    - Drilling systems, mud
    - Platform well control system
    - Pig receiver, riser pull-in
    - Dry tree related
    - Wet tree related
    - Export related
    - Drilling control, BOP
    - Drilling utilities
    - Subsea well control system
    - Separation and stabilization
    - Test separator
    - Inlet separator
    - Allocation metering system
    - Gas re-compression
    - Lift Gas

- **Cost, Norwegian content, contingency and allowance:** This section refers to information used by the software to estimate the cost of a project. For this work, the information was kept as the default values given by the software for all three concepts.

- **Economy/Production:** information about leasing interest rates of production unit and storage tank unit, and production profile must be input. This is used for calculation of NPV and other economic indicators. A generic production profile was used for all the cases of costs estimation perform. The production profile is used to perform the economic analysis, it does not have influence in the cost estimation. However, it must be input in order to get outputs from the software.

Having the cost data, a linear regression for the CAPEX, OPEX and DRILLEX, was performed for the three topside facilities considered. Linear equations were selected to represent the costs, this was the tendency that adjusted better to the data, besides previous studies have used linear equations to model the costs [17] [18]. The equations obtained are used as a proxy model to estimate the costs during the optimization.

The costs proxy models generated for the case of Wisting field are presented in the equations (4.5) to (4.11) below.

TLP:

$$E_{cap,TLP} = 0.0079 \cdot q_o^{capacity} + 29.81 \cdot q_g^{capacity} + 0.0115 \cdot q_w^{capacity} + 307.53 \cdot Nw^{field} + 11702.41 \quad (4.5)$$

$$E_{op,TLP} = 6.67E-4 \cdot q_o^{capacity} + 0.8930 \cdot q_g^{capacity} + 2.18E-4 \cdot q_w^{capacity} + 14.01 \cdot Nw^{field} + 613.93 \quad (4.6)$$

FPSO:

$$E_{cap,FPSO} = 0.0122 \cdot q_o^{capacity} + 42.64 \cdot q_g^{capacity} + 0.0173 \cdot q_w^{capacity} + 307.87 \cdot Nw^{field} + 15407.21 \quad (4.7)$$

$$E_{op,FPSO} = 9.42E-4 \cdot q_o^{capacity} + 1.4050 \cdot q_g^{capacity} + 3.63E-4 \cdot q_w^{capacity} + 14.01 \cdot Nw^{field} + 673.78 \quad (4.8)$$

Tie-back:

$$E_{cap,Tie-Back} = 0.0366 \cdot q_o^{capacity} + 12.74 \cdot q_g^{capacity} + 0.0477 \cdot q_w^{capacity} + 369.30 \cdot Nw^{field} + 21911.58 \quad (4.9)$$

$$E_{op,Tie-Back} = 5.50E-4 \cdot q_o^{capacity} + 0.1245 \cdot q_g^{capacity} + 1.82E-4 \cdot q_w^{capacity} + 14.26 \cdot Nw^{field} + 349.62 \quad (4.10)$$

DRILLEX (valid for all topside facilities):

$$E_{drill} = 253.45 \cdot Nw_{d,p+i} + 1.55E-11 \quad (4.11)$$

The standard error and R-squared for the costs linear regression is shown in Table 4.2.

Table 4.2. Linear regression statistics for costs equations

	Standard error	**R-squared**
$\mathbf{E_{cap,TLP}}$	255.96	0.993
$\mathbf{E_{op,TLP}}$	4.57	0.999
$\mathbf{E_{cap,FPSO}}$	279.65	0.991
$\mathbf{E_{op,FPSO}}$	6.30	0.998
$\mathbf{E_{cap,Tie\text{-}back}}$	446.37	0.990
$\mathbf{E_{op,Tie\text{-}back}}$	4.11	0.999
$\mathbf{E_{drill}}$	3.73e-12	1.000

The comparison between the costs data extracted from the cost estimation software and the results of cost obtained from the proxy models are presented in Figure 4.3 to Figure 4.9. For this figures the following nomenclature is used:

- Nw1 = 10 prod x 10 inj
- Nw2 = 15 prod x 15 inj
- Nw3 = 20 prod x 20 inj
- qo1 = 31449 stb/d
- qo2 = 94347 stb/d
- qo3 = 157245 stb/d
- qg1 = 53 MM scf/d
- qg2 = 88 MM scf/d
- qg3 = 124 MM scf/d

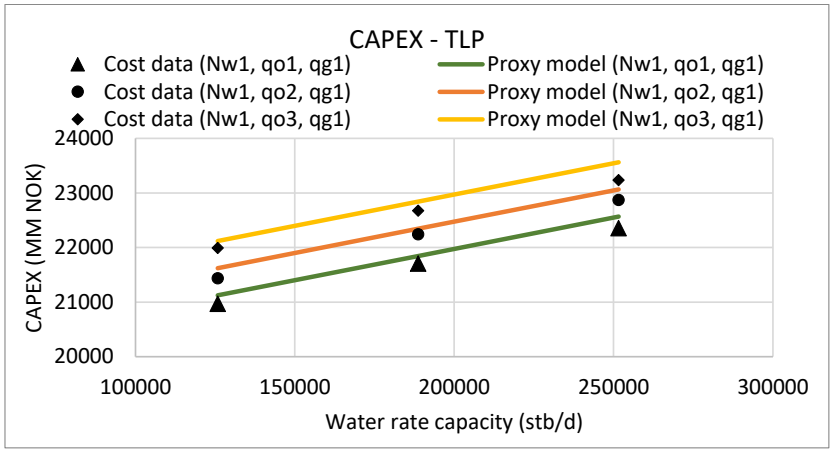

Figure 4.3. Comparison of CAPEX between cost data and cost proxy models for TLP concept

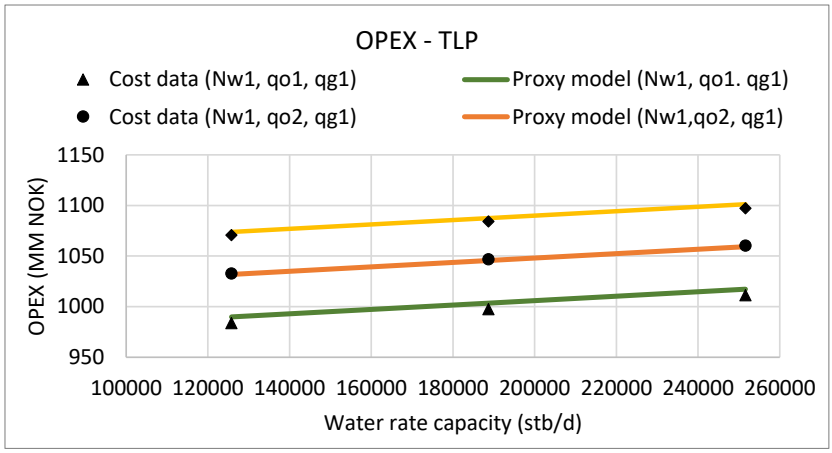

Figure 4.4. Comparison of OPEX between cost data and cost proxy models for TLP concept

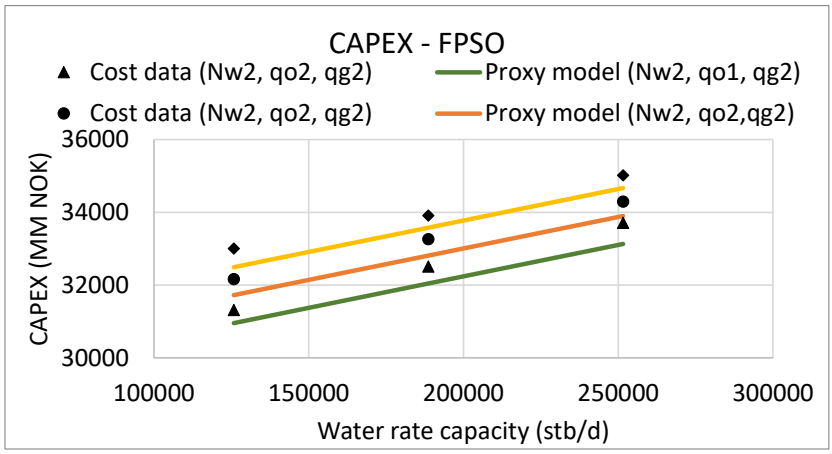

Figure 4.5. Comparison of CAPEX between cost data and cost proxy models for FPSO concept

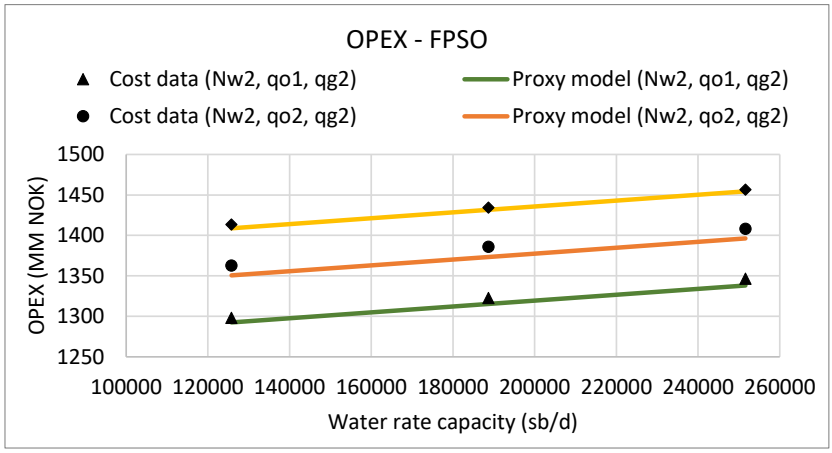

Figure 4.6. Comparison of OPEX between cost data and cost proxy models for FPSO concept

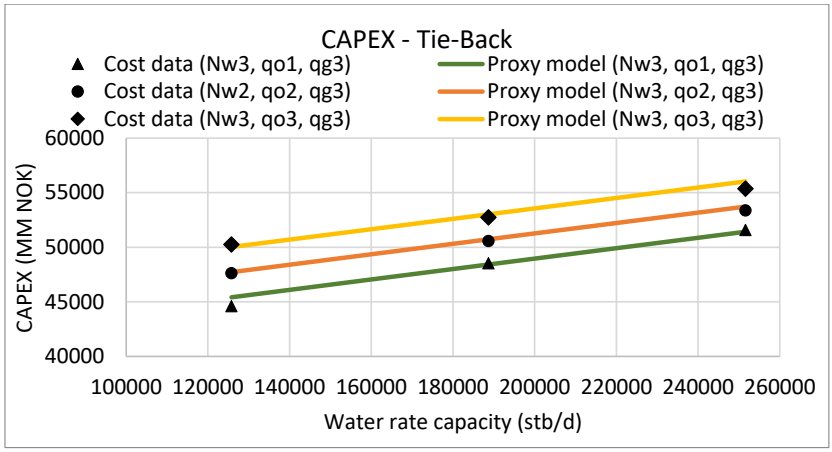

Figure 4.7. Comparison of CAPEX between cost data and cost proxy models for Tie-Back concept

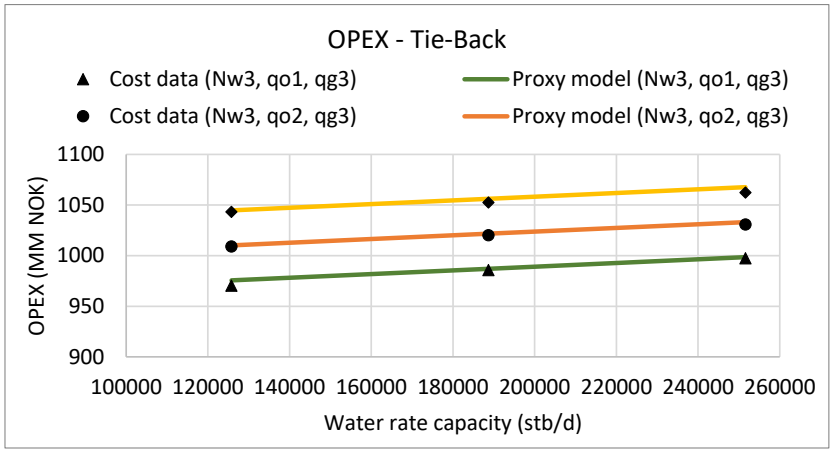

Figure 4.8. Comparison of OPEX between cost data and cost proxy models for Tie-Back concept

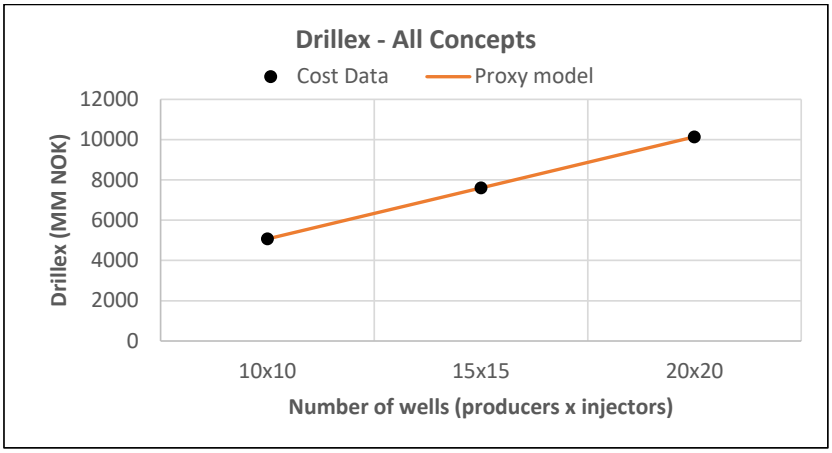

Figure 4.9. Comparison between DRILLEX cost data and cost proxy models for all concepts

The data used for the comparison shown in Figure 4.3 to Figure 4.9 is the same data used to generate the proxy models. Additional comparison was performed using different data to analyze the accuracy of the cost models. For this, the cost was estimated for four values of oil rate capacity (40 884, 50 318, 81 767 and 100 637 stb/d), three values of gas rate capacity (35, 88, 120 MMscf/d), a constant water rate capacity of 176000 stb/d and 20 production and 20 injection wells. The average relative error obtained between the proxy models and the data (combining the results from the three topside facilities) for the CAPEX was 13 %, for the OPEX was 60% and for DRILLEX was 0%. However, due to the fact that the contribution of OPEX to the NPV is small, the proxy models shown in equations (4.5) to (4.11) were still used.

When performing the calculation of NPV, the CAPEX is calculated as a single value and is distributed evenly during the first four years of the time horizon. The OPEX is a yearly average value, meaning that it has the same value for all the years of the field life. This OPEX spending profile was chosen because the cost data extracted from the cost estimation software was the yearly average and there was no information available regarding its variation in time.

In theory, CAPEX and OPEX are also affected by the drilling schedule. However, due to the fact that the commercial software outputs a lump-sum for CAPEX and OPEX without indicating its variation in time, this dependency was neglected. Therefore, CAPEX and OPEX were computed assuming that the maximum number of wells are available from year zero, which gives a slight overestimation of CAPEX and OPEX.

In the case of DRILLEX, this cost is estimated in each time step using the amount of wells (production and injection) drilled in a specific period.

4.3. NPV Estimation

In this work, the NPV is estimated through optimization. This indicator is the objective to maximize by changing the oil production profile and the drilling schedule of the field.

During the field development process, one of the main factors that is often used to compare field development alternatives is the Net Present Value (NPV). The NPV is the difference between the present value of cash inflow, represented by the revenues from hydrocarbon sales, and the present value of the cash outflow, represented by the costs, over a period. In this research, the net present value is estimated using Equation (4.12), which represents the NPV for an oil field where the main production is oil and the only expenditures are CAPEX, OPEX and DRILEX. This is the NPV equation used in this thesis.

$$NPV = \sum_{j=0}^{N} \frac{\left\{\Delta N_p^j \cdot P_o^j\right\} - \left\{E_{cap}^j + E_{op}^j + E_{drill}^j\right\}}{(1+DR)^j} \tag{4.12}$$

where,

j : Index of time period,
N : Total number of years,
DR : Discount rate (%),
ΔN_p^j : Cumulative oil produced in a period (stb),
P_o^j : Price of oil (NOK/stb),
E_{cap} : CAPEX (MM NOK),
E_{op} : OPEX (MM NOK),
E_{drill} : DRILLEX (MM NOK).

In an oil/gas production project, the NPV is at first negative due to the initial investment that needs to be done, before the start of production (CAPEX, DRILLEX). When production begins, the NPV increases and it becomes positive. A positive NPV means a profitable project. Figure 4.10 shows a typical NPV diagram for a generic oil/gas project.

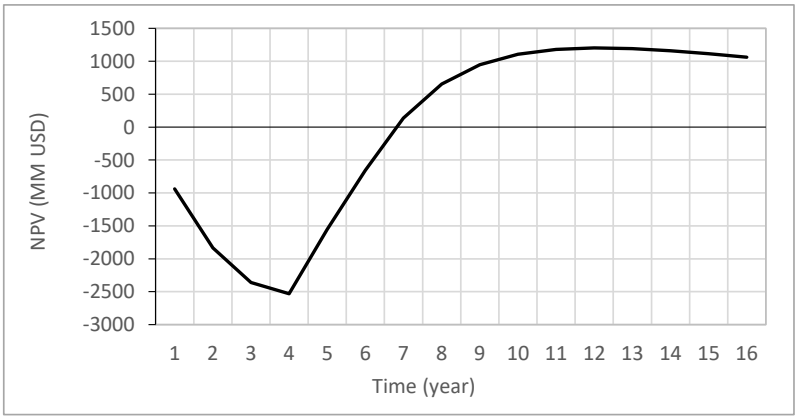

Figure 4.10**.** Typical NPV curve

Chapter 5

The NPV optimization problem for early field development planning

In the methodology developed, the NPV is estimated through optimization. This indicator is the objective to maximize by changing the oil production profile and the drilling schedule of the field. This chapter presents the optimization formulation used in this thesis, its application on a study case based on Wisting field and the validation of the optimization process using a brute-force optimization.

5.1. Background

Numerical optimization has been proposed extensively in previous works as a tool to find optimal field design features that maximize revenue and minimize cost. There are several studies available in the literature that use a variety of optimization techniques, types of models, model complexity, etc. to achieve this. A short review of some works relevant to this research is presented next.

- Jonsbråten [21] presented a mixed integer programming model for optimal development of an oil field under uncertainties in the oil price forecast. The model used a two-dimensional reservoir description and based on the reservoir size, the model simultaneously optimizes platform size, drilling program and production strategy.

- Nazarian [22] developed and applied an integrated field simulator, by coupling existing commercial reservoir and process simulators, to simulate the performance of an oil or gas field. The integrated field simulator was linked to an optimization routine, which enabled optimization at field level from reservoir to process. The simulator was tested with several case studies, covering topics like process optimization, optimum tie-in of satellite wells, optimal well location and field layout assessment. He demonstrated that using integrated simulation improves the capability to represent the performance of the field.

- Túpac et al. [23] developed and evaluated a system to improve oil field developments, where the position, type and geometry of wells were optimized to maximize NPV, considering some technical constraints like maximum well distance and trajectory.

- Litvak et al. [24] described the development and application of a new field development technology to optimize the location of new wells, drilling schedule, water and gas injection

strategies, production/injection rates and surface facilities, while handling associated risk and uncertainties in the reservoir description.

- Litvak & Angert [25] later extended the technology developed by Litvak et al. [24] for development of giant fields, with very large number of wells.

- Litvak, Onwunalu & Baxter [26] outlined the framework for simultaneous optimization of a broad range of field development decisions with subsurface uncertainties, providing capabilities for the evaluation of field development options with multiple reservoir descriptions.

- Storvold [27] developed an optimization model for decision support to increase hydrocarbon recovery and production lifetime of a field when different subsea solutions are evaluated. The model evaluates the installation of subsea boosting, subsea water separators and alternative routing solutions with the objective of maximize the net present value of the field.

- Alyan, Matin & Irwing [28] described the simulation study done in optimizing the field development plans for undeveloped tight carbonate reservoirs with limited production history and surveillance data. They also quantified the impact of reservoir geologic uncertainties on production. The optimization process allows identify potential opportunities to maximize production/recovery in the field through testing various orientations, spacing and placement of wells.

In this project, optimization is used to determine the optimum oil production and drilling schedules that give maximum NPV for a specific field concept. The optimization engine used is CPLEX, which uses a combination of branch-and-bound, cutting planes and simplex methods [29] [30]. Following, the optimization formulation is presented.

5.2. Optimization formulation

The objective function is to maximize the net present value of the production system

$$\max NPV \tag{5.1}$$

by changing the oil production rates, q_o^j, and the number of production wells drilled in a time step, $Nw_{drilled}^j$.

The optimization constraints are:
$\forall\, j \in \{1,2,..N\}$,

$$q_o^j \le q_{o,pot}^j \tag{5.2}$$

$$Nw_{drilled}^{min} \le Nw_{drilled}^j \le Nw_{drilled}^{max} \tag{5.3}$$

where $q_{o,pot}^j$ is the potential oil rate at time step j. $Nw_{drilled}^{min}$ and $Nw_{drilled}^{max}$ are, respectively, the minimum and maximum number of wells that can be drilled in a time step

The potential oil rate is represented by the proxy models introduced in chapter 2, and it is a non-linear function of the cumulative oil produced, Np^j, and the number of production wells in the field, Nw^j:

$$q_{o,pot} = q_{o,pot}\left(Np, Nw\right) \tag{5.4}$$

Piecewise linear approximation, using SOS2 models, is used to determine the potential oil rate in each time step.

Two additional operational constraints are: a maximum oil rate to prevent erosion in the elements of the production system $q_{o,erosion}^{max}$ and the capacity of water injection rate, $q_{w,inj}^{max}$ (valid for concepts with water injection):

$$q_o^j \leq q_{o,erosion}^{max} \tag{5.5}$$

$$q_{w,inj}^j \leq q_{w,inj}^{max} \tag{5.6}$$

In this methodology, the water injection is expressed as a function of the cumulative water injection, Wp_{inj}^j, obtained from the material balance model:

$$q_{w,inj} = q_{w,inj}\left(Wp_{inj}\right) \tag{5.7}$$

As mentioned in chapter 4, the costs depend on the production capacity of the processing facilities, $q_o^{capacity}$, $q_g^{capacity}$ and $q_w^{capacity}$, and the number of wells in the field:

$$E_{cap} = E_{cap}\left(q_o^{capacity}, q_g^{capacity}, q_w^{capacity}, Nw^{field}\right) \tag{5.8}$$

$$E_{op} = E_{op}\left(q_o^{capacity}, q_g^{capacity}, q_w^{capacity}, Nw^{field}\right) \tag{5.9}$$

$$E_{drill} = E_{drill}\left(Nw_{d,p+i}^j\right) \tag{5.10}$$

The OPEX (E_{op}) is expressed as an average value and remains equal in each time step. The variable Nw^{field} is the total number of production and injection wells in the field. For the case with water injection, the number of production and injection wells is assumed the same, then $Nw_{d,p+i}^j = 2 \cdot Nw_{drilled}^j$.

The oil, gas and water capacities of the processing facilities and the total number of wells are obtained as follow:

$$q_o^{capacity} \geq q_o^j \tag{5.11}$$

$$q_g^{capacity} \geq q_g^j \tag{5.12}$$

$$q_w^{capacity} \geq q_w^j \tag{5.13}$$

$$Nw^{field} \geq Nw^j \tag{5.14}$$

where $q_g^{\ j}$ and $q_w^{\ j}$ are the produced gas and water rate of the field at time step j, respectively. The gas rate is a non-linear function of the oil rate and the GOR and the water rate is a non-.linear function of the oil rate and the WC. The GOR and WC are obtained from the proxy models in chapter 3.

$$q_g = q_o \cdot GOR(Np, Nw) \tag{5.15}$$

$$q_w = \frac{q_o \cdot WC(Np, Nw)}{1 - WC(Np, Nw)} \tag{5.16}$$

To illustrate the optimization process, a simple example have been created in Excel. Let us assume we want to find the production profile and drilling schedule that give maximum profit of an oil field, with no water production, after five years of operation. To calculate the profit of the field, the NPV equation shown in chapter 4 is used.

Figure 5.1 shows the Excel spreadsheet created for this example. Here the NPV for each year is calculated in column L. The costs (columns I, J and K) are calculated using proxy models of the type shown in chapter 4. The revenues are calculated using the yearly oil production (column G) and oil price (column H).

	A	B	C	D	E	F	G	H	I	J	K	L
1	Time	qo-pp	qg_ppp	Nw-year	qo	qg	ΔNp	Oil Price	CAPEX	DRILLEX	OPEX	NPV
2	[year]	[stb/d]	[MMscf/d]	[-]	[stb/d]	[MMscf/d]	[stb]	[NOK/STB]	[1E6 NOK]	[1E6 NOK]	[1E6 NOK]	[1E6 NOK]
3												
4	0.0	47624	12	4	47624	12	0	645	31538	2027.7		-33565
5	1.0	134100	34	8	134100	34	3.2E+07	628		4055.5	1295	-18111
6	2.0	163829	41	12	163829	41	5.3E+07	611		1520.8	1295	12276
7	3.0	127364	32	15	127364	32	5.2E+07	594		0.0	1295	42545
8	4.0	61804	15	15	61804	15	3.4E+07	576		0.0	1295	61179
9	5.0	33184	8	15	33184	8	1.7E+07	559		0.0	1295	**69602**

Figure 5.1. Excel spreadsheet representing calculation of NPV during five years of production

The calculation of NPV for year zero and year one is as follows. The discount rate is input to cell M1 (not shown in Figure 5.1).

Year zero:
$$L4 = \frac{(G4 \cdot H4) - (I4 + J4 + K4)}{(1 - M1)^{A4}} \tag{5.17}$$

Year one:
$$L5 = L4 + \frac{(G5 \cdot H5) - (I5 + J5 + K5)}{(1 - M1)^{A5}} \tag{5.18}$$

To calculate the cost, the oil and gas rate capacities are the maximum values from columns E and F. Since there is not water production, the water rate capacity is zero. The number of wells are obtained from column D. Some assumptions made to calculate the costs are:

- All the CAPEX take place in year zero.
- The first group of wells are drilled in year zero, meaning that DRILLEX starts to count also from year zero.
- OPEX take place once the field start production. It starts to count from year one.

For the revenues, the trapezoidal rule is used to calculate the yearly oil production (cumulative production during a year) using the oil rate (column E) and the time step (column A). An

example of the oil production calculation for year one is shown in equation (5.19). Some simplifications made for this calculations are:

- ΔN_p represents all the oil that have been produced in a year. In Figure 5.1, cell G5 represent the oil produced from the beginning of year zero to the beginning of year 1.
- For year zero the cumulative oil produce is zero, since there was not production before that year.
- For the revenue, it is assume that the oil price remains constant in each time step, and the change takes place at the beginning of each year.

$$G5 = \frac{E5 + E4}{2} \cdot (A5 - A4) \cdot 355 \tag{5.19}$$

To find the maximum NPV after five years of production, the Excel's Solver is used. Here, the NPV at year five (cell L9) is the objective to maximize. The variables are the oil rate of each year (cells E4:E9) and the number of wells drilled in each year (cells D4:D9). The constraints considered are:

- Oil production rate cannot be higher than the oil production potential. This is: E4:E9 ≤ B4:B9.
- The number of wells drilled in each year is constrained by: 0 ≤ D4:D9 ≤ 4.
- For this example, no constraint of maximum oil rate to avoid erosion in the pipeline was considered.

The solver configuration for this example is shown in Figure 5.2.

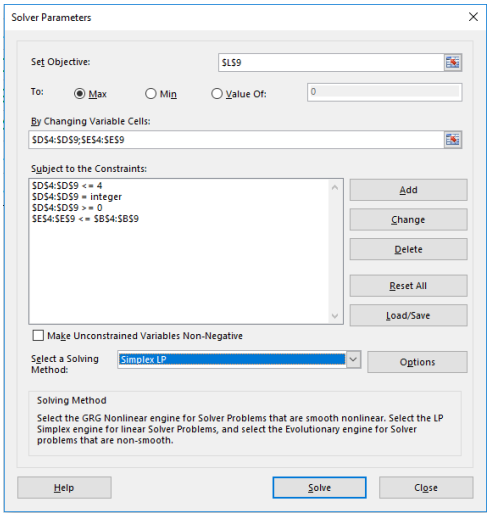

Figure 5.2. Solver setup to find maximum NPV

From Figure 5.2, it can be observed that the solving method selected is Simplex LP. This method requires that the objective function and the constraints are linear smooth functions of the optimization variables. Discontinuous function like MAX() or IF() cannot be used on equations that depend on the decision variables, since the Simple LP method cannot handler this kind of functions.

Additional calculations needed to solve this Excel example are:

- The oil production potential of oil and gas are obtained from proxy models, where these variables are expressed as function of the cumulative oil produced and the number of wells on the field. To determine these values, a table of the proxy models is stored in another spreadsheet in Excel. A two dimensional linear interpolation is used where, for each Np (calculated with the oil rate estimated in the optimization) and Nw, the oil and gas production potential is determined.
- The gas rate is assumed equal to the gas production potential and is used in the estimation of CAPEX and OPEX.

5.2.1. Linear reformulation

The optimization was reformulated as a Mixed Integer Linear Problem (MILP). The approach used here to solve the MILP formulation is a combination of the simplex algorithm and Branch and Cut method [31] (which is a combination of branch-and-bound and cutting planes). A more detailed explanation of branch and cut algorithm can be found in references [32] [33].

To reformulate the optimization, special ordered set models of type 2 (SOS2) [34] [35] [38] were used to linearly approach the non-linear functions in equations (5.4), (5.15) and (5.16). SOS2 is a set of consecutive non-negative variables, which sum must be equal to one and, at most, two adjacent members can be non-zero in a feasible solution.

SOS2 approximation in one dimension

Consider g is a continuous function, which values, for a set of breakpoints $\{x_i, i = 1,\ldots,N\}$, are known. The SOS2 approximation of g, $\tilde{g}$, and the independent variable can be written as follows:

$$\tilde{g}(x) = \sum_{i=1}^{N} \lambda_i \tilde{g}(x_i) \tag{5.20}$$

$$x = \sum_{i=1}^{N} \lambda_i x_i \tag{5.21}$$

where $(\lambda_i)_{1 \le i \le N}$ is a set of positive weighting factors.

The SOS2 condition applied on the weighting factors can be expressed as follows:

$$\sum_{i=1}^{N} \lambda_i = 1 \tag{5.22}$$

For a wider discussion of this topic, see [35].

SOS2 approximation in two dimensions

For this case consider g a function of x and y The SOS2 approximation of g, $\tilde{g}$, is expressed as follows:

$$\tilde{g}(x,y) = \sum_{i=1}^{N}\sum_{j=1}^{M}\Omega_{ij} g(x_i, y_j) \tag{5.23}$$

and the independent variables are:

$$x = \sum_{i=1}^{N}\sum_{j=1}^{M}\Omega_{ij} x_i \tag{5.24}$$

$$y = \sum_{i=1}^{N}\sum_{j=1}^{M}\Omega_{ij} y_i \tag{5.25}$$

where Ω_{ij} is a set of positive weighting factors, with the following conditions:

$$\sum_{i=1}^{N}\sum_{j=1}^{M}\Omega_{ij} = 1 \tag{5.26}$$

We then define the sets α_i and β_j by:

$$\forall i, \quad \alpha_i = \sum_{j=1}^{M}\Omega_{ij} \tag{5.27}$$

$$\forall j, \quad \beta_j = \sum_{i=1}^{N}\Omega_{ij} \tag{5.28}$$

The SOS2 formulation imposes that $(\alpha_i)_{1\le i\le N}$ and $(\beta_j)_{1\le j\le M}$ to be SOS2. Further discussion about this topic can be found in [35].

The details of the MILP formulation are presented in the Appendix E.

The tool used to perform the optimization calculations was AMPL. This is an algebraic modeling language to describe and solve problems for mathematical computing (optimization problems). In AMPL, the formulation of the optimization is done using declarative language elements like sets, parameter, decision variables, constraints and objectives. The structure of a problem in AMPL can be divided in a group of text files, each one containing different information. In this thesis, the file structure in AMPL consist of the following files:

- *Field-Opt.run:* this file calls the optimization solver, the other files used for the optimization, declares the solver options and triggers the optimization run.
- *Declaration.mod:* all the variables used in the optimization are declared here. This includes, decision variables, parameter, constraints and objective variables.
- *Data.dat:* here, the values of the parameters are introduced. The parameter are all the elements with constant values.

- *Optimization.mod:* in this file all the optimization formulation is declared.
- *Read_table.run:* if some parameter are stored in tables (for example, the proxy models of the production performance of the production system), this files is used for AMPL to read the information inside the table files.
- *Table_files.tab:* all the data presented in table format must be stored in a file with .tab extension.
- *Preprocessing.run:* here the sets are declared.
- *SOS2.run:* necessary to use SOS2 methods.
- *Output.run:* used to extract the desired results from the optimization run.
- *Output.out:* the results are stored in this file.

The optimization formulation was validated by comparing the results obtained for a synthetic field based on Wisting and a brute-force optimization perform in AMPL. This is presented in the following sections.

5.2.2. Application of the optimization formulation to a Wisting field case

The optimization formulation was tested on a synthetic field based on Wisting. For this case, a proxy model of the field production performance was created by coupling a reservoir in MBAL and a production system model in Pipesim. For the reservoir model, the properties shown in Appendix A were used and water injection with 100% of voidage replacement was assumed. The production system model was created using the properties presented in Appendix B and adding gas lift in each well. For the costs estimation, a TLP platform was used as topside facility, meaning that the costs were calculated with equations (4.5), (4.6) and (4.11).

For this case, the production profile and drilling schedule that give maximum profit were estimated using optimization. For this, some assumptions were considered:

- Field concepts: Gas Lift, Water Injection, TLP.
- Constant oil price: 500 NOK/stb (62.5 USD/stb).
- Discount rate = 8%.
- All wells start production from the beginning of the year they are drilled.
- A table of cumulative water injected vs. cumulative oil production was used to calculate the water injection rate. The table is shown in Appendix G.
- The time steps have a duration of one year
- The following constraint were applied:
    - The maximum number of production wells that can be drilled in a time step are four wells.
    - The maximum number of production wells in the field are 15 wells.
    - The maximum oil rate allowed to avoid erosion in the production system is 13000 stb/d.
- During the optimization, only the optimal drilling schedule of the production wells is computed. Therefore, to estimate the costs, it is assumed that the field has the same amount of production and injection wells.

The simulation was run in a workstation with an Intel® Xeon® W-2145 processor and 64 GB of memory. The running time of an optimization routing ranged between 9 seconds and 8 hour.

The results of the optimization are shown below: The optimum production profile is presented in Figure 5.3.The drilling schedule is shown in Table 5.1.

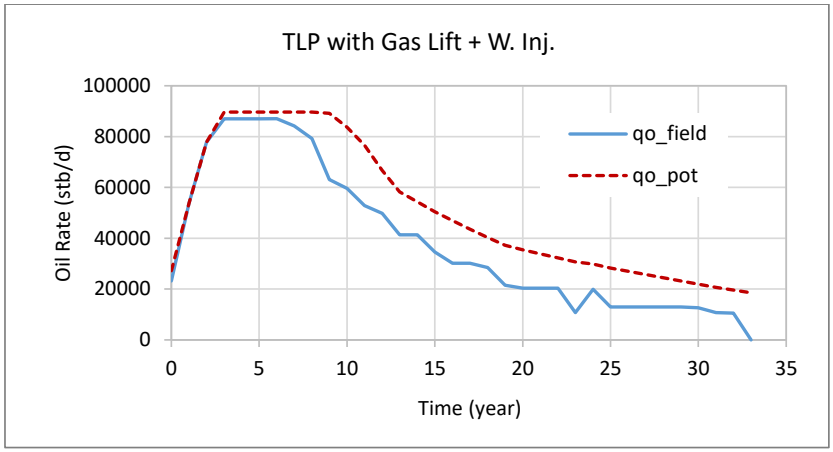

Figure 5.3. Optimum oil production profile and oil production potential for strategy TLP with GL + WI

Table 5.1. Optimum drilling schedule example case

Year	Nw drilled per year	Total Nw in field per year
1	4	4
2	4	8
3	4	12
4	3	15
5	0	15
…	0	15
33	0	15

From Figure 5.3, it can be observe that the optimal oil production rate is lower than the production potential rate of the field. This happens because, even though, for this case, the field has the capacity to produce at higher rates, a greater oil production would infringe one or more constraints in the optimization formulation.

The drilling schedule will be mostly influenced by the cost of drilling each well and the capacity of the strategy to produce revenues that overcome that cost. For this study case, the optimum schedule is to drill the maximum number of wells allowed in each time step until the total number of wells that can be drilled in the field is reached.

Figure 5.4 shows the profit obtained for the field configuration tested in this section. The figure shows the discounted cash flow (NPV of each year) and NPV (cumulative of yearly NPV). For this case, a maximum NPV of 72.46 billion NOK, obtained at the end of the life field (year 33), resulted from the combination of optimum production potential (Figure 5.3) and drilling schedule (Table 5.1).

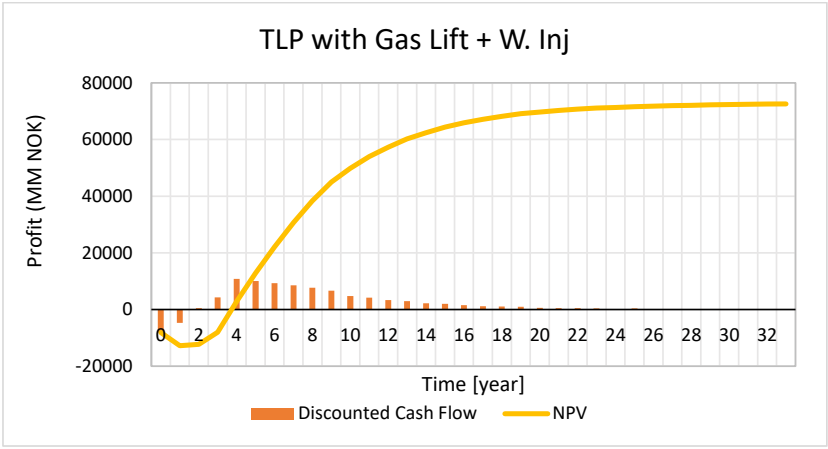

Figure 5.4. Profit obtained from optimization

5.2.3. Validation of optimization

In this section, the optimization formulation is validated against brute-force combinatorics. This brute-force combinatorics consisted of a sensitivity analysis, where the NPV is manually calculated for different oil production plateau rates in the production profile and fixing the number of wells from the beginning of production. The objective is to find the combination of production profile and number of wells that results in maximum NPV.

For the brute force optimization, AMPL was used to calculate the optimal production profile obtained with a specific plateau rate and fix number of wells that maximize the NPV of the field. This was performed for the same synthetic field used in the previous section and the same constraints and assumptions were applied. The number of wells used was 15, this is the maximum number of wells obtained in the optimization case shown in the previous section, and the values of plateau rate were:

Table 5.2. Plateau rates and number of wells used in brute-force optimization

Plateau rate (stb/d)
70 000
75 000
80 000
85 000
90 000
95 000

The optimal oil production profiles obtained for the six plateau rates used, compared against the production profile obtained using the optimization formulation (labeled as original), are presented in Figure 5.5 to Figure 5.10.

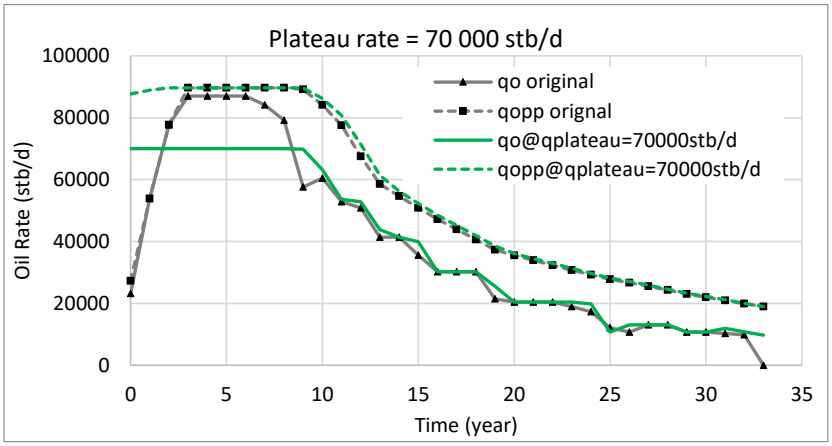

Figure 5.5. Comparison of production profile obtained with optimization formulation and brute-force optimization (Plateau rate 70 000 stb/d)

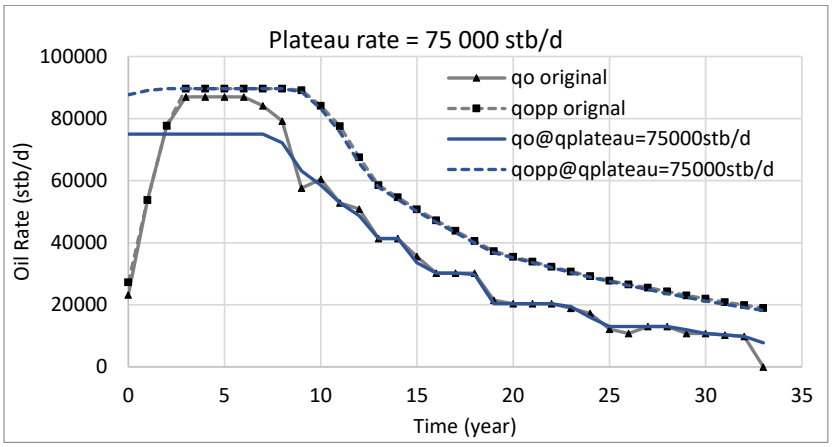

Figure 5.6. Comparison of production profile obtained with optimization formulation and brute-force optimization (Plateau rate 75 000 stb/d)

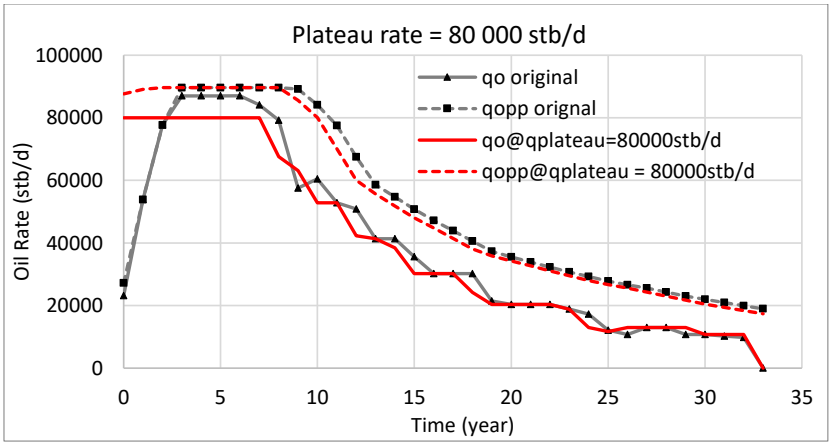

Figure 5.7. Comparison of production profile obtained with optimization formulation and brute-force optimization (Plateau rate 80 000 stb/d)

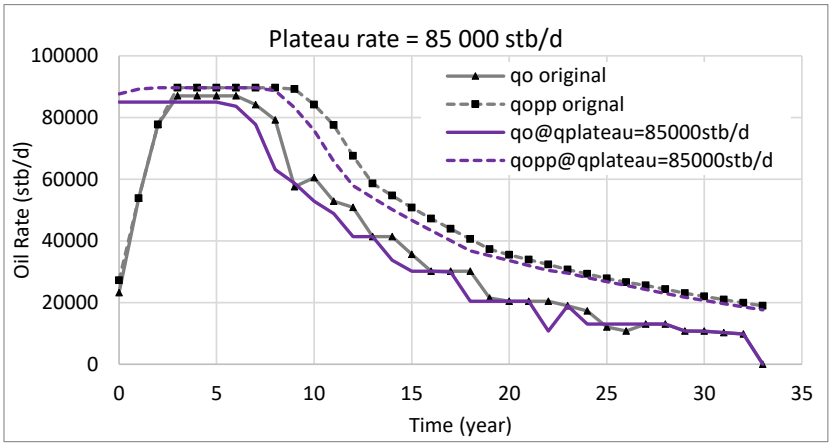

Figure 5.8. Comparison of production profile obtained with optimization formulation and brute-force optimization (Plateau rate 85 000 stb/d)

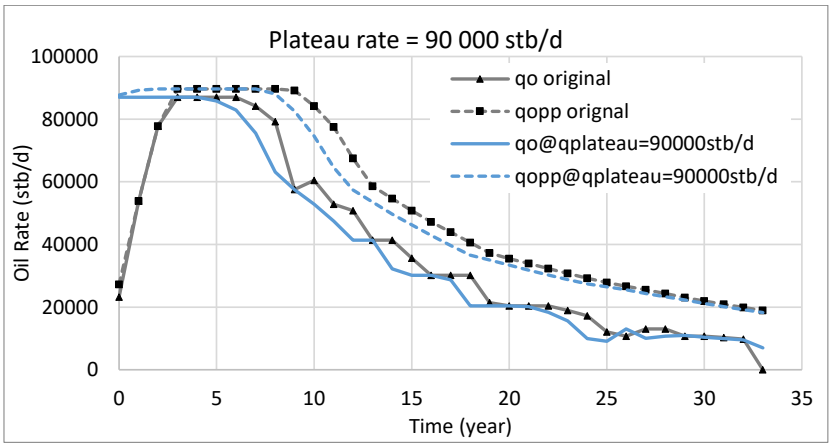

Figure 5.9. Comparison of production profile obtained with optimization formulation and brute-force optimization (Plateau rate 90 000 stb/d)

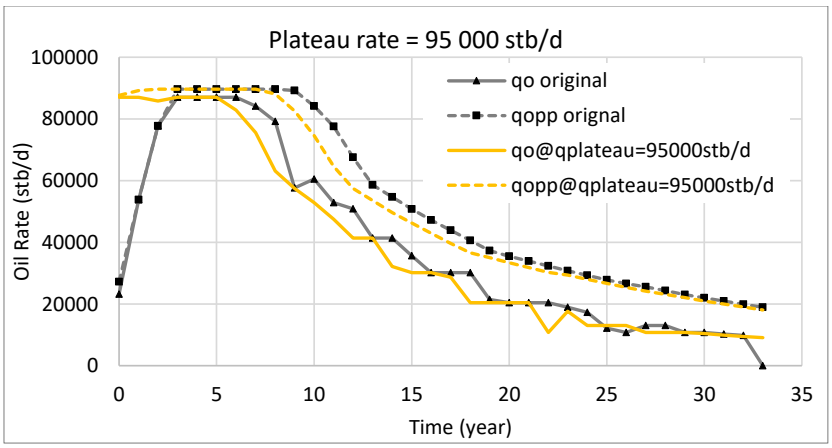

Figure 5.10. Comparison of production profile obtained with optimization formulation and brute-force optimization (Plateau rate 95 000 stb/d)

Figure 5.5 to Figure 5.10 show that, the production profile for all the plateau rates tested are similar to the original production profile in the decline phase. Moreover, for the profiles with plateau rate of 90 000 stb/d and 95 000 stb/d, the maximum oil rate obtained is the same as the one obtained for the original case, 86 996 stb/d. This means that the field cannot produce above that oil rate without ignoring some constraint. This shows that the production profile obtained with the optimization formulation presented in this chapter is optimal.

The maximum NPV obtained in the brute-force optimization is presented in Table 5.3.

Table 5.3. Maximum NPV obtained for validation of optimization formulation

Production profile	**NPV (billion NOK)**
original	72.46
qplateau = 70 000 stb/d	74.21
qplateau = 75 000 stb/d	77.43
qplateau = 80 000 stb/d	80.37
qplateau = 85 000 stb/d	82.73
qplateau = 90 000 stb/d	83.45
qplateau = 95 000 stb/d	83.42

The maximum NPV is obtained with a plateau rate of 90000 stb/d. However, as mentioned above the maximum feasible oil rate is 86 996 stb/d. To verify if this rate is really optimal, the optimization was repeated again using it as plateau rate. This gave as result a NPV of 83.64 billion NOK, which demonstrates that the maximum NPV is found with a production profile with plateau rate between 85 000 stb/d and 90 000 stb/d. The production profile obtained with this plateau rate is shown in Figure 5.11.

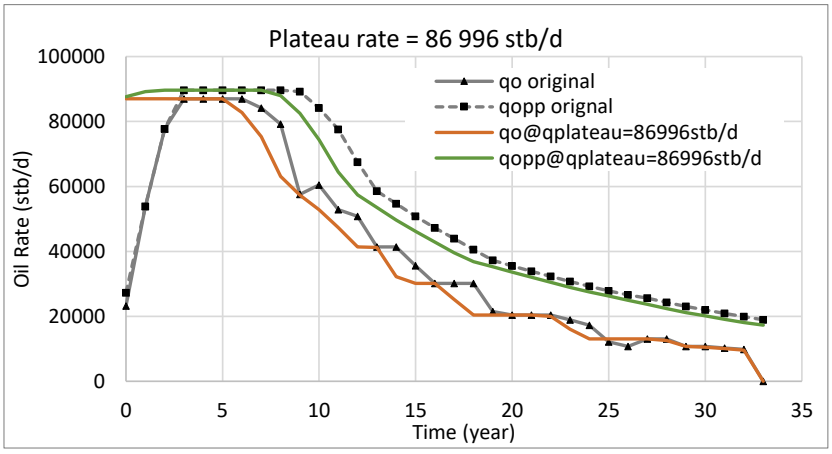

Figure 5.11. Production profile obtained with optimal plateau rate

The difference between the original NPV (obtained with the optimization formulation) and the maximum NPV obtained with the brute-force optimization is consequence of using a fixed number of wells in the second method. In the original optimization, a constraint on the maximum number of well that can be drilled in a time step was imposed. This generates a production profile with a built-up phase that is not seen in the brute-force optimization. As

consequence, both methods generate different revenues and, subsequently, different NPV values. Because of this, the calculations using the original optimization formulation were repeated, but in this case, the constraint on the maximum number of wells that can be drilled in a time step were dropped. The idea is to allow the program to find the optimal number of wells that must be drilled in each time step without restrictions. The results obtained are shown below.

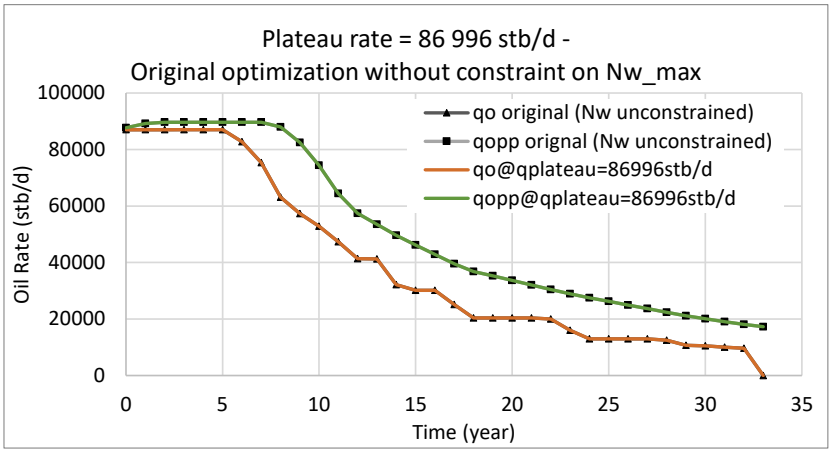

Figure 5.12. Comparison of optimal production profile obtained with the optimization formulation (without restriction on the maximum number of wells that can be drilled in a year) and the brute force optimization with plateau rate of 86 996 stb/d

When the original optimization formulation is used with no restriction on the maximum number of wells that can be drilled in a time step, the optimal drilling schedule consists of bringing all wells to stream from the start of production. In this case, the optimal production profile is the same as the one obtained for the case with plateau rate of 86 996 stb/d. The maximum NPV resulted was 82.65 billion NOK, which represents a relative error of 1.19% in comparison with the maximum NPV obtained with the brute-force optimization.

The results obtained with brute-force optimization, match with the ones obtained using the optimization formulation. In conclusion, it is valid to say that the optimization has been successfully verified and it can be used to determine optimal configurations of production systems in early field development.

Chapter 6

Uncertainty analysis specifications for early field development planning

This chapter presents the method used to perform uncertainty analysis to determine the potential outcome of NPV, with its associate probability, to support the decision process. The uncertainty variables considered, the type of uncertainty analysis used and a simple example of how the uncertainty analysis is implemented in this thesis are described below

6.1. Background

During early field development planning, there is a high level of uncertainty regarding the subsurface (e.g. initial volumes in place, fluid properties, formation deliverability, reservoir structure, etc.), cost figures (e.g. cost of equipment, subsea system, offshore structure) price of hydrocarbons, among others. Most of these uncertainties propagate into the calculation of production profiles (which, in this stage, almost never matches the profiles that the field actually produces) and forecasts expected from the field and further into estimations of revenue streams. Ultimately, uncertainties end up affecting the estimation of project economic indicators such as NPV and IRR over which decisions are made.

Therefore, it is of utmost importance to quantify the uncertainties of the most important elements considered in the value chain model and quantify the effect these uncertainties have on the final economic indicators that are taking into account in the decision process. The goal is to estimate a range of potential outcomes with their associated probability that allow field planners to take better decisions.

In this research, the uncertainties considered are:

1. Initial hydrocarbon volume in place.
2. Well productivity.
3. Costs figures (CAPEX, OPEX, DRILLEX).
4. Uncertainty in the layout of the subsea production system.

Variables 1 to 3 are, in principle, continuous in nature. Their range of variation and associated probability can be described with probability distribution functions. In this study, variable 4 was considered discrete, with three alternatives that are commonly employed when developing subsea fields.

The optimization formulation described in Chapter 5, finds optimal production profiles and drilling schedules that maximize the NPV of the project. The results of the optimization depend on the input described above. Initial volumes in place, well productivity and the layout of the production system affect the production potential curves of the system. Cost figures affect the estimation of the cash flow in each year.

During early phases, there is not much information about the system to make a very detailed design. A detailed design is required to be able to reduce the uncertainty in cost estimation. Therefore, cost figures usually have uncertainty associated with them that is reduced along the field development process. Typically, a normal distribution is used for cost with a standard deviation of 40% and is reduced to 20% during the field development process [36].

Often, in field development processes, due to lack of time and lack of integration and transfer of information between disciplines and departments involved, uncertainty is quantified with methods such as sensitivity analyses and spider plots that vary one variable at a time and evaluate the effect on the economic indicator. These methods does not capture effectively all potential variations that the economic indicators might exhibit. The method employed in this study to quantify the effect of the uncertainty on the optimization results and on the resulting NPV of the project is probability trees. The optimization will be executed several times with varying input, which is estimated by making an element-wise combination of alternatives in the probability tree. This method was favored over other methods due to its ease of implementation and low computational time required if low enough number of cases in the tree is used. For some specific cases, the optimization takes considerable time (on the range of hours) thus is unsuitable for other probabilistic methods based on sampling such as Monte Carlo or Latin Hypercube.

Angga [2] showed that Latin-Hypercube sampling and probability trees give similar solutions, which supports the decision to use probability trees in the present study.

Hydrocarbon prices are a big source of uncertainty when estimating the economic indicators of the field development project and development alternatives. When evaluating the effect oil or gas prices have on the project economics, the industry often executes sensitivity analyses varying the price within a range, but keeping it constant during the lifetime of the field.

The accurate and realistic prediction of future oil and gas prices is challenging and an area with active research where a variety of methods have been proposed. Al-Harthy [37] gives an overview of a few methods that can be used, namely Geometric Brownian Motion (GBM), mean reversion (MR) and mean reversion with jumps and assesses the validity of each method. These methods generate stochastic profiles of hydrocarbon prices with time that depend on a few input values and assumptions and that cover all possible price scenarios that could be expected in the future.

In the present study, the oil price used to compute the revenue stream has been considered constant with time. This assumption has been adopted because the uncertainty analysis method chosen, probability trees, is deemed to be incompatible with the use of more advanced methods such as the ones described above. If stochastic oil price models were to be employed, then it would be necessary to use stochastic methods to quantify uncertainty, such as Monte Carlo or Latin Hypercube. This will require computational running time that is deemed excessive and unsuitable for early stages of field development.

The following section presents the specifications of the uncertainty analysis used in this thesis. This is how the uncertainty variables were varied. At the end of this chapter, the uncertainty analysis is applied to a synthetic field case based on Wisting field.

6.2. Uncertainty analysis specifications

Uncertainty analysis is used in this thesis to study the probable range of NPV values that can be obtained as product of the variation of the following parameters:

1. Initial hydrocarbon volume in place.
2. Well productivity.
3. Costs figures (CAPEX, OPEX, DRILLEX).
4. Uncertainty in the layout of the subsea production system.

The uncertainty in the initial hydrocarbon volume in place (reservoir size) influences the results from the reservoir model. To account for different reservoir sizes, different reservoir models are needed. The well productivity and the uncertainty in the layout of the subsea production system influence the production system model. Subsequently, all three uncertainties are reflected on the proxy models of the production potential.

In Pipesim, the well productivity is an input variable of the well completion. In this thesis, horizontal completions are used in all the wells and the productivity index is determined using Joshi's model for steady-state horizontal well productivity [11]. Pipesim requires a number of inputs to estimate the productivity index when using Joshi model, among which are the horizontal and vertical permeability of the reservoir. The assumption made to generate the uncertainty in the productivity index was to vary simultaneously both permeability.

The uncertainty on the costs consists of varying simultaneously the CAPEX, OPEX and DRILLEX that resulted from the equations presented in section 4.2.1.

As mentioned before, probability tree was the method used to quantify the effect of uncertainty. For the uncertainty on the reservoir size, three initial hydrocarbon volume were used, representing P10, P50 and P90 percentiles. For the well productivity, three values of horizontal and vertical permeability were used in a range of ± 20 %. The costs were also varied in a range of ± 20 %, with a total of three costs values used. For the layout of the production system, Pipesim models were built for three different layouts. For variables 2-4, due to lack of information about their probability, it was considered that all the values used had the same probability.

The uncertainty variables that affect the production performance of the field (reservoir size, production system layout and well productivity) were varied individually to generate different production proxy models. In total, seven proxy models were created. The decision tree for these uncertainties is shown in Figure 6.1.

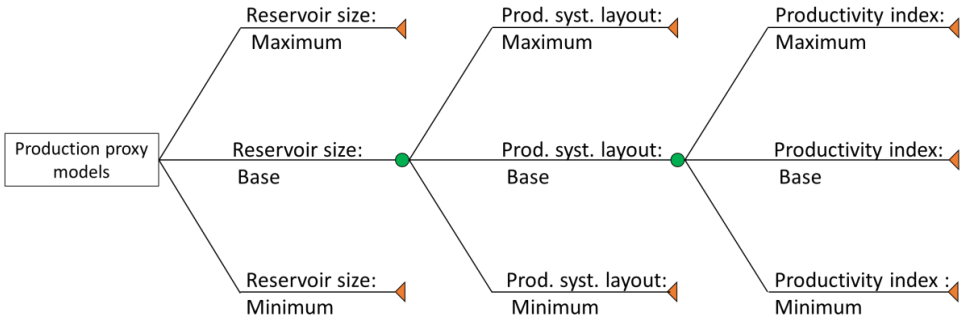

Figure 6.1. Decision tree for the uncertainty variables that affect the production performance of the field

The three costs values were combined with the seven proxy models generating a decision tree with 21 uncertainty cases. The uncertainty analysis consisted of applying the optimization process to each one this cases.

An example of applying the uncertainty analysis described to the same case used in the previous chapter is presented in the next section.

6.3. Application of uncertainty analysis

Uncertainty analysis was perform for the case presented in the previous chapter. This case consists of a synthetic field based on Wisting, which uses gas lift and water injection to support the production of the field and a TLP as a processing facility. The same optimization formulation and assumptions were applied. This is, to find the optimal oil production profile and drilling schedule that maximize the NPV of the fields. The assumptions considered for the optimization are repeated below:

- Field concepts: Gas Lift, Water Injection, TLP.
- Constant oil price: 500 NOK/stb (62.5 USD/stb).
- Discount rate = 8%.
- All wells start production from the beginning of the year they are drilled.
- A table of cumulative water injected vs. cumulative oil production was used to calculate the water injection rate. The table is shown in Appendix G.
- The time steps have a duration of one year
- The following constraint were applied:
    - The maximum number of production wells that can be drilled in a time step are four wells.
    - The maximum number of production wells in the field is 15 wells
    - The maximum oil rate allowed to avoid erosion in the production system is 13000 stb/d.
- During the optimization, only the optimal drilling schedule of the production wells is computed. Therefore, to estimate the costs, it is assumed that the field has the same amount of production and injection wells.

The reservoir size values used were: 818 MM stb (minimum), 1025 MM stb (base) and 1264 MM stb (maximum). This are the values shown in

Table 2.1 (chapter 2). The uncertainty on the production system layout consisted of: layout with clustered wells (base), layout with satellite wells and asymmetric layout with clustered wells. For this variable, there is not minimum and maximum case assigned since the variation is not numerical. For the productivity index, the values of horizontal and vertical permeability used in the original case (the one used in chapter 5) were varied ±20 %. Finally, the costs obtained from equations (4.5) to (4.11) were also changed in ±20 %.

The cumulative distribution function resulting from the uncertainty analysis is shown in Figure 6.2. From this analysis, it was obtained that the NPV can have values between 56.6 and 93.2 billion NOK.

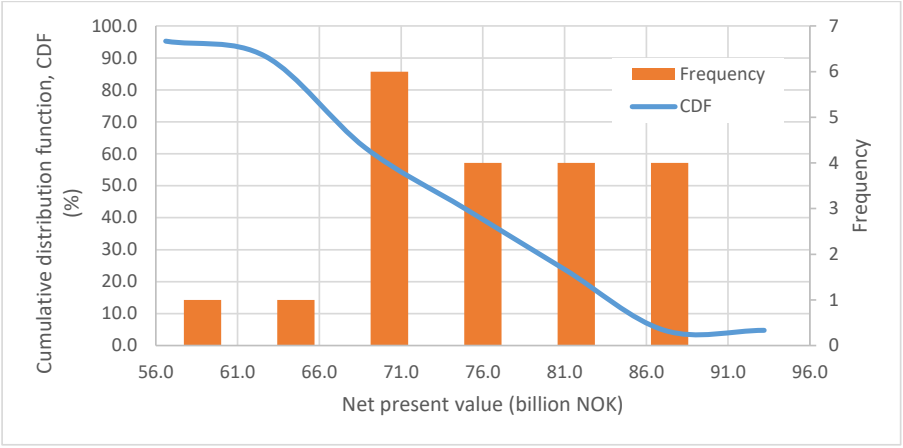

Figure 6.2. NPV probability

Chapter 7

Applying the decision-support methodology on the Wisting field case

The procedures described in previous chapters, namely:

- The method to create a proxy model to predict the production performance of the system based on the production potential concept using a series of pre-computed tables.
- The NPV optimization methodology to find optimal production and drilling schedules that maximize NPV.
- Uncertainty evaluation and quantification on the optimization results using probability trees.

Will be used together to define an integrated method to provide decision support to field planners during early phases of field development.
The method is applied to a synthetic case based on publicly available data about the Wisting field. The ultimate goal is to demonstrate the potential of the method and provide observations about performance, applicability and usefulness.

Wisting is an existing prospect that, at the moment of developing this thesis, was under development stage. Relevant information to model the field, like reservoir model, was not available. Therefore, aside from information available on public web domains, the models have been built based on assumptions or simplifications. For example: material balance was used to model the reservoir, the PVT properties of the fluid were calculated using simple black-oil model and all wells were considered identical in the network model. The methodology was used to compare different field development strategies and determine the best strategy to exploit the synthetic field

7.1. Evaluation of the method on Wisting field case

The work developed in this thesis is focused on the conceptual identification and selection stages of FDP. The methodology makes use of optimization of the yearly oil production rate (production profile) and the drilling schedule to maximize the NPV. Assessment of uncertainties is also used to support the decision process.

To reduce complexity and simulation time, proxy models of the production system are created, (production potential curves) from the coupling of standalone sub-surface and surface

simulators. Furthermore, additional proxy models are used for the costs estimation of the project.
To evaluate the methodology a series of steps were followed:

7.1.1. Step 1: Identification and selection of feasible field development strategies

This is the first step that takes place in field development. It is the conceptual screening of the project. Here, the technical concepts to exploit the field are manually identified. Then, field development strategies are created from the combination of all the selected technical concepts.

For the study case, three (3) recovery support methods and three (3) topside facilities were combined to form nine (9) field development strategies.

The recovery scenarios used are:

- Gas lifted wells (GL)
- Gas lifted wells + water injection (GL+WI).
- Multiphase boosting + water injection (MPB + WI).

The topside facilities considered are:

- Tension leg platform (TLP).
- Floating production storage and offloading (FPSO).
- Tie-back to existing platform.

Creation of models:

- Material balance was used to model the reservoir, using MBAL, a software from Petroleum experts.
- Network model in Pipesim.
- Excel to integrate both and generate production potential tables.
- Cost estimation in AMPL.
- Optimization in AMPL + CPLEX.
- Evaluation of uncertainties using Pipe-It.

Assumptions:

- PVT properties of the fluid were calculated using simple black-oil model.
- All wells were considered identical in the network model.

In this study, the methodology is tested on a single case study. However, the methodology was also successfully tested by Angga on the Safari field, a synthetic field proposed by AkerSolutions for detailed information on this work refer to reference [1] [2].

7.1.2. Step 2: Generation of proxy model of production potential

For each development strategy, production potential curves displaying oil rate, GOR and WC as function of cumulative oil production and number of wells were generated from the

integration of a reservoir model and a surface network model. Topside facilities were not considered during the generation of the production potential profiles since the first stage separator pressure was kept constant and this eliminates the pressure dependency between the two systems. The purpose of this proxy models is to use them to estimate the production performance of the field through optimization without needing to run the standalone models (reservoir and production network) in each optimization iteration. This reduces computation time while maintaining an accurate representation of the production system. A detailed explanation of how these proxy models are generated and a validation of their capacity to give a good representation of the production system were presented in chapter 3.

The reservoir was modeled as explained in chapter 3. The input data used in the model is presented in Appendix A and C. To account for the different recovery strategies, two types of reservoir models were built. For the first type, no water injection was considered and the average oil rate was constrained to a maximum of 110 000 stb/d. This constraint was an assumption made to account for the capacity of the processing facility. Since Wisting field is a prospect, there was no available information regarding the processing facilities. Therefore, this value of oil rate was taken from the processing capacity of Goliat field's FPSO. In the second type, the same average oil rate was used and water injection was implemented with a voidage replacement factor of 100%. In this work, the effect of different percentages of voidage replacement was not studied.

The surface network calculations were performed as explained in chapter 3. To express the influence of the number of wells, six models were built, each with different amount of production wells (1, 3, 6, 9, 12 and 15 wells). All wells were assumed identical. Joshi's model for steady-state horizontal well productivity was used [11].

Two types of production systems were modeled to account for the recovery strategies tested. For the first production system, a constant gas lift injection rate of 3 MM scf/d was included in all wells. This rate was determined using the "artificial lift performance operation" as explained in section 3.2.4. In the second production system, Framo Helico-Axial multiphase boosters with a maximum power consumption of 3 800 kW were selected from the network software library and added to each flowline. The detailed data used to build the network model is shown Appendix B.

The integration between the sub-surface and surface models is explained in chapter 3. The oil production potential for each recovery strategy is shown in Figure 7.1. Figure 7.2 shows the GOR curves, and the WC is presented in Figure 7.3. The numerical values corresponding to these production potential curves are presented in Appendix F.

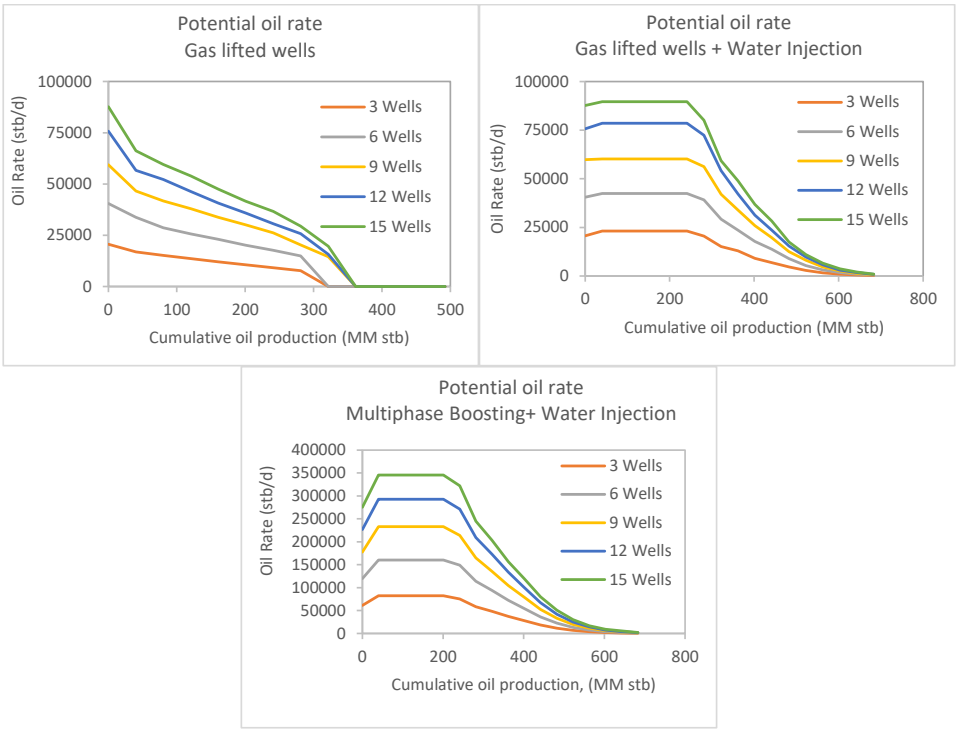

Figure 7.1. Potential oil rate for all the recovery scenarios

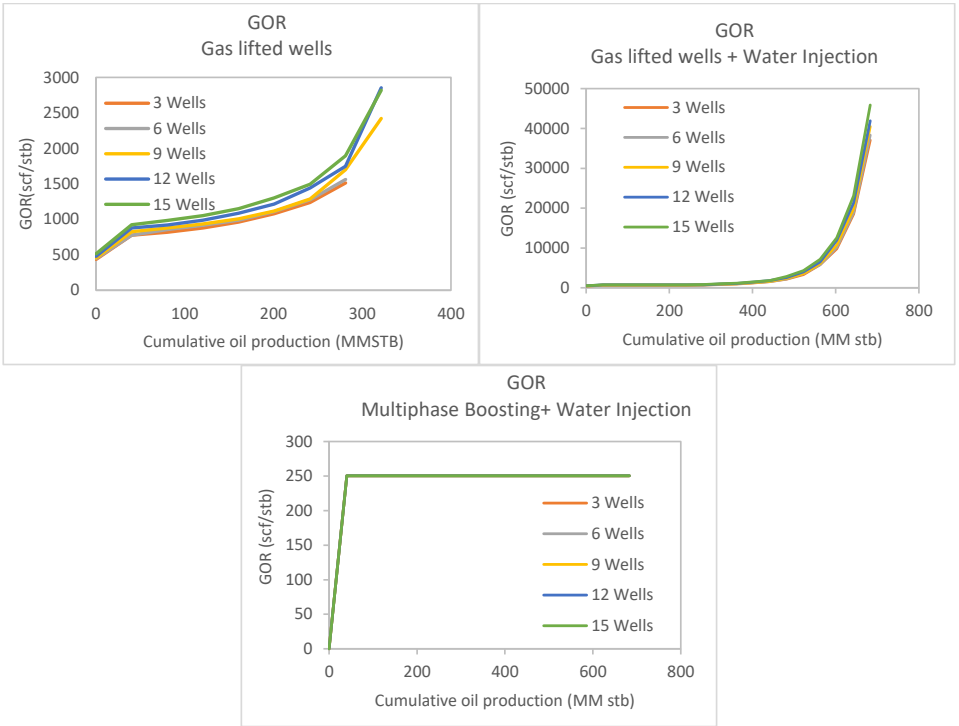

Figure 7.2. Potential GOR for all recovery scenarios

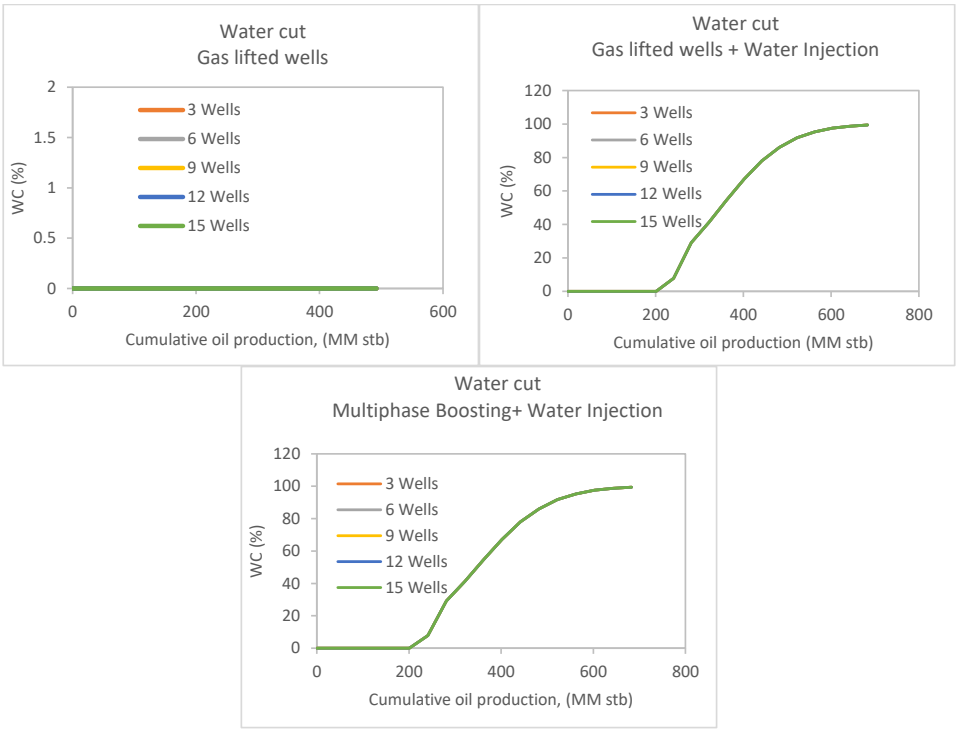

Figure 7.3. Potential water cut for all recovery scenarios

7.1.3. Step 3: Cost estimation

For the costs estimation, proxy model are used. These models consists of linear equations, where the cost of the project is expressed as function of the oil, gas and water rate capacities of the processing facilities and the number of wells. The cost equations used for this study case are the same as the ones presented in chapter 4. They are shown below.

TLP:

$$E_{cap,TLP} = 0.0079 \cdot q_o^{capacity} + 29.81 \cdot q_g^{capacity} + 0.0115 \cdot q_w^{capacity} + 307.53 \cdot Nw^{field} + 11702.41 \quad (4.5)$$

$$E_{op,TLP} = 6.67E-4 \cdot q_o^{capacity} + 0.8930 \cdot q_g^{capacity} + 2.18E-4 \cdot q_w^{capacity} + 14.01 \cdot Nw^{field} + 613.93 \quad (4.6)$$

FPSO:

$$E_{cap,FPSO} = 0.0122 \cdot q_o^{capacity} + 42.64 \cdot q_g^{capacity} + 0.0173 \cdot q_w^{capacity} + 307.87 \cdot Nw^{field} + 15407.21 \quad (4.7)$$

$$E_{op,FPSO} = 9.42E-4 \cdot q_o^{capacity} + 1.4050 \cdot q_g^{capacity} + 3.63E-4 \cdot q_w^{capacity} + 14.01 \cdot Nw^{field} + 613.78 \quad (4.8)$$

Tie-back:

$$E_{cap,Tie-Back} = 0.0366 \cdot q_o^{capacity} + 12.74 \cdot q_g^{capacity} + 0.0477 \cdot q_w^{capacity} + 369.30 \cdot Nw^{field} + 21911.58 \quad (4.9)$$

$$E_{op,Tie-Back} = 5.50E-4 \cdot q_o^{capacity} + 0.1245 \cdot q_g^{capacity} + 1.82E-4 \cdot q_w^{capacity} + 14.26 \cdot Nw^{field} + 349.62 \quad (4.10)$$

DRILLEX (valid for all topside facilities):

$$E_{drill} = 253.45 \cdot Nw_{d,p+i} + 1.55E-11 \quad (4.11)$$

7.1.4. Step 4: Optimization

For each development concept, the production profile and drilling schedule that give maximum profit were estimated using optimization. For this, some assumptions were considered:

- Constant oil price: 500 NOK/stb (62.5 USD/stb).
- Discount rate = 8%.
- All wells start production from the beginning of the year they are drilled.
- A table of cumulative water injected vs. cumulative oil production was used to calculate the water injection rate. The table is shown in Appendix G.
- The time steps have a duration of one year
- The following constraint were applied:
    - The maximum number of production wells that can be drilled in a time step are four wells.
    - The maximum number of production wells in field is 15 wells.
    - The maximum oil rate per well allowed to avoid erosion in the production system is 13000 stb/d.
    - The maximum water injection per well is 6290 stb/d (valid for the cases with water injection).
- During the optimization, only the optimal drilling schedule of the production wells is computed. Therefore, to estimate the costs, it is assumed that the field has the same amount of production and injection wells.

The simulations were run in a workstation with an Intel® Xeon® W-2145 processor and 64 GB of memory. The running time of one optimization case ranged between 9 seconds and 8 hour.

The results of the optimization are shown below: The optimum production profile for three strategies (all the recovery methods with TLP) is presented in Figure 7.4 to Figure 7.6. The resulting production profiles for all cases are presented in the Appendix H.

From the production profiles obtained, it was observed that the topside facilities do not have influence on the oil production rate. The topside facility affect the costs and, subsequently, the NPV. The NPV depends on both costs and production profile Therefore, the topside facility should, in theory, influence the production profile. However, the results show that this influence is negligible for the cases studied

Regarding the influence of the recovery methods over the oil production profile, the cases with gas lifted wells gave the lowest oil production. In addition, for these cases, the optimal production schedule consist of producing at the field potential rate.

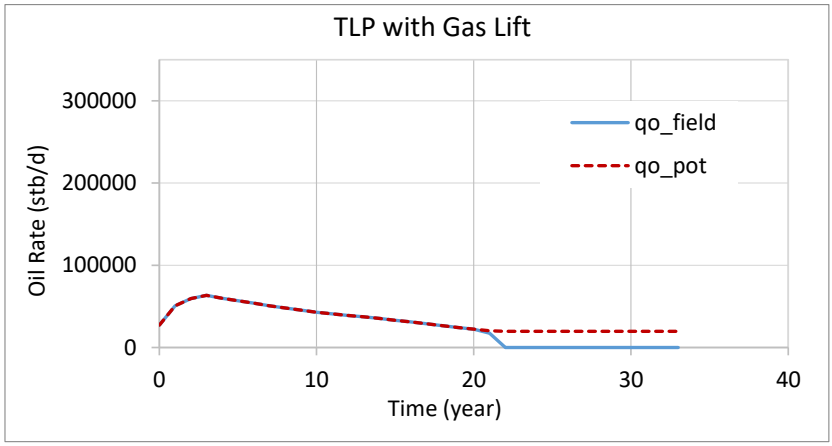

Figure 7.4. Optimum oil production profile and oil production potential for strategy TLP with Gas Lifted wells

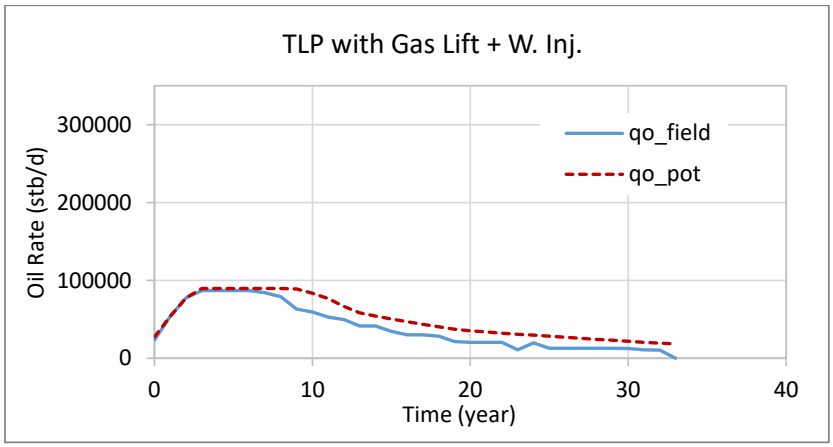

Figure 7.5. Optimum oil production profile and oil production potential for strategy TLP with GL + WI

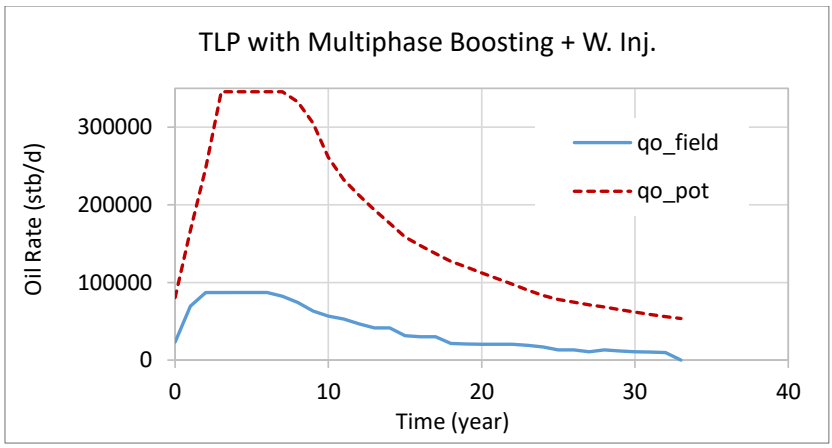

Figure 7.6. Optimum oil production profile and oil production potential for strategy TLP with MPB + WI

The cases with gas lift + water injection and multiphase boosting + water injection gave similar production profiles. For these cases, it was obtained that, the optimal production rate is lower than the production potential rate of the field. This happens because, even though, for theses cases, the field has the capacity to produce at higher rates, a greater oil production would infringe one or more constraints in the optimization formulation. The influence of the oil production is reflected on the revenues, higher production gives higher revenues, and on the costs since a higher production means processing facilities with higher capacity are needed.

The drilling schedule for all the development strategies is shown in Table 7.1. This parameter will be mostly influenced by the cost of drilling each well and the capacity of the strategy to produce revenues that overcome that cost. For this study case, the drilling schedule remains mostly the same regardless the strategy used. The optimum schedule is to drill the maximum number of wells allowed in each time step until the total number of wells that can be drilled in the field is reached. The combinations of Tie-back and FPSO, the most costly platforms, with GL, the scenario with less oil production, are the only strategies that give a lower number of wells drilled.

Table 7.1. Optimum drilling schedule for all strategies

	Number of wells drilled per year						**Total Nw**
Year	**1**	**2**	**3**	**4**	**5**	**…**	
TLP + GL	4	4	4	3	0	0	15
FPSO +GL	4	4	4	2	0	0	14
Tie-back + GL	4	4	4	2	0	0	14
TLP + GL + WI	4	4	4	3	0	0	15
FPSO +GL + WI	4	4	4	3	0	0	15
Tie-back + GL + WI	4	4	4	3	0	0	15
TLP + MPB + WI	4	4	4	3	0	0	15
FPSO + MPB + WI	4	4	4	3	0	0	15
Tie-back + MPB + WI	4	4	4	3	0	0	15

Table 7.2 shows the NPV obtained for each strategy. This results are shown at an abandonment rate of 20 000 stb/d. This rate was chosen because, for some strategies, the cash flow becomes negative when the oil rate drops at approximately 20 000 stb/d, negative cash flow means that the revenues are lower than the expenses.

Table 7.2. Maximum NPV obtained for each development strategy

NPV (billion NOK)			
	TLP	**FPSO**	**Tie-back**
GL	45.29	39.94	36.88
GL + WI	71.19	64.98	60.02
MPB + WI	74.71	69.67	63.01

Based on Table 7.2, it can be concluded that the best development strategy to exploit this synthetic field would be to use a TLP platform in combination with MPB + WI. This conclusion is done using a deterministic calculation, i.e. assuming that there is no uncertainty in the input. However, in reality there are many uncertainties related with the reservoir volumes and properties, fluid characteristics, costs, etc. To perform a proper field development study, an analysis and quantification of uncertainties is necessary. This is performed in the step 5.

7.1.5. Step 5: Analysis of uncertainties

The effect of uncertainty was evaluated using discrete cases with probability trees. Uncertainties in the production potential curves (proxy models) and the costs were considered.

For the potential curves, uncertainties on the size of the reservoir (initial oil in place), the layout of the production system (Figure 7.7) and the Joshi's steady state productivity index (PI) were used. The steady state productivity model of Joshi, involves several reservoir parameters to calculate the productivity index of a well. However, to simplify the process, the uncertainty in PI was accounted only with uncertainty in the horizontal and vertical permeability (Kh and Kv).

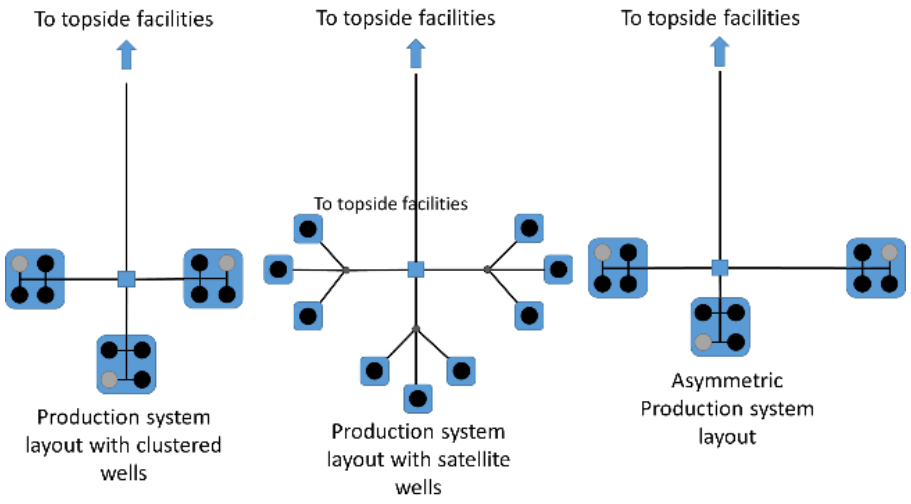

Figure 7.7. Uncertainty in production system layout

Seven production potential curves were generated for each recovery strategy. This resulted in 21 uncertainty cases (the type of topside facility has a negligible influence on the production potential curve). Figure 7.8 presents a decision tree diagram showing these cases and their corresponding probability.

Since the methodology was tested in a synthetic reservoir based on public data of Wisting field, there is no information available about the layout configuration of the subsea system or the productivity index. Therefore, the uncertainty values used for these two parameters where assumed to have equal probability. This means that, each one of the three cases of production system layout has a probability of 1/3, and the same applies for the cases of productivity index (each has a probability of 1/3). In the cases of the reservoir size, the uncertainty used correspond to information of higher, lower and based volumes available in public domain. It was assumed that these values correspond to the P10, P50 and P90 percentiles of a normal distribution with the probability values shown in Figure 7.8.

The costs values obtained from the cost proxy models were varied in ±20% to account for uncertainty in these variables. This results in three uncertainty cases in which CAPEX, OPEX and DRILLEX were varied simultaneously. They are shown in Figure 7.9.

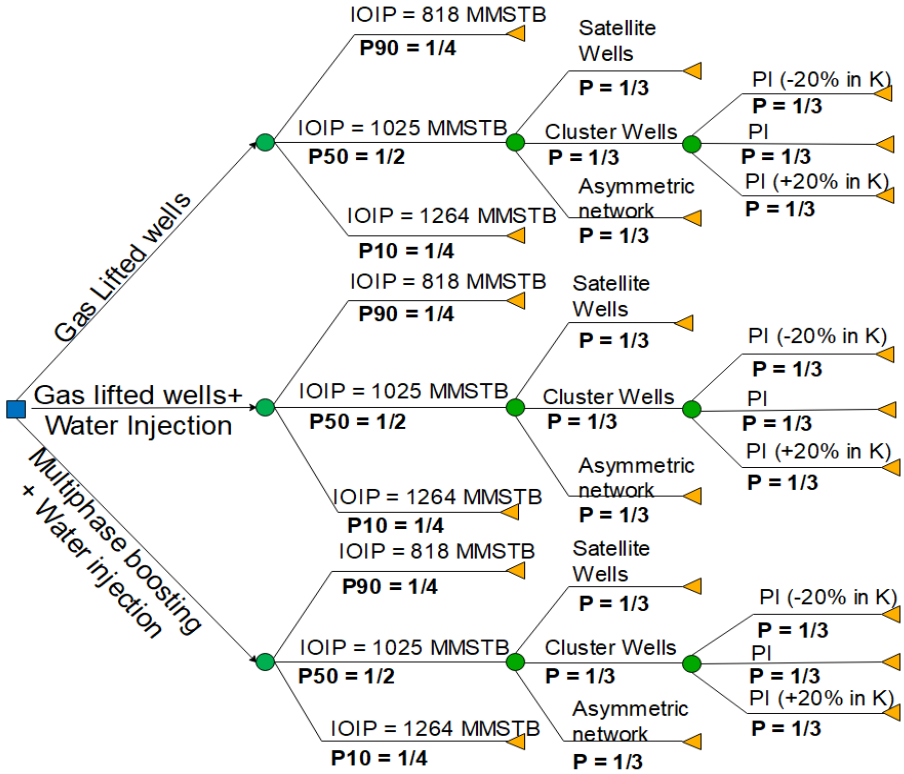

Figure 7.8. Decision Tree diagram for potential curves uncertainty

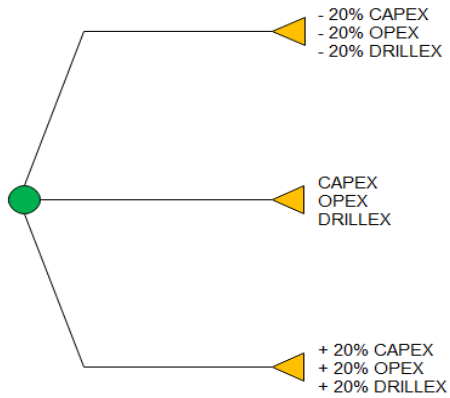

Figure 7.9. Decision tree diagram for costs uncertainty

The cost uncertainty was applied to the 21 curves of production potential, resulting in 63 uncertainty cases. Additionally, the 63 cases were repeated for each topside facility, giving 189 simulations for the uncertainty analysis. Step 4 was applied for each one of these cases.

The software Pipe-It [7] was used to setup the uncertainty analysis. This software allows running the optimization while varying the inputs of production potential curves and costs. This

is done automatically, Pipe-It is configured to select each production potential proxy model and vary the cost in the established range. Then, it executes the AMPL file to run the optimization. Finally, the results of each optimization run is stored by Pipe-It.

Figure 7.10 shows the NPV's cumulative distribution function obtained in the uncertainty analysis. From this, it is possible to identify the probability that the NPV takes a value between a specific range. In the case of this analysis, the NPV can range between 17.85 and 95.72 billion NOK. The P10, P50 and P90 values are shown on Table 7.3.

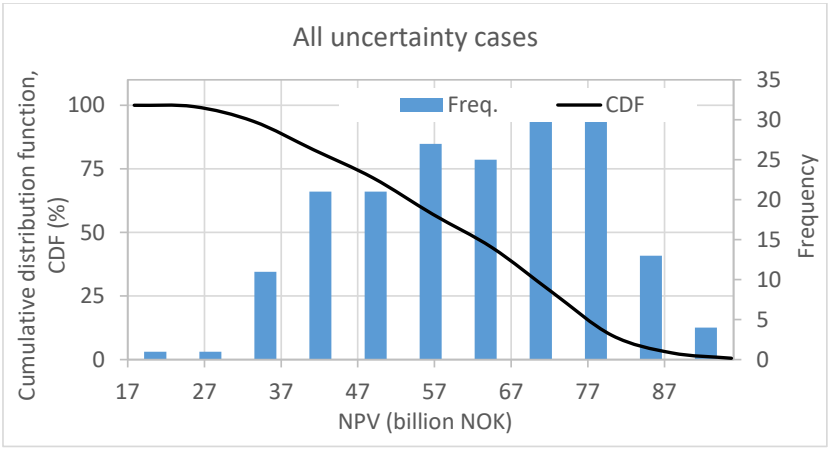

Figure 7.10. NPV's cumulative density function. All uncertainty cases

Table 7.3. NPV's probabilities

NPV (billion NOK)			
	P10	**P50**	**P90**
All cases	35.98	60.99	79.93

Figure 7.11 and Figure 7.12 compare the influence of each recovery scenario and each topside facility over the NPV, respectively. Figure 7.11 shows that the recovery scenario that give the highest values of NPV is MPB + WI, follow closely by GL + WI, the less profitable scenario is GL. These results are influenced by the amount of production that can be obtained from each scenario.

The topside facilities influence the NPV through the costs. Figure 7.12 shows that the most profitable facility is TLP, since it has the lower costs. The next is the FPSO and finally the Tie-back to existing facilities. Tie-back to existing facilities does not account costs of platform. However, the costs of the pipeline and umbilical system is higher in comparison to TLP and FPSO due to the larger distance they need to cover (150 km).

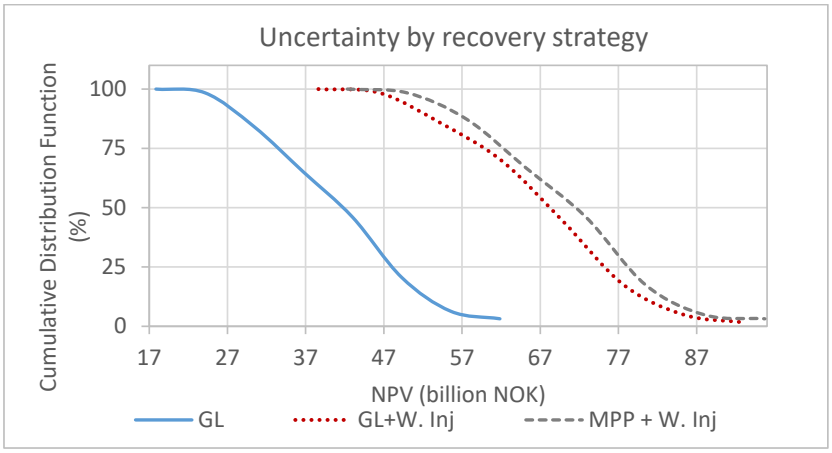

Figure 7.11. Comparison of NPV's cumulative density function for all recovery scenarios

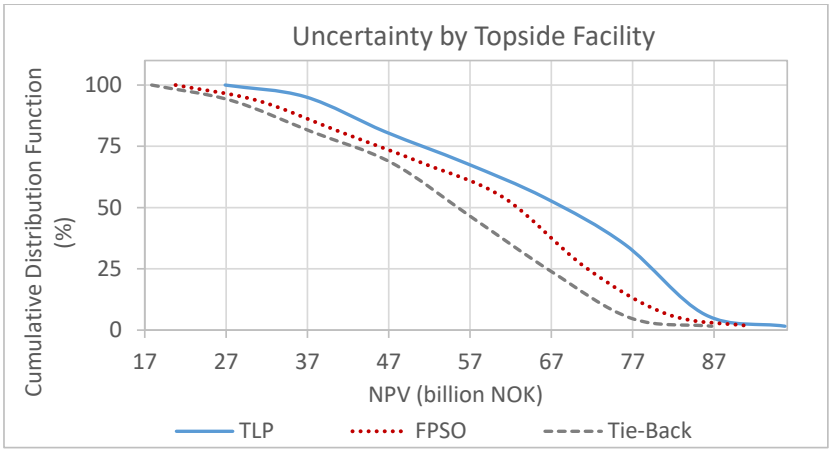

Figure 7.12. Comparison of NPV's cumulative density function for all topside facilities

The results from Figure 7.11 and Figure 7.12 are in accordance with what was obtained before in the step 4 of this methodology (Table 7.2).

The P10, P50 and P90 values for the three recovery scenarios and the three topside facilities concepts are shown in Table 7.4.

Table 7.4. NPV probabilities. Recovery scenarios and topside facilities

NPV (billion NOK)			
	P10	**P50**	**P90**
GL	27.83	41.68	53.95
GL + W. Inj	51.61	68.15	82.26
MPB + W. Inj	55.73	71.37	84.95
TLP	40.33	68.27	84.63
FPSO	33.79	62. 58	79.44
Tie-back	30.52	55.45	74.18

7.2. General observations

An automated methodology that uses integrated asset modeling, mathematical optimization and analysis of uncertainties to perform field design in early stages of the field development process, was developed. The methodology employs proxy models of the production system that reduce complexity and computational simulation time. Mathematical optimization is used to determine the best production profile and well drilling schedule that maximize economic profit for a specific field development strategy. The effect of uncertainty and several design alternatives is quantified using probability trees.

The methodology was evaluated in a synthetic field where the profitability of nine development strategies was compared. The development strategies were obtained from the combination of three recovery scenarios (GL, GL + WI and MPB + WI) and three topside facilities (TLP, FPSO and Tie-back). As result, the best strategy was determined using the NPV as main decision factor, other factors were the oil production and drilling schedule. The best strategy was TLP with MPB + WI. This strategy generated the highest production and required the lowest costs, resulting in the highest profitability.

The effect of uncertainty was evaluated using discrete cases with probability trees (a total of 189 cases). Uncertainties in the reservoir, the production system layout, productivity index and cost were considered. From this analysis, it was determined that the NPV has a probable values that range from 18 to 96 billion NOK.

Angga [1] [2] evaluated the methodology on the Safari Field. He successfully determined the field plateau duration and rate that maximize the NPV and study the effect of cost uncertainties. From the evaluation perform with the Wisting field case and the one perform by Angga, it is valid to say that the methodology provide decision support when performing field planning and demonstrated to successfully find optimal field design features in an automated manner while quantifying the effect of uncertainties.

Chapter 8

Applicability of cold flow and heat tracing for handling wax deposition in subsea pipelines of remote offshore, low pressure and temperature oil reservoirs

The subsea production and transport of untreated reservoir fluids require overcoming phenomena that restrict the flow or disturb its smoothness. The discipline in charge of challenging these problems is called Flow Assurance. A common flow assurance issue for Wisting-like fields is wax deposition. The deposition of wax occurs often in flow of untreated reservoir oil in wells, surface and subsea production systems and flowlines conducting untreated oil. This phenomenon increases the pressure drop inside the pipeline and can cause pipe blockage.

Wax is a compound consisted of heavy paraffinic components which are fully dissolved in the hydrocarbon mixture at high temperature, but tends to precipitate as a solid-like soft material when the temperature declines below a certain level referred to as Wax Appearance Temperature (WAT). The formed wax tends to deposit on the pipe wall, as it is normally colder than the core of the flowing stream, forming a layer of sticky solid paste that restricts the flow.

Calculation models to predict the wax build-up in a pipe cross section are based on molecular diffusion mechanism of wax crystals driven by concentration gradient from the center outwards. This is combined with shear dispersion of the accumulated wax crystals by the flowing fluid. Such models are used today in engineering calculations for predicting wax build-up and for mapping wax restriction along pipe sections with constant or declining flow stream temperature. Computational wax build-up routine can be linked to flow simulator.

The conventional techniques for wax deposition mitigation and removal are chemical, thermal and mechanical. The chemical management consists in the injection of substances into the pipeline to control wax. Chemical removal techniques consists of injecting solvents or dispersants. Thermal management can be of two types, passive and active. The passive thermal management technologies consists of applying insulation to cover the pipeline or use cold flow technology. Active thermal management consist in maintaining the temperature of the flow above the WAT to avoid wax formation. The mechanical management consists of carrying on regular pigging to scrape the wax from the pipe wall.

The focus of this chapter is to analyze novel flow assurance techniques for the control of wax deposition in the production pipeline for a field with the characteristics of Wisting. The first approach is to extract, from the fluid stream, the wax-creating material before entering the flowline, a concept commonly known as "Cold Flow". The second approach is Electrical Heat Tracing, which consists of heating the pipeline wall with the purpose of maintaining the production stream above the wax appearance temperature. For both studies, the pipe-flow dynamics were analyzed. However, the detailed design of each technology falls out of the scope of this study.

For Cold Flow, the particular system analyzed consists of a reactor unit at the inlet to the flowline, where the thermal solubility of the wax-creating molecules is reduced by cooling. Subsequently, solid wax is deposited in the reactor piping and wax free crude enters the flowline. The reactor is regenerated periodically. Three types of reactors were simulated: a non-insulated pipe section, a passive cooler with a bundle of parallel pipes and an active cooler. Sensitivity analysis were performed for all three cases varying the external convective coefficient, the reactor pipeline diameter and the WC.

For Electric Heat Tracing, four strategies were employed to avoid wax deposition in subsea flowlines transporting untreated crude oil from subsea wells to a host installation. The strategies are distinct by the configuration of deploying the heat tracing along the pipe and by the activation schedule (continuous or alternating heating cycles). The study demonstrates quantitatively that the electrical power required for maintaining wax-free flow depends strongly on the employed strategy. In conclusion, the study ranks the strategies according to their computed energy efficiency, thus providing quantitative benchmarks for preliminary wax control assessment.

The author claims no ownership or rights on the Cold Flow or Electrical Heat Tracing technologies. This work consisted in analyzing and studying the feasibility of those concepts for a real system (using a reference case based on Wisting field's characteristics).

8.1. Background

To the author's knowledge, the idea of Cold Flow comes from the work of Coberly [39], who showed that the presence of solid particles in the bulk fluid decreases the tendency of wax crystals to deposit. Various concepts of Cold Flow have been presented in the literature and some have been registered in patents. Merino-Garcia & Correa presented a review of existent patents that use Cold Flow technologies for the control of wax deposition [40]. Furthermore, Al-Yaari reviewed wax deposition problems in flow assurance and addressed techniques for wax deposition mitigation [41]. Both authors mention the following equipment for wax control:

- The wax eater (Kellog, Brown and Root, Halliburton) [42] [43];
- Cold seeding (NEI, Calgary, Canada and Marathon Oil, Houston, Texas) [44];
- High-shear heat exchanger (Kellog, Brown and Root, Halliburton) [43];
- Pressure surge (Kellog, Brown and Root, Halliburton) [43];
- Flash cooling (Shell Western E&P Inc., Houston, Texas) [45];
- Oil or solvent injection (C-Fer Technologies, Edmonton, Canada);
- Magnetic conditioning (Magwell. Boerne, Texas, and Halliburton).

Cold flow can also be applied to handle gas hydrates and several technologies have been developed [46]: Anti-agglomerate; the SINTEF cold flow technology [47]; the NTNU cold flow

hydrate technology [48]; and HYDRAFLOW [49]. Watson, Speranza, & LaCombe, performed a study comparing these four technologies, highlighted possible obstacles that need to be overcame and showed the effect in the production profile for a specific system [46]. Akpabio and Vinatovskaja, performed comparison studies of three cold flow technologies for gas hydrate mitigation (SINTEF, NTNU and HYDRAFLOW) against conventional technologies (injection of inhibitors and direct electrical heating). Both concluded that Cold Flow technologies offer a better solution for the flow assurance problems in deep-water and arctic environment, and are especially suited for long distances [50] [51].

In relation with using electric heating to avoid wax formation, many studies evaluating the efficiency of these technologies, can be found in the literature. Denniel and Laouir [52], worked on the development of heated PiP technology and demonstrated its high efficiency, where low linear power inputs (20 to 40 W/m of pipe) were sufficient for the prevention of hydrate or wax formation. Later, they applied the technology to a 20 km tie-back to maintain indefinitely the fluid temperature 26 ^{o}C above ambient temperature.

Escobar-Remolina, Barrios and Silva [53] applied electric heating technology to a well production line along 900 meter in a Colombian field, where an extra-heavy oil was been produced. They managed to increase the daily oil production of the well in 160%. Pedersen, Kullbotte, Børnes and Marthinsen [54], performed laboratory experiments where an ice plug was formed in a 4.5 m long 30 inches pipejoint and melted using direct electrical heating (DEH). The experiments showed that 3% of the ice plug got melted at an ambient temperature of -2 ^{o}C and a current of 1300 A for 48 hours, while increasing the current to 1500 A melted 6% of the ice plug in the same period of time.

Tzotzi et al. [55] presented the hydrate formation inside an EHT-PiP system and its safe and controlled dissociation using active heating. Finally, Lirola, Pouplin, Settouti and Agoumi [56] presented an overview of two active heating solutions: distributed and local; as a conclusion, they provided guidelines about which technology is the most adequate depending on the oil properties.

8.2. Flow assurance issues: Wax deposition

The main flow assurance issues that affect the production of hydrocarbons through wells, flowlines and risers are hydrates, waxes, asphaltenes, slugging, naphthenates, scales, corrosion, erosion and emulsions [57]. The main interest of this thesis is to analysis technologies of flow assurance for the control and mitigation of wax deposition in subsea production pipelines, other issues fall outside the scope of this work. Below is a brief description of wax deposition.

Wax deposition takes place when the production fluid temperature drops below the wax appearance temperature (WAT) and the paraffin components in the crude oil precipitate and deposit on the pipeline wall. The wax particles deposit in the inner pipe wall forming a layer, which increase in thickness with time and can lead to serious flow related problems like excessive pressure drop and pipe blockage. The deposition occurs if there is a temperature gradient between the bulk flow and the pipe wall. Therefore, once the fluid reaches thermal equilibrium with the ambient, wax deposition ceases.

Several factors influence wax precipitation, for example fluid composition, flow rate, temperature gradient, pipe wall temperature, crude oil temperature, oil viscosity, etc. Wax deposition occurs due to the action of driving forces, also known as mechanisms, which help in

the transportation and/or precipitation of wax particles. The most relevant wax deposition mechanism are molecular diffusion and shear dispersion.

8.2.1. Molecular diffusion

Molecular diffusion of wax molecules starts when the pipe wall reaches the wax appearance temperature, and wax starts to precipitate in the region closest to the wall. Thus, a concentration gradient is created between the wax dissolved in the bulk flow and the wax remaining in solution close to the pipe wall. A molecular diffusion process then occurs when the wax dissolved in the bulk flow is diffused toward the pipe wall where it precipitates. Based on the results of Bern et al. and Brown, et al., molecular diffusion is the main responsible for wax deposition [58] [59]. This is especially valid for systems at high temperatures and high heat flux conditions [60]. The driving force for molecular diffusion is the concentration gradient (dc/dr) along the direction r (pipe radius), where c is the concentration of paraffin at a certain location [61].

8.2.2. Shear dispersion

Shear dispersion occurs during flow, when particles are suspended in the flowing oil and move in the same direction and speed of the flow. Due to the velocity gradient, shear is greater in the proximities of the pipe wall, so the particles tend to move towards the center of the pipe. This effect usually causes the transport of the precipitated wax to be predominantly far from the wall. Brown et al. [59] discusses that laboratory evidence indicates that the effect of shear dispersion is not significant in comparison with molecular diffusion. Additionally, Bern et al. [58] and Burger et al. [60], state that the shear dispersion is dominant when flow is at low temperature and low heat flux, and when there is a high concentration of wax crystals in the flow.

8.3. Wax Deposition Modelling in OLGA

In this section, the wax deposition models that are available in the commercial simulator OLGA are described.

OLGA has a wax deposition module to model wax precipitation and deposition. The calculation is made based on a pre-calculated table that contain information of each wax-forming component [62]. This table has information like the number and name of wax components, their molecular weights, liquid densities, cloud point temperatures, concentration of wax components in HC mixture, etc. OLGA uses the table as an input file for the calculation of wax deposition. The simulator has three models: RRR (Rygg, Rygdahl and Rønningsen) model, Matzain model and HEATANALOGY model.

8.3.1. RRR (Rygg, Rydahl and Rønningsen) Model

The RRR model is a wax deposition model for multiphase flow in pipelines. Rygg, Rydahl and Rønningsen created this model in 1998 [63]. It takes into account both molecular diffusion and shear dispersion mechanisms. In the model, wax deposition affects the pressure drop since it decreases the pipe diameter. In addition, it influences the heat exchange of the fluids with the environment, because the wax acts as an insulation layer between the wax bulk flow and the pipe wall. The increase in the thickness of the wax layer is a volume rate

calculated as the sum of the contribution of molecular diffusion and shear dispersion:

$$l_{\max} = \frac{Vol_{wax}^{diff} + Vol_{wax}^{shear}}{(1+\phi)2\pi rL} \tag{8.1}$$

where

$l_{\max}$ = rate of increase in thickness for the wax layer (m/s).

ϕ = wax porosity (it can be used as a tuning parameter in OLGA [62]).

r = current inner pipe radius (m).

L = length of the pipe section (m).

Vol_{wax}^{diff} = volume rate of wax deposition by molecular diffusion (m^3/s).

Vol_{wax}^{shear} = volume rate of wax deposition by shear dispersion (m^3/s).

The two volume rates of wax deposition terms are calculated with the following equations:

By molecular diffusion (function of composition)

$$Vol_{wax}^{diff} = \sum_{i}^{N\max} \frac{D_i\left(c_i^b - c_i^w\right)S_{wet}MW_i}{\delta\rho_i} 2\pi rL \tag{8.2}$$

where

c_i^b, c_i^w = molar concentration of the wax component i, dissolved in the bulk oil phase and at the wall, respectively (mol/m^3).

S_{wet} = fraction of wetted circumference.

$N_{\max}$ = number of wax components.

MW_i = molar weight of wax component i (kg/mol).

ρ_i = density of the wax component i (kg/m^3).

D = diffusion coefficient (m^2/s).

δ = thickness of the laminar sublayer (m).

In OLGA, the diffusion coefficient D is calculated with Hayduk-Minhas correlation [62].

By shear dispersion (Burger, Perkins & Striegler correlation, 1981 [60])

$$Vol_{wax}^{shear} = \frac{k^* C_{wall}\dot{\gamma}A}{\rho_{wax}} \tag{8.3}$$

where

k^*, is the shear deposition rate constant (kg/m2).

C_{wall}, is the volume fraction of the precipitated wax in the oil at the inner wall temperature.

$\dot{\gamma}$, shear rate at the wall (s^{-1}).

A, surface area available for deposition (m^2).

ρ_{wax}, average wax density (kg/m^3).

The RRR model does not take into account any removal mechanism. It assumes that all the wax transported to the wall sticks to the surface when the temperature is below the WAT.

8.3.2. Matzain Model

The Matzain is a semi-empirical kinetic model that predicts wax thickness based on experimental tests conducted on South Pelto oil in the Gulf of Mexico [63]. The model takes into account shear stripping alongside molecular diffusion and shear dispersion as wax deposition mechanisms. The shear stripping is a wax reducing mechanism. A drawback of the Matzain model is that it is based on experiments carried out only for South Pelto oil.

8.3.3. Heat Analogy

This is a proprietary model used in OLGA for wax deposition in pipelines. The model takes into account molecular diffusion, shear dispersion and shear stripping as mechanism of deposition. No further details of the model are provided in the manual of the software [62].

8.4. Flow assurance technologies

Wax deposition can be remediated or prevented by chemical, thermal or mechanical methods or by a combination of them. The chemical and thermal methods are inhibitor injection, and insulation and heating, respectively. The mechanical method consist of pigging, where a pig (pipeline inspection gauge) passes through the pipeline to scrape off the wax deposited in the pipe wall. This thesis focuses in two flow assurance technologies to mitigate and remove wax deposition, Cold Flow and Electric Heat Tracing.

8.4.1. Cold Flow

Cold Flow is a novel technology focused on the transportation of multiphase flow through the production system without the hindrance of wax and/or hydrates deposition. The principle of Cold Flow is based on the fact that waxes and hydrates need a temperature differential between the production fluid and the pipe wall to precipitate. Then, the precipitation of solid wax and/or hydrate particles can be avoided by eliminating the temperature gradient. This is accomplished by cooling the production fluid to ambient temperature in a component, where all waxes and/or hydrates are precipitated before entering the production system. Solid deposits are then removed from the cooling section and transported as a solid dispersion. Different Cold Flow methods can be found in the literature [41]:

- The wax eater,
- Cold seeding,
- High-shear heat exchanger,
- Pressure surge,

• Flash cooling,
• Oil or solvent injection,
• Magnetic conditioning.

Cold flow has the potential of been a cost-effective solution to wax and/or hydrate formation in deep-water and long-distance production pipelines. With Cold Flow, the costs of using chemical control methods and insulation are avoided. However, to date, there are no hydrocarbon production systems operating with Cold Flow.

8.4.2. Electrical Heat Tracing (EHT)

Electrical heat tracing is an active heating technology to avoid the formation of waxes and/or hydrates. This technology was developed by TechnipFMC and its performance have been tested in the Islay Project, located in the Northern North Sea [64].

EHT consists of 3-phase heat tracing cables installed in a standard Pipe-In-Pipe (PiP), between the outer wall of the inner pipe and the thermal insulation layer, connected at the far end in star connection. Four heat trace cables, made of three copper cores, and two DTS optical fibers spiraled, form the system, as shown in Figure 8.1. The heat is generated through Joule resistivity effect and is transferred through conduction to the inner wall of the production pipe. The EHT does not need the use of a current return path as far as the system is balanced, so no additional umbilical cable is required.

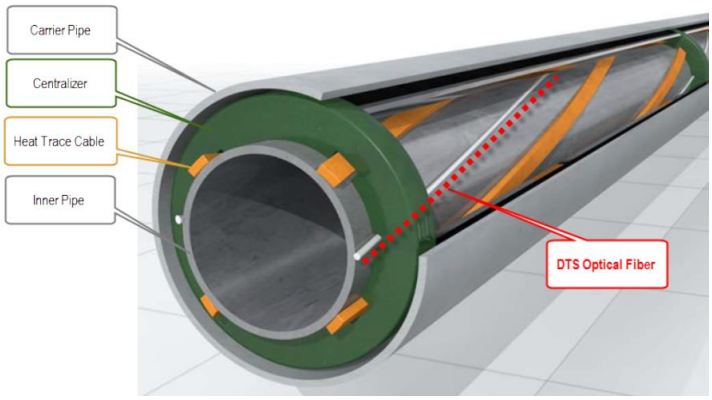

Figure 8.1. Electrical Heat Trace [65]

EHT presents many benefits in comparison to other active heating technologies [66]. In the first place, the EHT configuration separates the active heating system from the PiP insulation system, so they are independent and efficiently integrated. In addition, the direct contact between the heating system and the inner pipe ensures optimum delivery of heat, which results in lower power consumption.

8.5. Cold Flow study

In this section, the studies performed on the Cold Flow approach are present. First is a description of three Cold Flow concepts, which were considered in this study. Then, the cases

used to analyze and compared each concept are explained. Finally, the results are presented and discussed.

8.5.1. Cold Flow Concepts for Wax Flow Assurance

Three Cold Flow concepts were studied to assess their feasibility as flow assurance methods for control of wax deposition. They are a non-insulated pipe section, a passive cooler with a bundle of parallel pipes and an active cooler. They consist of inducing, by cooling, the formation, precipitation and deposition of wax in a dedicated section of the production system. This section is then periodically "cleaned" and the inert wax particles are sent together with the production fluids. The criterion used to determine the length of the section is that the thickness of wax deposited at the end of the section has to be less than 1% of the total pipeline diameter. Practically, this occurs when the fluid reaches thermal equilibrium with the surroundings.

8.5.2. Non-Insulated Pipe Section

The non-insulated Pipe Section concept (Figure 8.2) consists of connecting a pipe section without insulation (loop), at the beginning of the main transportation pipeline, cooled by sea currents [40] [41] [43]. The section must be long enough to ensure that all the wax is deposited there. This means that the fluid has to exit the loop at thermal equilibrium with the surroundings.

Two pipe sections are placed in parallel so, when one has a significant amount of wax, it is then closed for wax removal, and the production fluids are diverted through the other section. During the wax removal, a pig crushes the wax accumulations on the wall and the residues are sent together with the flow in the main transportation line.

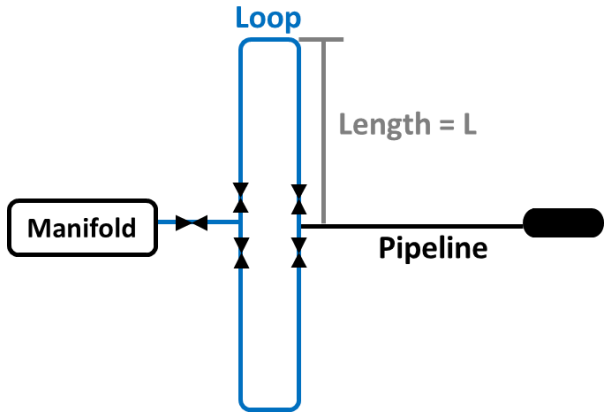

Figure 8.2. Non-insulated pipe section concept

8.5.3. Passive Cooler with a Bundle of Parallel pipes

This concept consists in installing a passive cooler, made of parallel pipe segments, cooled by sea currents (Figure 8.3). The wax will deposit in the walls of the cooler. To eliminate the wax, the heat exchanger can be pigged or its walls can be heated [67]. A feasibility study was performed where the number of parallel segments in the cooler and their length were the studied

parameters. The aim was to find a combination were a thermodynamic equilibrium between the fluid and the surroundings were guaranteed at the outlet of the heat exchanger.

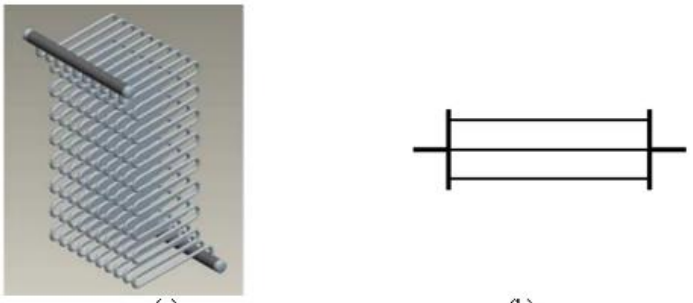

Figure 8.3. Passive cooler with a bundle of parallel pipes. (a) 3D isometric of a parallel pipe heat exchanger with natural cooling, (b) modelling approximation

8.5.4. Active Cooler

This concept consists in connecting an active heat exchanger at the beginning of the system. The goal is to find the minimum duty needed to cool down the fluid until it reaches the temperature of the surroundings. This concept is the most difficult to pig, since the typical active heat exchangers are shell and tubes and the geometry is significantly more complex than the other two cases. An alternative method to remove the wax deposited inside the heat exchanger is to heat the walls of the equipment by introducing a hot fluid.

8.5.5. Cases

The study was divided in 3 cases, each one representing one cold flow concept. Additionally, a base case representing the original production system was created.

The original production pipeline has a horizontal length of 8 km, with an internal diameter of 6.69 inches. The fluid enters the pipeline with a mass flow of 17.51 kg/s, which represents a standard flow rate of $14x10^3$ Sm3/d for 32 API, a gas specific gravity of 0.95, a temperature of 70 ^oC, a water cut of zero, a GVF of 0.085 and a WAT of 22 ^oC. The outlet pressure was 25 bara. The surrounding temperature was 4 ^oC. The external coefficient of convective heat transfer with seawater is 500 W/m-K. Figure 8.4 shows a sketch of the flowline diagram used in OLGA.

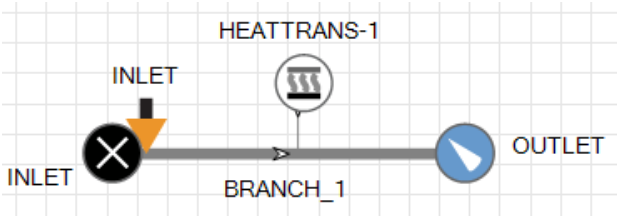

Figure 8.4. Schematic flowline diagram used in OLGA

Three layers compose the pipeline wall: steel, concrete and polypropylene. Their properties are given in Table 8.1.

Table 8.1. Wall material properties

	Steel	Concrete	Poly-Propylene
Thickness (cm)	1	0.6	0.30
Conductivity (W/m-K)	50	1.7	0.12
Density (kg/m^3)	7850	2250.0	960.00
Capacity (J/kg-K)	485	880.0	1675.00

The wax deposition model used was RRR. The simulation time was 90 days, with a maximum time step of 1000 s and a minimum of 1 s. The information given above was used for all the cold flow cases.

8.5.6. Case 1: Non-Insulated Pipe Section

A sensitivity study to determine the required length of the pipe section (cooling length) was performed for three different subcases:

Case 1.1: Influence of the external convective coefficient of heat transfer. The required cooling length of the pipe section was found for several values of convective coefficient of heat transfer. The values used were within the range of expected free convection coefficients for water [68], and are given in Table 8.2.

Case 1.2: Influence of pipe diameter. The required pipe section length was determined for different values of pipe diameter (Table 8.2).

Case 1.3: Influence of water cut. Three values of water cut were studied in this subcase (Table 8.2).

Table 8.2. Sensitivity variables values used for Case 1

Case 1.1	Case 1.2	Case 1.3
Convective coefficient (W/m^2-C)	**Pipe diameter (in)**	**Water cut (fraction)**
500	6.69	0.00
1000	8	0.15
2000	9	0.30
3000	10	
	11	

Since OLGA is a 1D software, the pipe section was modelled as an equivalent pipeline section attached at the beginning of the original production system described on the base case. This means that the length of the equivalent pipe section is two times the length of the loop (Figure 8.5).

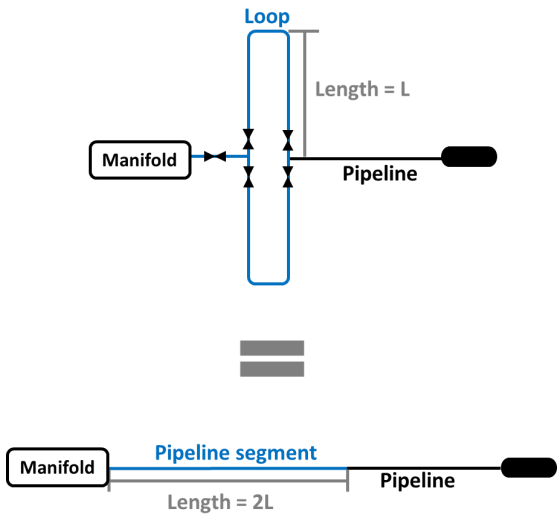

Figure 8.5. Equivalent one-dimensional loop used in OLGA simulations

In this case, the equivalent 1D pipe section does not have insulation. This means that its wall consists only of one material, steel, with a thickness of 1cm. The rest of the pipeline has the wall configuration mentioned in the base case.

8.5.7. Case 2: Passive Cooler with a Bundle of Parallel Pipes

For this case, two sensitivity variables were taken into account. The first one was the number of cooler's parallel segments and, the second one, their length. In the same way as case 1, this case was divided into two sub-cases. The first subcase, model the cooler with two parallel segments (case 2.1), and the second uses three parallel segments (case 2.2). Figure 8.6 shows a sketch of the model for case 2.2 in OLGA.

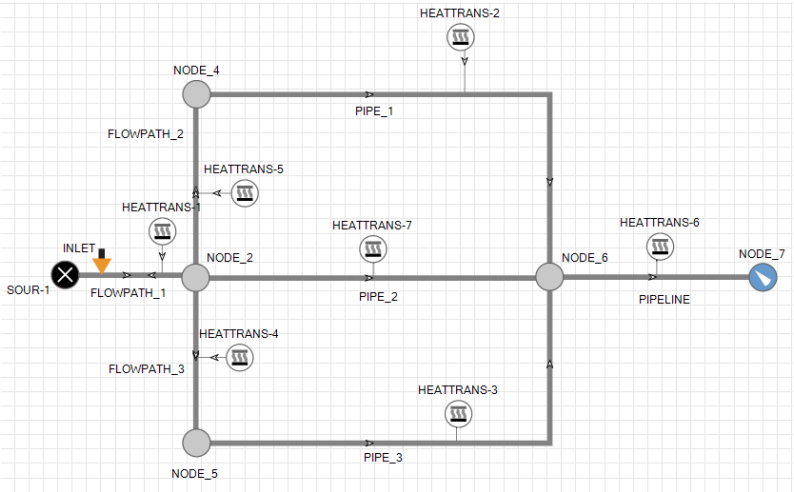

Figure 8.6. Schematic diagram of Case 2 used in OLGA

In both subcases, the fluid is distributed evenly through all the parallel segments and the distance between segments is 1 m (FLOWPATH_2 and FLOWPATH_3 in Figure 8.6). The cooler pipes diameter is 3 inches and the wall material is steel with thickness of 0.4 cm without insulation.

8.5.8. Case 3: Active Cooler

Here, a heat exchanger was added to the system, and the minimum duty to avoid wax deposition in the pipeline was determined. Unlike the other cases, in case 3, external forced convection is used to cool down the flow to ensure the fluid leaves the heat exchanger at thermal equilibrium with the surroundings. A sketch of the model is shown in Figure 8.7.

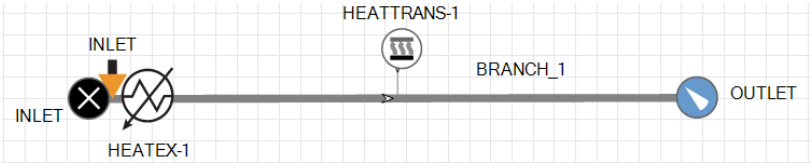

Figure 8.7. Schematic diagram of Case 3 used in OLGA

8.5.9. Results of Cold Flow study

The criterion used to determine the loop length for Case 1 was that the wax thickness at the end of the loop had to be at least 1% of the pipeline diameter after a production of 90 days. This criterions was defined by the author. Figure 8.8 shows the required cooling length that meets the criteria in each subcase. Additionally, the added pressure drop and the wax thickness profile for all the subcases are given in Figure 8.9 and Figure 8.10, respectively. For all cases, the added pressure drop was calculated with Equation (6.1). In general, all cases required a loop length of at least 3 km to allow most of the wax to deposit in the section.

$$AddedPressureDrop[\%] = \frac{\Delta p_{basecase} - \Delta p_{new}}{\Delta p_{basecase}} \qquad (6.1)$$

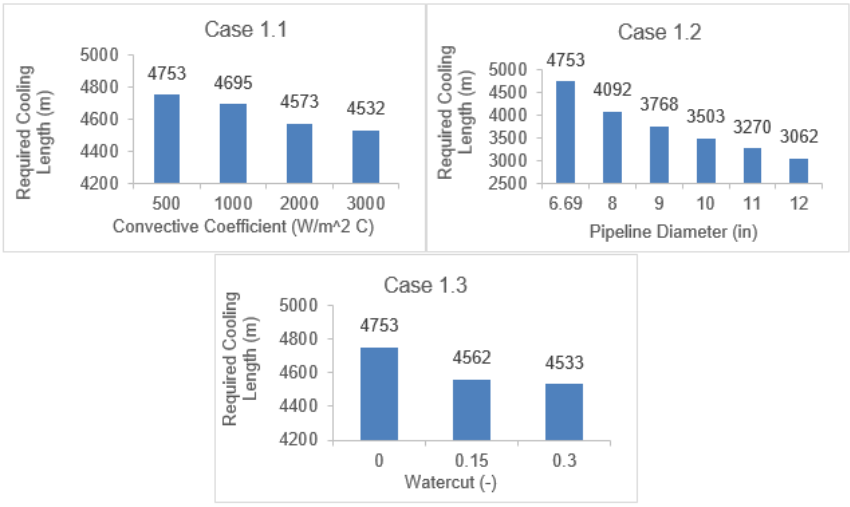

Figure 8.8. Required cooling length for Case 1 after 90 days of production

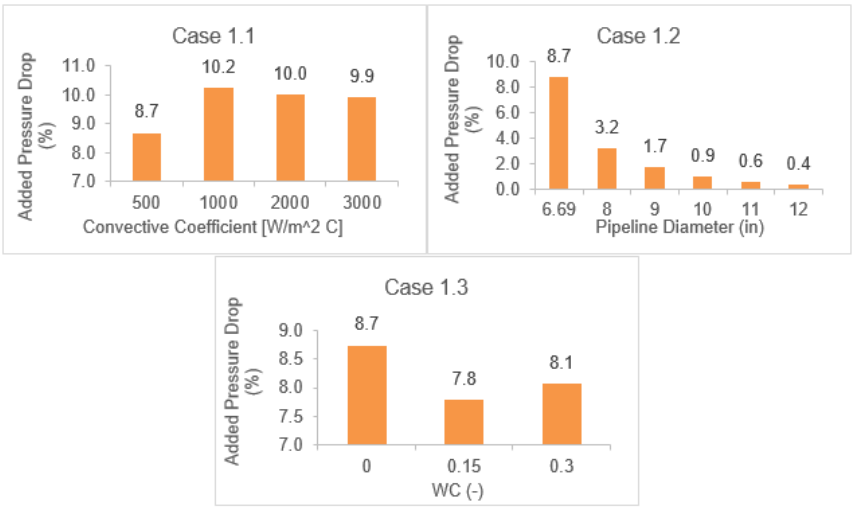

Figure 8.9. Added pressure drop for Case 1 after 90 days of production

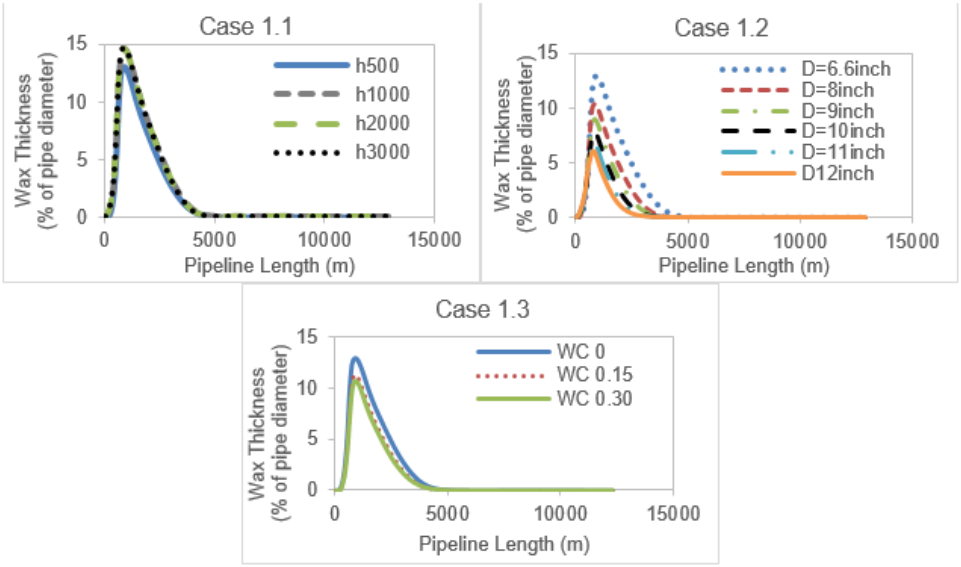

Figure 8.10. Wax thickness profile for Case 1 after 90 days of production

Figure 8.8 to Figure 8.10 show that the pipeline diameter has the biggest influence in the required length of the non-insulated pipe section. According to the results of the sensitivity analysis performed in subcase 1.2, the biggest diameter provides also the smaller cooling length, pressure drop and maximum wax thickness. With bigger diameter, the heat transfer, between the bulk flow and the surroundings, is larger and the required cooling length is smaller. An increase in pipe diameter from 6.69 in (base case diameter) to 12 in (maximum diameter studied) give a decrease in the required cooling length of 35.58% (from 4753 m to 3062 m). It also give a decrease of 95.40% in the added pressure drop (from 8.7% of added pressure for a diameter of 6.69in to 0.4% of added pressure for a diameter of 12 in).

Changes in the outer convective coefficient and stream water cut do not have much influence in the required cooling length. For the pressure drop, the water cut has a smaller influence compared with the convective coefficient. An increment in the convective coefficient of 2500 W/m^2 C, decreases the required cooling length in 4.65%, but increases the pressure drop of 1.2%. In the other hand, a water cut of 30% gives a decrease of 4.63% in the required cooling length and of 0.6% in the pressure drop.

An important conclusion from the feasibility study performed on Case 1 is that this technology is more attractive for long transportation distances (> 50 km). For example, comparing with the system used here (8 km pipeline), the minimal cooling length obtained (Case 1.2, using a 12 inches diameter pipeline) represents 38.28% of the original production pipeline, while for a pipeline of 50 km, would represent only 6.12%.

The results shown in this section might depend strongly on the fluid characteristics, rates and pipeline dimensions. Thus, direct extrapolation of these observations to other subsea production systems is not recommended.

Figure 8.11 and Figure 8.12 show the results obtained for Case 2. Here, the number of cooler segments has a big influence in their required cooling length. For two segments, the length was 2.3 km, which represents 28.75% of the original production system. While, for three segments the length was 1.6 km, representing 20% of the original production system. This means that, with the parallel pipe passive cooler (case 2) the space needed can be much less than that needed for the non-insulated pipe section (case 1). However, a disadvantage is that the added pressure drop needed will be bigger in comparison with that of the non-insulated pipe section, this is due to the smaller diameter pipes use in the cooler, yet this pressure drop will decrease with the increase of the number of cooler segments.

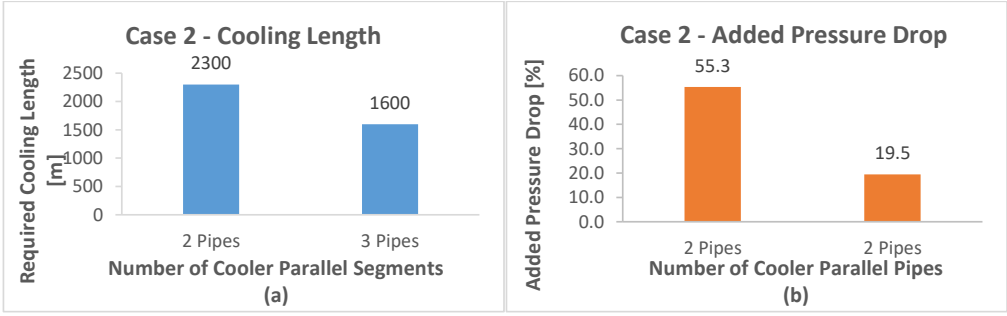

Figure 8.11. Results for Case 2 after 90 days of production. (a) required cooling length. (b) added pressure drop

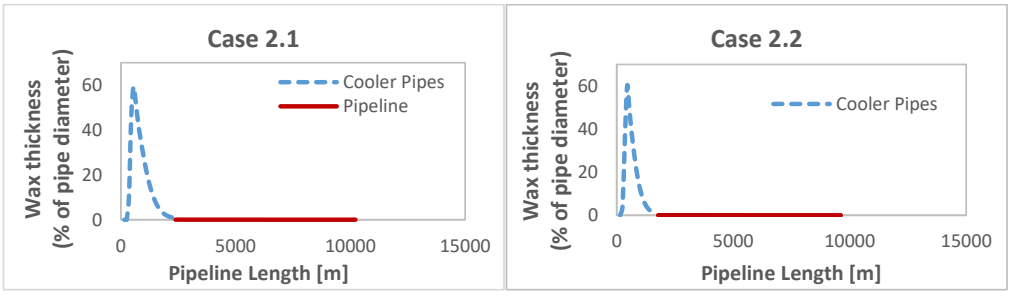

Figure 8.12. Wax thickness profile for Case 2 after 90 days of production

For Case 3, a heat exchanger was connected at the beginning of the production system. Here the required duty that guarantee thermal equilibrium between the production fluid and the surrounding was 2.2 MW. To compare, a subsea heat exchanger with forced cooling advertised by the company NOV have a typical cooling capacity of 10 to 20 MW per unit [69]. The added pressure drop was 0.61 bara, this value is not taking into account the pressure loss through the heat exchanger. This case is the more efficient to control wax deposition, however is the less friendly for pigging due to the complex structure of heat exchangers. Figure 8.13 shows the wax thickness profile for Case 3 after 90 days of production.

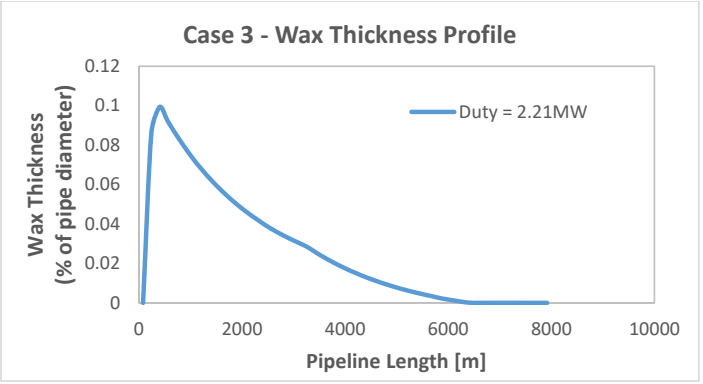

Figure 8.13. Wax thickness profile for Case 3 after 90 days of production

8.6. Electrical Heat Tracing study

This section presents the feasibility study perform on Electrical Heat Tracing. For this, four heating strategies to avoid the formation of wax particles in subsea pipelines, were applied to a synthetic field. Two pipeline lengths were considered in this study: 8 km and 50 km. The strategies consisted of warming up the wall of the pipeline to keep the bulk flow temperature above the wax appearance temperature. The heating effect results from the heat generated when an electric current flows through a conductive material. The four strategies are:

- *Strategy 1: Continuous heating of the whole pipeline*. For a period of 90 days, the total length of the pipeline was continuously heated and the minimal power required to keep the bulk flow above the WAT was calculated.

- *Strategy 2: Continuous heating of a section of the pipeline*. Here, the pipeline was divided into two sections. In the first section, which goes from the beginning of the flowline until a certain length, the flow was allowed to naturally cool down. In the other section, which goes from the end of the first section to the end of the pipeline, the wall of the pipeline was continuously heated to maintain the flow over the WAT. The point, in the pipeline, at which the temperature of the flow reaches the WAT, determines the length of the sections. For the pipeline of 8 km, the first 2.4 km were not heated and the heat was applied in the remaining 5.6 km. For the pipeline of 50 km, the heating was applied in a section of 49.7 km. The minimal power required to avoid wax formation in the pipeline inner wall was calculated.

- *Strategy 3: Intermittent heating of the whole pipeline*. The total length of the pipeline was intermittently heated by periods of 1 day, 12 hours, 8 hours and 4 hours respectively, over 90 days. The minimal power consumption required to avoid wax formation was calculated.

- *Strategy 4: Continuous heating of the pipeline by sections*. In this strategy, the pipeline was divided into sections of equal lengths and heat was applied every other section for a period of 90 days. Two section lengths were tested: 500 m and 100 m. The minimal power required was calculated.

The strategies were tested with two pipeline lengths: 8 km and 50 km. The four strategies were applied in the 8 km pipeline, while only strategies 1, 2 and 3 were used in the 50 km pipeline. The forth strategy was not implemented in the 50 km pipeline due to the high amount of sections, which made difficult the setup of the simulation.

The influence of the insulation was also studied. For this, all the strategies were tested twice, with insulation and without insulation in the pipeline.

8.6.1. Study Case

The production system used consists of a horizontal pipeline, with an internal diameter of 17 cm. The fluid enters the pipeline with a mass flow of 17.51 kg/s, which represents a standard flow rate of 14e03 Sm3/d for 32 API gravity. Other parameters used are presented in Table 8.3.

The pipeline's wall materials were the same as the one used in the study of Cold Flow. The information is presented in Table 8.1.

The wax deposition model used was RRR. The total simulation time was 90 days, with a maximum time step of 1000 s and a minimum of 1 s. The information given above was used for all the strategies.

Two criteria were used to determine the minimum required power. In one criterion, the fluid temperature in the pipeline cannot be less than the WAT. The second criterion, defined by the author and applied in strategies 3 and 4, was that the maximum thickness of the wax layer deposited in the pipeline could not be higher than 1% of the pipeline ID.

Table 8.3. Parameter used for Study Case

Property	**Value**
Oil specific gravity	0.87
Gas specific gravity	0.95
Fluid inlet temperature (°C)	70.00
GVF	0.09
Water cut	0.00
WAT (°C)	22.00
Ambient temperature (°C)	5.00
Outlet pressure	25.00
External convective coefficient for heat exchange (W/m-K)	500.00

8.6.2. Results and Discussion

The aim of the study is to generate conclusions about the efficiency of each active heating strategy and to rank them based on this criterion. The author chose to quantify the efficiency of a strategy by computing its average power consumption per meters of pipeline. The lower the average power consumption is, the more efficient the strategy is.

It is important to highlight that the results showed for the third strategy (intermittent heating of the whole pipeline) correspond to the heating period of 1 day, as the most efficient period with the lower percentage of wax formation along the pipeline.

Figure 8.14 shows the required power consumption per meter for both pipeline lengths with insulation. For this case, strategy 1 and strategy 2 were the less power-consuming strategies, both for the 8km and the 50km pipelines, with a power consumption per meter no greater than 400 W/m. On the other hand, for both pipeline lengths, strategy 3 tripled the energy requirements with a power consumption per meter of 1500 W/m, been the less energy-efficient strategy. Strategy 4, only applied to the 8 km pipeline, had a medium power consumption per meter of 850 W/m for sections of 500 m and 750 W/m for sections of 100 m.

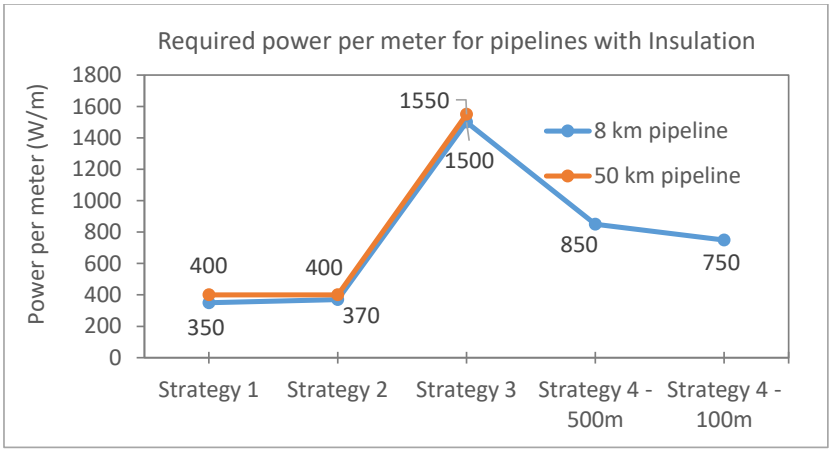

Figure 8.14. Required power consumption per meter of pipeline with insulation for both pipeline lengths, 8 km and 50 km

Figure 8.15 shows the required power consumption for both pipeline lengths when there is no insulation in the pipelines. In this case, the power consumption for all studied strategies increased considerably in comparison with the case when the pipelines have insulation. Strategies 1 and 2 were still the most power-efficient. However, the required power consumption per meter increased to 5200 W/m in strategy 1 and 5300 W/m in strategy 2, for both pipeline lengths. For strategy 3, (both pipeline lengths) and strategy 4, with pipeline segments of 500 m, the power consumption per meter was 22000 W/m, resulting in the less power-efficient strategies. Strategy 4 with pipeline segments of 100 m had medium power consumption of 12000 W/m.

Based on the results obtained, one can conclude that to avoid wax formation, it is best to continuously heat the entire pipeline or its critical section, where the fluid temperature drops

below the WAT. This means that strategies 1 and 2 are the most efficient compared to the others, been their power consumption per meter less than half of that required by the other strategies.

The less efficient strategy is intermittent heating. This strategy has non-heating periods where, for all the cases analyzed (1 d, 12 hr, 8 hr and 4 hr), the fluid temperature drops below the WAT (where wax can potentially precipitate). High power rates are then required to heat the fluid again to a temperature above the WAT.

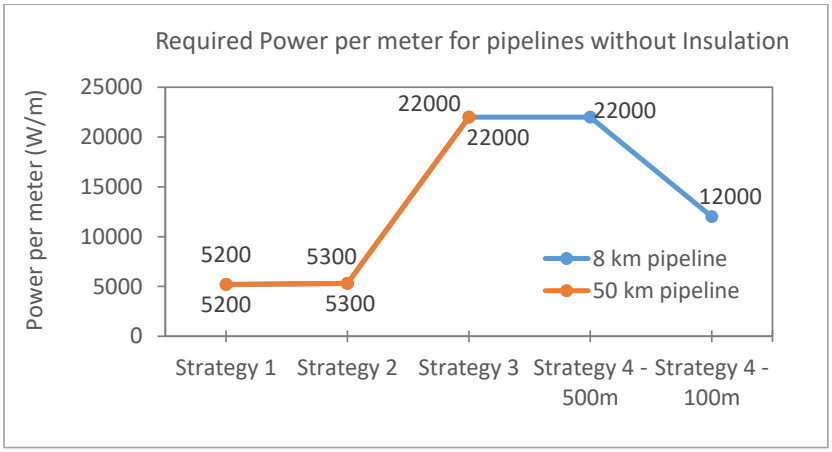

Figure 8.15. Required power consumption per meter of pipeline without insulation for both pipeline lengths, 8 km and 50 km

In strategy 4, where the heating was applied in intercalated segments of equal lengths, the power required in the heated sections depends on the segment length. The power has to be such that, it guarantees that the fluid temperature will not drop below the WAT in the non-heated sections. In other words, the temperature at the end of the heated sections has to be high enough to avoid wax formation in the subsequent non-heated sections.

Pipeline insulation helps to reduce the heat transfer between the bulk flow and the ambient. Thus, the power needed to heat the fluid above a certain temperature is lower when the pipeline has insulation. It was observed that, on average, a decrease of 86% in the overall heat transfer coefficient leads to a decrease of 93% in the required power.

To confirm the results obtained, the total power consumption is analyzed below.

Figure 8.16 and Figure 8.17 show the total power consumption of all studied strategies for both pipeline lengths, and for pipelines with insulation (Figure 8.16) and without insulation (Figure 8.17). In both figures, it can be seen that strategies 1 and 2 were still the most power-efficient strategies, while the less efficient was strategy 3.

In strategy 1, the power consumption per meter, along the 8 km pipeline, was at most 5% lower than the one in strategy 2. In other words, strategy 2 required a higher power capacity installed in the pipeline. On the other hand, the total power consumption of strategy 1 was 33% higher than strategy 2, when the pipeline has insulation (Figure 8.16), and 40% higher than strategy 2 for pipeline without insulation (Figure 8.17). This means that, for this specific case, where the

pipeline length was 8 km and the heated section in strategy 2 was 5.6 km, it is most energy-efficient to apply strategy 2.

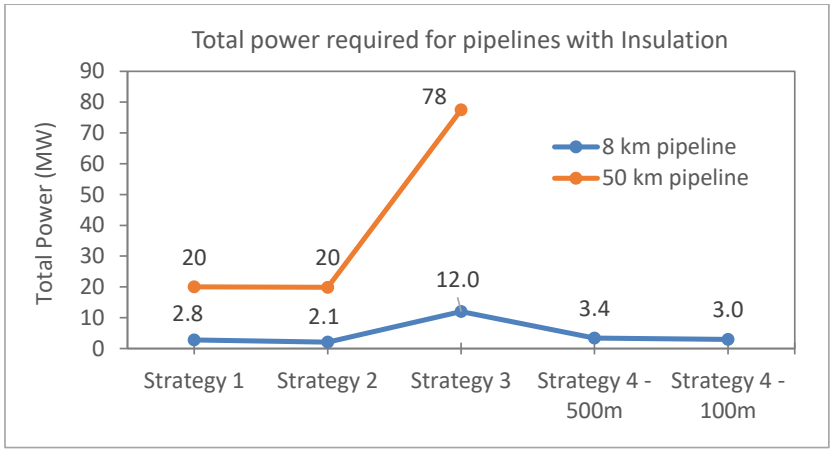

Figure 8.16. Total power required for pipelines with insulation

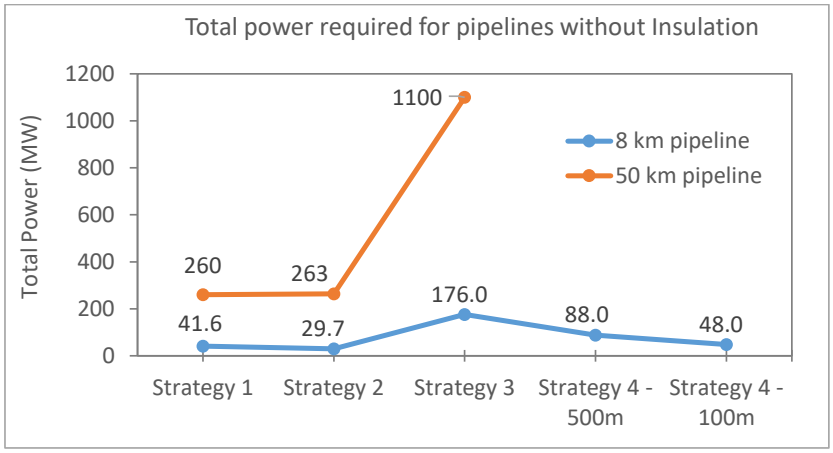

Figure 8.17. Total power required. For pipeline without insulation

In the case of the 50 km pipeline, for pipeline with insulation, the total power consumption of strategy 1 and 2 was the same. For pipeline without insulation, the total power consumption of strategy 1 was 1.15% lower than for strategy 2. Since the heated section in strategy 2 had almost the same length as in strategy 1, the total power consumption was similar for both strategies.

Figure 8.16 and Figure 8.17 confirms that strategies 3 and 4 require the highest power consumption, been the less power-efficient one, strategy 3, intermittent heating.

It is important to highlight that the total power consumption depends on the pipeline length. It is economically more efficient to apply heating to the shorter pipelines since they require less power consumption.

8.7. Observations

The aim of this study was to analyze novel approaches for the control of one of the most typical flow assurance issues for offshore oil fields (Wisting-like fields), wax deposition. Considering solutions to possible flow assurance issues is an important part of the field development planning of a field.

Two strategies were considered in this study, Cold Flow and Active Heat Tracing. The analysis were performed using a commercial 1D mechanistic multiphase flow simulator. The wax deposition was model using RRR model, which consider molecular diffusion and shear dispersion as wax deposition mechanisms. The most important observations are presented below for each approach analyzed.

8.7.1. About Cold Flow

Three wax cold flow concepts were successfully studied for installation at the upstream end of the main transportation pipeline. The main contribution of this study is the simplified technical validation of the wax cold flow concept in a synthetic case of a Wisting-like field. The validation consisted of performing a numerical estimation of required cooling distances and performance of three cooling arrangements: a non-insulated pipe section, a parallel pipe heat exchanger with natural cooling and a heat exchanger with forced cooling. The analysis was performed with a commercial 1D mechanistic multiphase flow simulator. The main conclusions of this study are:

- For the non-insulated pipe section concept, the required length of the loop was at least 3 km, which can be impractical for some production systems. For most cases, the added pressure drop due to the presence of the loop was negligible (around 10%).

- When using a passive cooler with a bundle of parallel pipes the required length for cooling was reduced considerably (30 – 50%) compared with the case 1. However, the lengths and diameters required might still be too large for placing them inside a compact subsea structure. Another drawback of this concept is that the cooler uses smaller pipe diameters, which means that the pressure drop will increase and the pipe will get block in shorter times, needing to be cleaned often.

- In the active cooler case, the minimal duty obtained was comparable with subsea heat exchangers advertised by a manufacturer. The disadvantage of this concept is that it is difficult to pig due to the complexity of the equipment and the added pressure drop. The authors didn't perform a review or studied methods to remove wax in such equipment. However, the following reference [67] is given as a possible solution.

8.7.2. About Electric Heat Tracing

Four strategies of electric heating were studied for two pipeline lengths, 8 km, and 50 km. Their required power consumption was compared with each other and the most efficient strategies were determined. At the same time, the effect of having insulation in the pipeline was addressed.

- The most power-efficient strategies are strategy 1 and strategy 2, where the pipeline or a section of it, is continuously heated.

- The less power-efficient strategy is intermittent heating of the pipeline (strategy 3), since the fluid needs to be heated above the WAT after every non-heated period.

- For strategy 4, heating by sections, it is important to determine an optimal section length that guarantees the lower power consumption and the lower formation of wax in the no-heated sections.

- We have also concluded that insulation plays an important role in active heating, since it reduces the heat transfer between the fluid and its surroundings, lowering the power requirements. A decrease of 86% in the overall heat transfer coefficient led to a decrease of 93% in the required power.

- Finally, the total power consumption of any strategy depends on the length of the pipeline to be heated.

Chapter 9

Effect of cold flow wax control method on Wisting study case

In the study case presented in this thesis (Chapter 2), pipeline insulation was the technique considered to avoid wax. In this chapter, the Cold Flow method that was studied in Chapter 8 is applied to this study case to control wax. The Cold Flow method consists of having an additional section of uninsulated flowline where production fluids cool to seabed temperature and all wax present in the fluid precipitates on the walls. This pipe section is then pigged frequently, and the wax slurry is transported to the FPSO together with the production stream. Results presented in chapter 8 are used in this chapter to modify the input and parameters of the models used in Chapter 7 and their effect on the results presented earlier is evaluated.

It was considered that the implementation of this flow assurance concept to the study case has the following main consequences:

- The pressure drop from well to topside facilities is increased due to the additional pipe length and the higher viscosity of the low temperature oil. This will therefore reduce the magnitude of field production potential values compared to the original case.
- Change in capital and operational expenditures related to the wax control loop.

The other study presented in Chapter 8, regarding alternative operational modes of electric heat tracing for pipeline, was not considered nor integrated further with the field development decision support method. The implementation of this technology would affect mainly the capital and operational costs. The CAPEX would experience an increase associated to the costs of the heat tracing system. The OPEX would experience a decrease associated to the reduction in chemical injection fluids, and an increase associated to the costs of maintenance of the heat tracing system and power consumption. However, it is considered that these changes would be modest and could therefore be accounted for by performing uncertainty analyses on the cost figures and the production potential. In addition, the implementations of heat tracing would not have an important effect on the production potential curves, since these proxy models capture the performance behavior of the field only.

9.1. Cold flow system

The Cold Flow system used in this chapter correspond to the uninsulated pipe section concept presented in section 8.5.2. However, due to the fact that the technology is novel, immature and yet untested in the field, there are no cost figures available for this concept yet. Therefore, the

cost figures of the Cold Flow system were taken from Vinatovskaja [51], who performed a feasibility study and an economic evaluation of the SINTEF-BP Cold Flow Technology, which is similar to the technology considered in Chapter 8. The values reported are presented in Table 9.1.

Table 9.1. Cost estimation of SINTEF-BP Cold Flow Technology

Component	Unit Number	Costs per unit (Cost per meter) (USD)*	Cost per unit (NOK)
Extra pipeline	4092	600	5 400
Reactor unit	1	15 000 000	135 000 000
Splitter	1	1 500 000	13 500 000
Subsea pump	1	3 000 000	27 000 000
Subsea Separator	1	3 000 000	27 000 000
	Total	22 500 000	224 586 000
* Data presented by Vinatovskaja.			

Besides the costs associate to the application of the Cold Flow system, there is a reduction in CAPEX associated to the pipeline. Since Cold Flow enables using an uninsulated pipeline downstream the wax control loop, the costs of the insulation has to be eliminated from the CAPEX estimation performed to generate the cost models in Chapter 4. According to reference [50], the deployment of the bare steel pipeline in subsea environment would cost between 0.5 and 0.8 MM USD per kilometer instead of 1 MM USD per kilometer for the insulated pipeline. This means a reduction of 20 – 50 % in the cost of pipeline installation.

Regarding the OPEX, BP concluded that the wax Cold Flow technology generates savings of around 10% compare to other solutions [50] [51].

Applying the wax Cold Flow method to the study case presented in this thesis affects the production performance of the field due to changes in pressure drop between wells and separation facilities and in the cost figures. To consider these effects, new production potential proxy models, and CAPEX and OPEX equations were generated considering additional expenses and saving mentioned earlier. The Cold Flow concept was applied to the most cost-effective development strategy obtained in the evaluation presented in chapter 7. This is, using TLP as topside facility and multiphase boosting and water injection (MPB + WI) for production support. The results obtained were compared against the original results to evaluate the effect that the implementation of a wax Cold Flow method has on the optimization results. Additionally, the effect of uncertainties such as reservoir size, productivity index, CAPEX and OPEX was evaluated.

Other risks and expenses associated with the novel technology, for example complete failures, frequent breakdowns, frequent maintenance and intervention, development and qualification costs were not considered in the evaluation.

9.2. Generation of production potential proxy models

For the new proxy model of the production potential, the well/network model was changed to include an additional pipeline section after each manifold. This section represents the Cold Flow system and has a length of 4092 m, which is the required cooling length for an 8 inches pipeline presented in Figure 8.8 (Chapter 8). The tank model used to simulate the reservoir remained the

same as the one used in the original study case. The new proxy models were generated as explained in Chapter 3, and Figure 9.1 shows the production potential oil rate curves obtained against the original curves from the base study case.

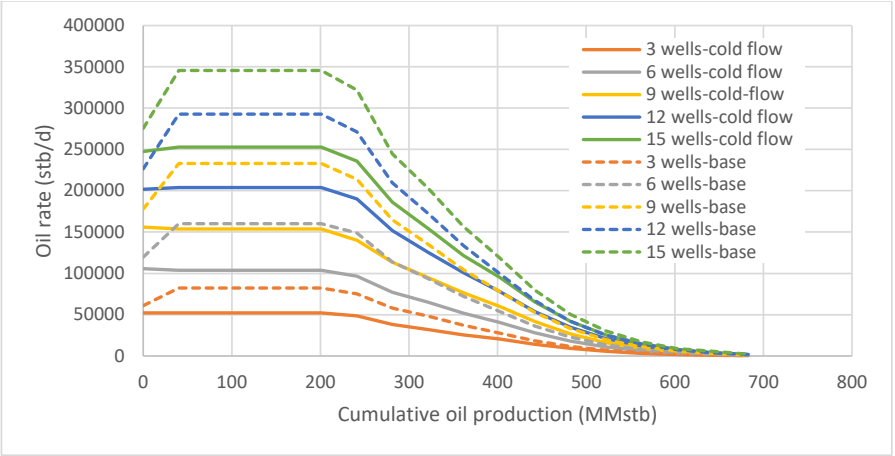

Figure 9.1. Proxy model of oil production potential. Comparison between the base study case and the case with Cold Flow

9.3. Generation of cost models

The capital and operational expenditures were modified based on the cost information of the SINTEF-BP Cold Flow Technology. For the CAPEX, the costs associated to the pipeline installation were reduced by 35% to represent the savings of using bare pipelines instead of insulated pipelines. At the same time, the cost of the extra pipeline used to cool down the production stream and the components of the Cold Flow loop (Table 9.1) were added. The OPEX was reduced by 10% as indicated above.

These changes were applied to the cost data to generate the cost equations used in Chapter 7, using TLP platform. The CAPEX associated to the pipeline installation and the OPEX were different for each cost data point, while the CAPEX associated to the cold flow system was a constant value applied to each cost data point. Then, new cost equations were generated from a multivariable linear regression ((9.1 and (9.2).

$$E_{cap,TLP} = 0.0074 \cdot q_o^{capacity} + 29.83 \cdot q_g^{capacity} + 0.0106 \cdot q_w^{capacity} + 264.59 \cdot Nw^{field} + 11588.29 \quad (9.1)$$

$$E_{op,TLP} = 6.00E-4 \cdot q_o^{capacity} + 0.8037 \cdot q_g^{capacity} + 1.96E-4 \cdot q_w^{capacity} + 12.61 \cdot Nw^{field} + 552.54 \quad (9.2)$$

9.4. Optimization to estimate production and drilling scheduling

The optimization formulation presented in Chapter 5 was applied with the new proxy models generated in this chapter using the same assumptions considered in section 5.2.2. Figure 9.2 shows the comparison between the production profile obtained with the original study case (presented as “no cold flow” in the plot’s legend) and in the case applying cold flow (presented as “cold flow” in the plot’s legend). Table 9.2 presents the drilling schedule obtained in the

original study case and the case applying the Cold Flow. Finally, the comparison between the NPV obtained for both cases is presented in Table 9.3.

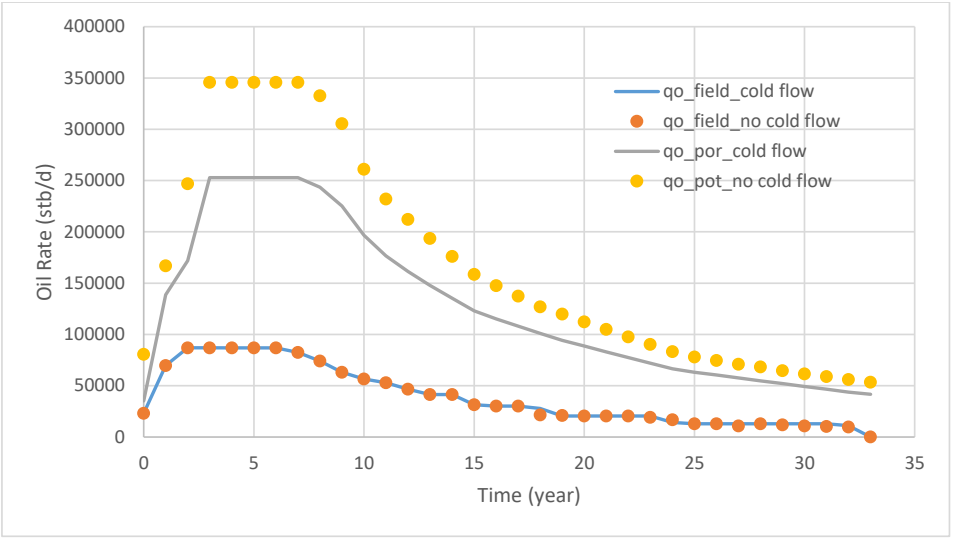

Figure 9.2. Production potential comparison between the original study case and the case with Cold Flow

Table 9.2. Drilling schedule comparison between the original study case and the case with Cold Flow

	Number of wells drilled per year						**Total Nw**
Year	**1**	**2**	**3**	**4**	**5**	**…**	
Wisting study case (no cold flow)	4	4	4	3	0	0	15
Study case with cold flow	4	4	4	3	0	0	15

Table 9.3. NPV comparison between the original study case and the case with Cold Flow

Case	**NPV (billion NOK)**
Original study case (no cold flow)	74.71
Study case with cold flow	78.64

Although the production potential of the field is reduced when applying Cold Flow, the optimal production profile obtained for this new case remains the same in comparison to the original study case (Wisting study case). The reduction in the production potential occurs because the pressure drop in the production system increases when applying Cold Flow. However, the optimal production profile is the same in the cases with and without the Cold Flow because the constraints consider in the optimization formulation make infeasible a higher oil production. If a different case were studied, where the field had to be operated at potential or close to potential, the application of Cold Flow method could have a more important impact in the optimal production profile when compared against the results obtained here.

From Table 9.2, it is observed that applying Cold Flow to the Wisting study case, does not influence the drilling schedule of the production system. The same drilling schedule was

obtained for both cases, which is to drill the maximum number of wells allowed in each time step until reaching the total number of wells that the field can have.

The NPV obtained for the case with Cold Flow is higher than the one obtained originally in the Wisting study case, been the relative error between both values 5.26%. Since the production profile for both cases is the same, which means that the revenues is also the same, the difference in NPV is consequence of the changes in cost. The application of Cold Flow represents a reduction in CAPEX and OPEX, which generates a lower NPV for the case with Cold Flow.

9.5. Uncertainty analysis

The effect of uncertainty was evaluated using discrete cases with probability trees. Uncertainties in the production potential curves (proxy models) and the costs were considered. More specifically, the uncertainty variables studied were, the reservoir size, productivity index, CAPEX and OPEX. For the CAPEX, uncertainty in the cost associate to the pipeline installation and uncertainty in the costs associated to the components of the Cold Flow system were contemplated.

For the uncertainty on the reservoir size and productivity index, the same values used in the Wisting study case (section 7.1.5) were used in this analysis. Figure 9.3 shows the decision tree diagram that represents the uncertainties for the production potential curves.

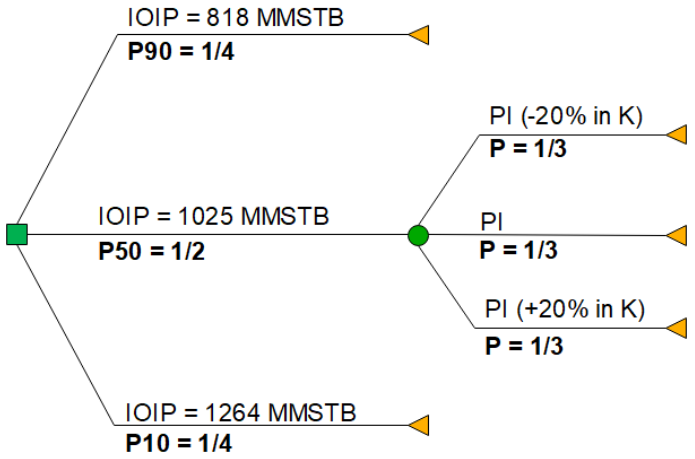

Figure 9.3. Decision tree diagram for uncertainty in production potential (study case with cold flow)

As mentioned previously, the application of Cold Flow to the production system results in a reduction in the cost of pipeline installation in the range of 20% to 50%. Considering this information, the cost figures of CAPEX estimates in section 9.3 where changed using three percentages of reduction in cost, 20%, 35% and 50% (the cost associated to the installation of the Cold Flow system and the OPEX remained constant) and linear regression was perform to get new cost equations. A similar process was performed for the uncertainty in the CAPEX associated to the installation of the Cold Flow system. The cost values given in Table 9.1 were change in a range of ±20 %, while maintaining the cost of the pipeline and the OPEX installation

constant. Finally, the OPEX used in the optimization, was varied in a range of ±20 %, while keeping constant the CAPEX. Figure 9.4 shows the decision tree diagram for the uncertainties in cost considered in this analysis.

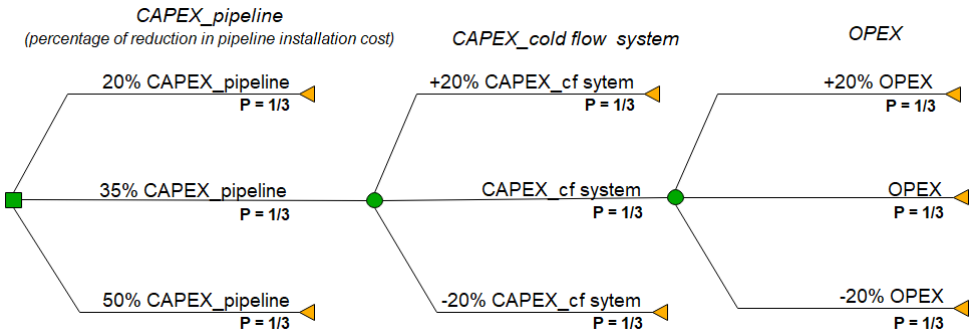

Figure 9.4. Decision tree diagram for cost uncertainty (study case with cold flow)

The uncertainty in the production potential curves and in the cost were combined to give 35 uncertainty cases, to which the optimization problem was applied. For each uncertainty case, the maximum NPV was estimated. It was obtained that the NPV can range between 63.67 and 92.38 billion NOK. This can be observed in Figure 9.5, which shows the cumulative distribution function of the NPV obtained for this analysis.

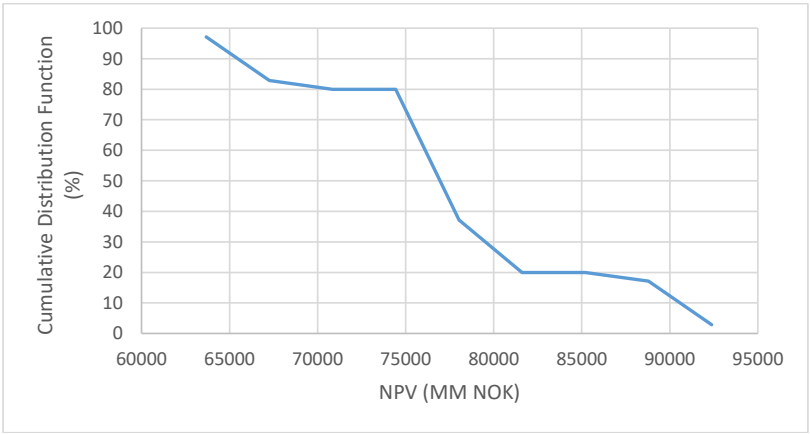

Figure 9.5. NPV's cumulative distribution function (study case with cold flow)

Table 9.4. NPV's probabilities, comparison between original study case and case with cold flow

NPV (billion NOK)			
	P10	**P50**	**P90**
Study case with cold flow	66.01	78.64	89.96

In the case of the uncertainty analysis, it is not possible to compare the results obtained here and in the base case (Wisting study case), because for both cases the uncertainty variables considered were not the same. For the Wisting case, uncertainty in the production system layout and DRILLEX were analyzed, while these variables were dropped out from the Cold Flow analysis. In addition, for the Cold Flow CAPEX and OPEX were varied individually in the

uncertainty analysis, while in the base case CAPEX, OPEX and DRILLEX were varied simultaneously. For this, the results of each uncertainty analysis show the effect of different parameters over the NPV.

9.6. General Observations

The field development method presented in this thesis was used to determine the optimal production profile and drilling schedule of the Wisting study case combined with the flow assurance technology, Cold Flow. The development strategy used in this analysis was to use TLP as processing facility and multiphase boosting plus water injection for production support, which was demonstrated to be the most cost-effective strategy in chapter 7.

The implementation of Cold Flow to the Wisting study case, affects the production potential curves that represent the production performance of the field and the cost figures. Therefore, new proxy models were generated using information obtained in chapter 8 and cost information from SINTEF-BP Cold Flow Technology.

With the new proxy models, numerical optimization was performed. From this, it was concluded that, although the implementation of Cold Flow to the study case reduces the production potential of the field, due to the increase in pressure drop, the optimal production profile did not change in comparison with Wisting study case. This occurs because, the production profile obtained is defined by the optimization constraints imposed, and a higher production profile would be infeasible. The implementation of Cold Flow to a different case that requires to produce at or close to the field potential, could have a more important impact on the optimal production profile.

Regarding the drilling schedule, applying Cold Flow to the Wisting study case does not affect the results of this parameter. The same drilling schedule was obtained for the Wisting study case and the case applying Cold Flow.

The NPV obtained using Cold Flow resulted to be marginally higher than the one obtained in Wisting study case. This difference was consequence of the reduction is cost thanks to the implementation of the Cold Flow system.

Finally, an uncertainty analysis was performed considering uncertainty is the reservoir size, well productivity index, CAPEX associated to the pipeline installation, CAPEX associate to the Cold Flow system and OPEX. It was obtained that the NPV can range between 63.67 and 92.38 billion NOK.

Chapter 10

Conclusions and recommendations

This chapter presents a summary of the results obtained and the main conclusions extracted from these results. At the end of this chapter, recommendations for future works based on this study are presented.

The first result obtained is a verification and a substantiation on a field scale methodology to provide decision support on field design in early stages of the field development process. The methodology comprises of the following steps:

- Representing the production performance of the integrated reservoir-well network system with a proxy model. The proxy model consists of oil production potential, GOR and WC tables expressed as function of the cumulative oil produced and the number of production wells. These proxy models are obtained by coupling a reservoir tank model with a steady-state well/network model.

- Develop linear models for cost figures such as CAPEX, OPEX and DRILLEX by applying linear regression on cost values for varying number of wells, maximum oil, water and gas rates.

- Formulate an efficient mathematical optimization problem to find optimal production and drilling schedule that maximize NPV using the proxy model of the production system and linear cost functions for CAPEX, OPEX and DRILLEX. The non-linearities are represented with piece-wise linear functions using SOS2 variables.

- Uncertainty analysis on the results of the optimization using probability trees.

If several development alternatives are considered, then cost proxy models and production performance proxy models should be derived for each.

While the overall methodology presented here might be similar to the conventional ones practiced by the industry or presented in previous research, the details of the modeling and the formulation of the optimization, as suggested and verified in this thesis, are novel and constitute improvement.

The methodology has been applied to produce and monetize a synthetic reservoir based on data on the Wisting Field.

Nine (9) development strategies were compared and ranked. The strategies were obtained from the combination of three recovery methods (gas lifted wells, gas lifted wells with water injection and multiphase boosting with water injection) and three topside facilities (TLP, FPSO and Tie-Back). The best- case strategy, i.e. the one that gives the highest profit, was determined.

Observations on the obtained results suggest that:

- The optimal oil production profile is mainly influenced by the recovery method used. The effect of the type and cost of topside facility over the amount of oil produced resulted to be negligible.

- When using gas lifted wells, optimal production is obtained when operating close to the production potential. When water injection and/or multiphase boosting are added, the recovery capacity of the field increases. However, in such cases it is not optimal anymore to produce at potential rate. The highest production is obtained using multiphase boosting with water injection.

- The drilling schedule is mainly influenced by the costs of drilling a well and the capacity of the strategy to generate enough revenue to overcome that cost. For the case studied here, the drilling schedule is not affected greatly by the strategy used. It consists of drilling the maximum number of wells allowed in each time step until the total number of wells that can be drilled in the field is reached. In this thesis, the effect of increasing the maximum number of wells allowed in the system was not addressed.

- The best development concept to exploit the synthetic field studied was using TLP combined with multiphase boosting and water injection. This result was somehow expected, since the topside facility that generate the lowest costs is TLP and the recovery method that produced the highest oil rate along the field life is multiphase boosting with water injection.

- The effect of uncertainty was evaluated using discrete cases with probability trees. A total of 189 cases were analyzed, where uncertainty in the reservoir size, network layout, productivity index and costs were considered. It was determined that the NPV probability ranges between 18 and 96 billion NOK approximately. When applying uncertainty analysis, different field configurations were evaluated, meaning that additional proxy models had to be created. Therefore, they correspond, in a way, to slightly different fields than the original case

- The proposed methodology successfully finds optimal field design features while quantifying the effect of uncertainty with running times suitable for current field development workflows.

Additionally, the method was applied on a field with Cold Flow for wax control. The Wisting study case was changed to include the effect of Cold Flow on the production performance proxy models and the cost equations. The main observations of the results obtained are:

- The implementation of cold flow to the study case reduces the production potential of the field, due to the increase in pressure drop. However, the optimal production profile did not change in comparison with Wisting study case, due to the optimization constraints imposed. The implementation of cold flow to a different case that requires

producing at or close to the field potential could have a more important impact on the optimal production profile.

- Regarding the drilling schedule, applying cold flow to the Wisting study case did not affect the results of this parameter when compared against the base case.

- The NPV obtained using cold flow resulted to be marginally higher than the one obtained in Wisting study case. This difference was consequence of the reduction is cost thanks to the implementation of the cold flow system.

- The effect of uncertainty in the reservoir size, well productivity index, CAPEX associated to the pipeline installation, CAPEX associate to the cold flow system and OPEX was evaluated using probability trees. It was obtained that the NPV can range between 63.67 and 92.38 billion NOK.

The above complete the list of observations on the field development part of the dissertation. Following are results and observations obtained in the two tasks investigated in flow assurance part.

In the first task, a sensitivity analysis of three cold flow approaches for wax control in a subsea production pipeline was performed. These was done for a synthetic production system with a production pipeline of 8 km. The three concepts approaches are: 1) a non-insulated pipe section, 2) a parallel pipe heat exchanger with natural cooling, and 3) a heat exchanger with forced cooling. The sensitivity analysis consisted in study the influence of the external convective coefficient of heat transfer, pipe diameter and water cut. For concepts (1) and (2), the minimum required cooling length was determined. For concept (3) the minimum duty needed to cold down the fluid to ambient temperature, was found.

The results obtained are valid for the particular study case analyzed in this thesis, the conclusion might change for another cases. The most relevant results are:

- For the non-insulated pipe section concept, the required loop length obtained is about 3 km. Therefore, this concept can be useful for remote production systems where the cooling length of the loop can be considered small in comparison with the total system length. For most cases studied, the added pressure drop due to the presence of the loop was negligible (around 10%).

- The required cooling length of the parallel pipe heat exchanger with natural cooling was reduced considerably (30% - 50%) compared with the non-insulated pipe section concept. However, the lengths required might still be too large for some production systems. Another drawback of this concept, in comparison with concept (1), is that the cooler uses smaller pipe diameters, which means that the pipe will get blocked in shorter times, needing to be cleaned often.

- The minimal duty obtained for concept (3) was comparable with subsea heat exchangers advertised by a manufacturer. The disadvantage of this concept is that it is difficult to pig due to the complexity of the equipment and the added pressure drop.

In the second flow assurance task, four strategies of electric heating were studied for two pipeline lengths, 8 km, and 50 km. The strategies were: (1) continuous heating of the whole

pipeline, (2) continuous heating of the critical section of the pipeline, (3) intermittent heating of the whole pipeline, and (4) continuous heating of intercalated pipeline sections. The required power consumption of each strategy was determined and compared against each other. At the same time, the effect of having insulation in the pipeline was addressed. Conclusions derived from the results are:

- The most power-efficient strategies are to continuously heat the whole pipeline or the critical section of pipeline. The critical section of the pipeline goes from the point at which the produced fluid reach the WAT to the downstream end of the pipeline.

- The less power-efficient strategy is heating intermittently the pipeline (strategy 3). This is because, during the non-heated periods, the fluid temperature falls below the WAT and it needs to be heated above this point in every subsequent heated period. This conclusion was observed for all the periods tested, the results can differ for other periods.

- For strategy 4, heating by sections, it is important to determine an optimal section length that guarantees a low power consumption and low wax formation in the non-heated sections.

- Insulation plays an important role in active heating, since it reduces the heat transfer between the fluid and its surroundings, lowering the power requirements.

- The total power consumption depends on the length of the pipeline to be heated.

The above concludes the results and the observations of the flow assurance part of the dissertation.

10.1. Recommendations for future works

For future works on the automated methodology for field development, it is recommended to:

- Increase the flexibility of the method by adding the option to choose the objective variable. Besides NPV, possible objective variables could be oil/gas recovery, operational flexibility, CO2 emissions, break-even point, etc.

- Explore formulations for performing multi-objective optimization.

- Improve the optimization formulation to reduce the running time. For this, it is suggested to perform a study on the optimal number of break points used for the piecewise linear approximation of the non-linear functions, as well as perform a study comparing different PWL approximation models.

- Modify the methodology to allow the option of work with multiple independent reservoirs.

- Analyze the effect of the reservoir model used by comparing the results obtained using reservoir simulator versus material balance.

- For the uncertainty analysis, include additional uncertainties like water breakthrough time, water coning, oil price, etc. In addition, perform the uncertainty analysis using stochastic methods, like Monte Carlo or Latin Hypercube, instead of probability trees.

- Include the effect of flow assurance technologies on the proxy models of the production potential and costs.

For future works on the feasibility studies on cold flow concepts and active heating strategies, it is recommended to expand the studies by testing other operating conditions, liquid properties and different wax deposition models. In addition, it is recommended to perform experimental studies of the topics analyzed to validate the results obtained in this work.

References

[1] Angga, I G. A. G. “Automated Decision Support Methodologies for Field Development: The Safari Field Case. Petroleum Engineering, Specialization Project. NTNU-Norway. 2018.

[2] Angga, I G. A. G. “Automated Decision Support Methodology for Field Development: The Safari Field Case”. Master Thesis. NTNU-Norway. 2019

[3] NORWEGIAN PETROLEUM DIRECTORATE. NPD FactPages. [ONLINE] Available at: http://factpages.npd.no/FactPages/Default.aspx?culture=en. [Accessed 4 December 2018].

[4] Jahn, F., Cook, M. and Graham, M. (2008). Hydrocarbon Exploration and Production. Volume 55. Second edition. Amsterdam. Elsevier Science. ISBN: 9780080568836.

[5] Barroux, C. C., Duchet-Suchaux, P., Samier, P. & Nabil, R. “Linking reservoir and surface simulators: how to improve the coupled solutions”. SPE European Petroleum Conference. Paris, France. 24-25 October 2000.

[6] Schlumberger, Avocet Integrated Asset Modeler, 2014.1

[7] Petrostreamz, Pipe-It.

[8] Stanko, M., “Petroleum Production Systems”. Compendium in Field Development and Operation Course dictated at the Petroleum and Geoscience Department, NTNU. 2019.

[9] Petroleum Experts IPM, MBAL, v13.0, 2016.

[10] Schlumberger, “PIPESIM® v12.02”, 2012.

[11] Joshi, S., D., “Horizontal Well Technology”, Tulsa-Oklahoma, Pennwell Books, 1991.

[12] Schlumberger, PIPESIM 2012.2 Open Link Reference Manual. 2012

[13] Petroleum Experts IPM, GAP, v11.0, 2016.

[14] Schlumberger. “ECLIPSE 2019.2,” 2019.

[15] NORWEGIAN PETROLEUM DIRECTORATE. NPD FactPages. [ONLINE] Available at: https://factpages.npd.no/FactPages/default.aspx?nav1=field&nav2=PageView%7CAll&nav3=43686. [Accessed 16 December 2019].

[16] Olaussen, S., Beck, L., Falt, L., Graue, E., Jacobsen, K., Malm, O. and South, D. “Gullfaks Field-Norway East Shetland Basin, Northern North Sea”. American Association of Petroleum Geologists. Pub. Id: A020 (1992). 1992.

[17] Nunes, G., Hemerly Cost, A., de Figueiredo,J. “An Integrated Field Development Methodology for Improving FEL1”. Offshore Technology Conference Brasil. Rio de Janeriro. 2017.

[18] Nunes, G., da Silva, A and Esch, L. “A Cost Reduction Methodology for Offshore Projects”. Offshore Technology Conference. Texas. 2018.

[19] Kuznetzov, M. Sevastyanova, K. Tarasov, P. Zilber, V. and Nekhaev, S. “Capital Cost Estimation Method for Artic Offshore Oil Projects”. SPE Artic and Extrem Environments Conference & Exhibition. Moscow, Russia. 2011.

[20] Acona, “ACES v5.0”, 2018.

[21] Jonsbråten, T., “Oil Field Optimization under Price Uncertainty”. The Journal of the Operational Research Society, 1998, 49(8), 811-818. doi:10.2307/3009962.

[22] Nazarian, B. “Integrated Field Modeling”. PhD Thesis. NTNU. Norway. 2002.

[23] Tupac, Y. J., Almeida, L. F., and Vellasco, M. M. B. R., “Evolutionary Optimization of Oil Field Development”, Society of Petroleum Engineers, Houston, Texas, USA, 2007, doi:10.2118/107552-MS.

[24] Litvak, M. L., Gane, B. R., Williams, G., Mansfield, M., Angert, P. F., et al., “Field Development Optimization Technology”, Society of Petroleum Engineers, Houston, Texas, USA, 2007. doi:10.2118/106426-MS.

[25] Litvak, M. L., & Angert, P. F., “Field Development Optimization Applied to Giant Oil Fields” Society of Petroleum Engineers, The Woodlands, Texas, USA, 2009. doi:10.2118/118840-MS.

[26] Litvak, M. L., Onwunalu, J. E., & Baxter, J., “Field Development Optimization with Subsurface Uncertainties”. Society of Petroleum Engineers, Denver, Colorado, USA, 2011. doi:10.2118/146512-MS.

[27] Storvold, V. S., “Optimization of investment decisions and production planning in aging offshore petroleum fields”. Master Thesis, NTNU, Norway, 2012.

[28] Alyan, M., Martin, J., & Irwin, D., “Field Development Plan Optimization for Tight Carbonate Reservoirs”. Society of Petroleum Engineers, Abu Dhabi, UAE 2015, doi:10.2118/177695-MS.

[29] Bradley, S., Hax, A. and Magnanti. (1997) Applied Mathematical Programming. Addison-Wesley. Chapter 2-9. ISBN-13: 978-0201004649. ISBN-10: 9780201004649.

[30] Taylor III, B. (2013) Introduction to Management Science. Edition 1. Online Module C: Integer Programming: The Branch and Bound Method. Pearson. ISBN-10: 0-13-275191-7. ISBN-13: 978-0-13-275191-9.

[31] IBM, "IBM ILOG AMPL v12.2 — USER'S GUIDE", 2010.

[32] Grötschel, M., Holland, O., "Solution of large-scale symmetric travelling salesman problems", Mathematical Programming, 1991, 51, 141–202.

[33] Padberg, M., & Rinaldi, G, "A Branch-and-Cut Algorithm for the Resolution of Large-Scale Symmetric Traveling Salesman Problems", SIAM Review, 1991, 33(1), 60-100, http://www.jstor.org/stable/2030652.

[34] Codas, A., Campos, S., Camponogaram E., Gunnerud, V., Sunjerga. S. (2012) "Integrated Production Optimization of Oil Fields with Pressure and Routing Constraints: The Urucu Field". Comput Chem Eng. 46,178–189, https://doi.org/10.1016/j.compchemen g.2012.06.016.

[35] Silva T. L., Camponogara E. (2014). "A Computational Analysis of Multidimensional Piecewise-Linear Models with Applications to Oil Production Optimization". Eur J Oper Res. 232(3). 630–642. https://doi.org/10.1016/j.ejor.2013.07.040.

[36] Hall, N. A., Delille, S. "Cost Estimations Challenges and Uncertainties Confronting Oil and Gas Companies". 2011 AACE International Transactions. 2011.

[37] Al-Harthy, M. H. (2007). "Stochastic Oil Price Models: Comparison and Impact". The Engineering Economist. 52:3, 269-284. DOI: 10.1080/00137910701503944

[38] Hoffmann, A., Stanko, M. (2017). "Short-Term Model-Based Production Optimization of a Surface Production Network with Electric Submersible Pumps Using Piecewise-Linear Functions". Journal of Petroleum Science and Engineering. 158. 570–584, https: //doi.org/10.1016/j.petro l.2017.08.063.

[39] Coberly, C. (1942) "Method of preventing wax deposits in tubing". US Patent No. 2303823 A.

[40] Merino-Garcia, D. and Correra, S. (2008). "Cold Flow: A Review of a Technology to Avoid Wax Deposition". Taylor & Francis Group, Ed, 26, 446-459. https://doi.org/10.1080/10916460600809741

[41] Al-Yaari, M. (2011) Paraffin Wax Deposition: Mitigation & Removal Techniques. SPE Saudi Arabia section Young Professionals Technical Symposium. Dhahran, Saudi Arabia. 14-16 March 2011. SPE-155412-MS.

[42] Berson, R. A. (2000). "Method for Making Slurry". US Patent No. 6070417 A.

[43] Fung, G., Amin,R., Fleyfel, F. and O'Sullivan, J. (2003). "Method for Reducing Solids Buildup in Hydrocarbon Steams Produced from Wells". US Patent No. 6656366 B1.

[44] Nenniger, J. (1991). “Process for Inhibiting Formation of Wax Deposits”. CA Patent No. 1289497 C.

[45] Knowles, W. T. (1987). “Choke Cooling Waxy Oil”. US Patent No. 4697426 A.

[46] Watson, M. J., Speranza, A. and LaCombe, M. (2015). “Rigorous Integrated Production Modelling of Cold Flow Technology”. Offshore Technology Conference Brazil. Rio de Janeiro, 27-29 October 2015. OTC-26291-MS.

[47] Larsen, R., Lund, A. and Argo, C. B. (2003). “Cold Flow – a Practical Solution”. 11th International Conference on Multhiphase Flow “Multiphase 03” BHR Group. San Remo, Italy. 11-13 June 2003.

[48] Gudmundsson, J. S. (2002). “Cold Flow Hydrate Technology”. 4th International Conference on Gas Hydrates. Yokohama.19-23 May 2002, 5pp.

[49] Azarinezhad, R., Chapoy, R., Anderson, R. and Tohidi, B. (2008). “HYDRAFLOW: A Multiphase Cold Flow Technology for Offshore Flow Assurance Challenges”. 2008 Offshore Technology Conference. 5-8 May 2008. OTC 19485.

[50] Akpabio, M. G. (2013). “Cold Flow in Long Distance Subsea Pipelines”. Master Thesis. NTNU, Trondheim.

[51] Vinatovskaja, E. (2015). “Cold Flow in the Arctic: a Feasibility Study”. Master Thesis. University of Stavanger, Stavanger.

[52] Denniel, S. and Laouir, N. (2001). “Active Heating for Ultra-Deepwater PiP and Risers”. Offshore Technology Conference, Houston, Texas, 31 April - 3 May 2001. OTC 13138.

[53] Escobar-Remolina, J., Barrios, W. and Silva, B. (2012). “Production Increase with Electric Heating Production Line Technology in an Extra-Heavy Oil Field in Colombia: Successful Case of Flow Assurance”. SPE Annual Technical Conference and Exhibition, San Antonio, Texas, USA, 8-10 October 2012. SPE 159219.

[54] Pedersen, A., Kullboteen, H., Børnes, A. and Marthinsen, T. (2007). “Laboratory Experiments of Melting Ice Plugs in Pipelines by Applying Direct Electric Heating”. Seventeenth International Offshore and Polar Engineering Conference, Lisbon, Portugal, 1-6 July 2007.

[55] Tzotzi, C., Parenteau, T., Kaye, D., Turner, D., Bass, R., Morgan, J., Zakarian, E., Rolland, J. and Decrin, M.-K. (2016). “Safe Hydrate Plug Dissociation in Active Heating Flowlines and Risers - Full Scale Test”. Offshore Technology Conference, Houston, Texas, USA, 2-5 May 2016. OTC-27051-MS.

[56] Lirola, F., Pouplin, A., Settouti, N. and Agoumi, J. (2017). “Technical Assessment and Qualification of Local and Distributed Active Heating Technologies”. 13th Offshore Mediterranean Conference and Exhibition, Ravenna, Italy, 29-31 March 2017.

[57] Theyab, M. A. (2018) Fluid Flow Assurance Issues: Literature Review. SciFed Journal of Petroleum. Volume 2. Issue 1.

[58] Bern, P. A., Withers, V. R. and Cairns, J. R. (1980) Wax Deposition in Crude Oil Pipelines. European Offshore Petroleum Conference and Exhibition. London, UK. 21-24 October 1980. EUR 206.

[59] Brown, T. S., Niessen, V. G. and Erickson, D. (1993) Measurement and Prediction of the Kinetics of Paraffin Deposition. 68th Annual Technical Conference and Exhibition of the Society of Petroleum Engineers, Houston, USA. 3-6 October 1993. SPE 26548.

[60] Burger, E. D., Perkins, T. K. and Striegler, J. H. (1981) Studies of Wax Deposition in the Trans-Alaska Pipeline. Journal of Petroleum Technology. Vol 33. 1075-1086. https://doi.org/10.2118/8788-PA.

[61] Gupta, A. and Anirbid, S. (2015) Need of Flow Assurance for Crude Oil Pipelines: A Review. International Journal of Multidisciplinary Science Engineering. Vol 6. No 2. ISSN 2045-7057.

[62] OLGA®. User Manual

[63] Rosvol, K. (2008). "Wax Deposition Model". Master Thesis. NTNU, Trondheim.

[64] Fisher, R. C., Hall, S. Cam, J-F. and Delaporte, D. (2012) Field Deployment of the World's First Electrically Trace Heated Pipe in Pipe. Offshore Technology Conference. Houston, USA. 30 April-3 May 2012. OTC 23108.

[65] Decrin, M-K., Nebell, F. de Naurois, H. and Parenteau, T. (2013) Flow Assurance Modelling Using an Electrical Trace Heated Pipe-In-Pipe: Flow Qualification to Offshore Testing. Offshore Technology Conference. Houston, USA. 6-9 May 2013. OTC 24060.

[66] de Naurois, H., Delaporte, D., Helingoe, M. and Greder, H. (2011) Evaluation Qualification of Electrical Heat Trace Pipe in Pipe for a SS Flow Line and Selection for an Application on a Subsea Field in UK, ISLAY. Offshore Technology Conference. Houston, USA. 2-5 May 2011. OTC 21396.

[67] Empig (2017). [ONLINE] Available at: http://empig.no/technology/

[68] Bergman, T., Lavine, A., Incropera, F. and Dewitt, D. (2011). "Fundamentals of Heat and Mass Transfer". 7th Edition, John Wiley & Sons, Inc. Jefferson City.

[69] NOV (2017). [ONLINE] Available at: http://www.nov.com/Segments/Completion_and_Production_Solutions/Subsea_Production_Systems/Subsea_Cooling.aspx

Appendix A

Input data for material balance model

Table A.1. Tool Options

Reservoir fluid	Oil
Tank model	Single Tank
PVT model	Simple PVT
Production History	By Tank
Compositional model	None

Tank input data

Table A.2. Tank parameters

Tank Type	Oil
Temperature (°C)	17.7
Initial Pressure (bara)	71.4
Porosity (%)	25.0
Connate Water Saturation (fraction)	0.1
Water Compressibility (1/psi(	Use Corr
Gas Cap (downhole ratio)	0.0
Original Oil In Place (MMstb)	1025.0

Table A.3. Water influx

Model	Hurst-van Everdingen-Modified
System	Linear Aquifer
Boundary	Infinite Acting
Reservoir thickness (m)	125
Reservoir width (m)	2200
Aquifer Permeability (mD)	400

Table A.4. Relative permeability

Hysteresis	No
Modified	No
Water Sweep Eff. (%)	100
Gas Sweep Eff. (%)	100

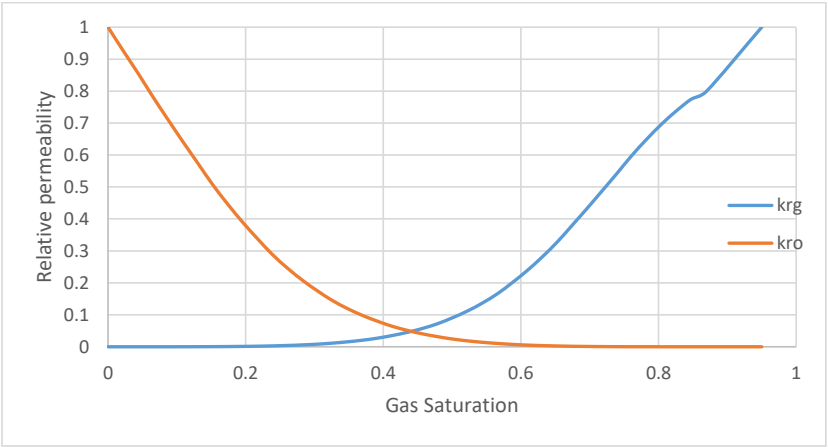

Figure A.1. Oil to Gas relative permeability

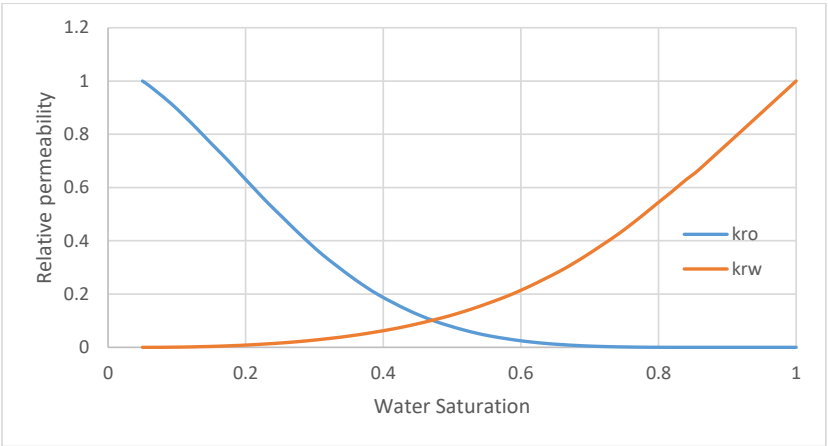

Figure A.2. Oil to Water relative permeability

PVT data

Table A.5. Black oil model

Formation GOR (Sm3/Sm3)	44.6
Oil gravity (API)	39.0
Gas gravity (sp. gravity)	0.8795
Pb, Rs, Bo correlation	Standing
Oil viscosity correlation	Beggs et al.

Table A.6. Tank prediction data

Avg. oil rate (stb/d)	110000.0
Water Void Replac. (%)	100.0
Avg. Water Inj Rat (stb/d)	6290.0
Water Sat. Breakthrough (fraction)	0.3
Gas Sat. Breakthrough (fraction)	0.0

Appendix B

Input data for surface network model

Horizontal completion properties

Table B.1. Reservoir data

Static pressure (bara)	**Input from Res. Model**
Temperature (ºC)	17.7

Table B.2. IPR model

Distributed Pi (Infinity Conductivity)	
Model Type	SS Oil (Joshi)
Rextn (m)	621.65
Tichkness (m)	125.00
Kx (mD)	1200.00
Ky (mD)	1200.00
Kz (mD)	600.00
Eccent (m)	0.00
Rw (in)	9.63
Skin	0.00

Tubing data

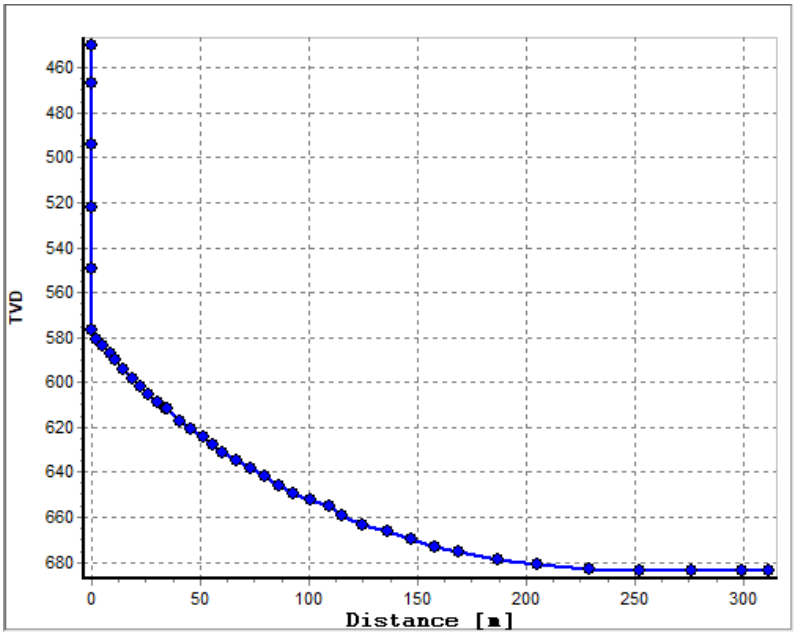

Figure B.1. Tubing layout

Geothermal survey

Table B.3. Geothermal survey

TVD (m)	Ambient Temp (ºC)
576.71	4.0
585.47	5.4
594.09	6.8
606	8.1
615.45	9.5
626.12	10.9
640.49	12.3
653.25	13.6
665.88	15.0
688.16	16.4
920	17.8

Table B.4. Tubing configuration

Bottom MD	**ID**	**Wall Thickness**	**Roughness**	**Casing ID**
(m)	(in)	(in)	(in)	(in)
576.71	4.89	0.29	0.001	20.00
585.47	4.89	0.29	0.001	20.00
594.09	4.89	0.29	0.001	13.38
606.00	4.89	0.29	0.001	12.25
615.45	4.89	0.29	0.001	12.25
626.12	4.89	0.29	0.001	12.25
640.49	4.89	0.50	0.001	7.00
653.25	4.89	0.50	0.001	7.00
665.88	4.89	0.50	0.001	7.00
688.16	4.89	0.50	0.001	6.00
920.00	4.89	0.50	0.001	6.00

Flowlines data

Pipe: Well – Manifold

Table B.5. Properties

Inner Diameter (in)	4.8900
Wall Thickness (in)	0.3370
Roughness (in)	0.0018
Total Length (m)	20
Elevation (m)	-450
Ambient Temp (ºC)	40

Table B.6. Heat transfer

U Value	Calculate
Pipe coating K (Btu/hr/ft/F)	0.1156
Pipe coating thickness (in)	0.9843
Pipe conductivity (Btu/hr/fr/F)	31.7919
Ambient Fluid	Water
Ambient Fluid Vel. (ft/s)	0.5741
Pipe Burial (in)	0.0000
Ground Conductivity Half buried (Btu/hr/ft/F)	0.8092

Pipe: Manifold – Riser base

Table B.7. Properties

Inner Diameter (in)	7.8130
Wall Thickness (in)	0.4320
Roughness (in)	0.0018
Total Length (m)	10000
Elevation (m)	-450
Ambient Temp (°C)	4

Table B.8. Heat transfer

U Value	Calculate
Pipe coating K (Btu/hr/ft/F)	0.1156
Pipe coating thickness (in)	0.9843
Pipe conductivity (Btu/hr/fr/F)	31.7919
Ambient Fluid	Water
Ambient Fluid Vel. (ft/s)	0.5741
Pipe Burial (in)	0.0000
Ground Conductivity Half buried (Btu/hr/ft/F)	0.8092

Pipe: Riser base – Sea level

Table B.9. Properties

Inner Diameter (in)	10.02008
Wall Thickness (in)	0.365
Roughness (in)	0.0018
Total Length (m)	450
Elevation inlet (m)	-450
Elevation outlet (m)	0
Ambient Temp inlet (°C)	4
Ambient Temp outlet (°C)	0

Table B.10. Heat transfer

U Value	Calculate
Pipe coating K (Btu/hr/ft/F)	0.1156
Pipe coating thickness (in)	0.9843
Pipe conductivity (Btu/hr/fr/F)	31.7919
Ambient Fluid	Water
Ambient Fluid Vel. (ft/s)	1.3095

Pipe: Sea Level – Sink

Table B.11. Properties

Inner Diameter (in)	10.02
Wall Thickness (in)	0.37
Roughness (in)	0.0018
Total Length (m)	30.00
Elevation inlet (m)	0.00
Elevation outlet (m)	30.00
Ambient Temp inlet (ºC)	0.00
Ambient Temp outlet (ºC)	0.00

Table B.12. Heat transfer

U Value	Calculate
Pipe coating K (Btu/hr/ft/F)	0.1156
Pipe coating thickness (in)	0.9842
Pipe conductivity (Btu/hr/fr/F)	31.7919
Ambient Fluid	Air
Ambient Fluid Vel. (ft/s)	16.4042

Black oil model data

Table B.13. Data used for black oil model

WC (fraction)	Input from Res. Model
GOR (Sm3/Sm3)	Input from Res. Model
Gas S.G.	0.8795
API	39
Dead Oil Viscosity Corr.	Beggs & Robinson
Live Oil Viscosity Corr.	Beggs & Robinson
Rs, Bo Corr.	Standing

Appendix C

Black oil tables

Table C.1. Black oil table 1

Temperature	Pressure	Bubble point pressure	Gas Oil Ratio	Oil FVF	Oil viscosity	Gas viscosity
(oC)	(bara)	(bara)	(Sm3/Sm3)	(m3/m3)	(cP)	(cP)
16.35	200	64.40	43.86	1.09	3.38	0.0208
16.35	175	64.40	43.86	1.09	3.25	0.0192
16.35	150	64.40	43.86	1.09	3.11	0.0173
16.35	125	64.40	43.86	1.09	2.99	0.0156
16.35	100	64.40	43.90	1.10	2.85	0.0139
16.35	75	64.40	43.90	1.10	2.72	0.0127
16.35	69	64.40	43.86	1.10	2.69	0.0124
16.35	64.4	64.40	43.86	1.10	2.66	0.0123
16.35	60	64.40	40.99	1.10	2.80	0.0121
16.35	50	64.40	34.54	1.08	3.13	0.0118
16.35	40	64.40	28.09	1.07	3.52	0.0115
16.35	30	64.40	21.64	1.05	3.96	0.0113
16.35	20	64.40	15.12	1.04	4.49	0.0111
16.35	10	64.40	8.26	1.02	5.17	0.0109
16.35	5	64.40	3.61	1.01	5.70	0.0107
16.35	3	64.40	1.67	1.01	6.06	0.0105
16.35	2	64.40	0.77	1.00	6.37	0.0104
16.35	1	64.40	0.01	1.00	6.93	0.0102

Table C.2. Black oil table 2

Temperature	Pressure	Bubble point pressure	Gas Oil Ratio	Oil FVF	Oil viscosity	Gas viscosity
(oC)	(bara)	(bara)	(Sm3/Sm3)	(m3/m3)	(cP)	(cP)
17.70	200	67.60	34.91	1.06	5.43	0.0204
17.70	175	67.60	34.94	1.07	5.24	0.0188
17.70	150	67.60	34.94	1.07	5.06	0.0170
17.70	125	67.60	34.94	1.07	4.86	0.0154
17.70	100	67.60	34.94	1.07	4.67	0.0139
17.70	75	67.60	34.94	1.08	4.47	0.0127
17.70	69	67.60	34.91	1.08	4.42	0.0125
17.70	67.6	67.60	34.94	1.08	4.42	0.0124
17.70	60	67.60	31.02	1.07	4.74	0.0122
17.70	50	67.60	25.88	1.06	5.19	0.0119
17.70	40	67.60	20.71	1.05	5.70	0.0117
17.70	30	67.60	15.58	1.04	6.25	0.0115
17.70	20	67.60	10.41	1.02	6.85	0.0113
17.70	10	67.60	5.20	1.01	7.53	0.0112
17.70	5	67.60	2.26	1.01	7.94	0.0111
17.70	3	67.60	1.08	1.00	8.15	0.0111
17.70	2	67.60	0.45	1.00	8.29	0.0110
17.70	1	67.60	0.00	1.00	8.51	0.0109

Appendix D

Proxy models used for validation of production potential approach

Case 1:

Table D.1. Validation case 1 characteristics

IOIP (MMstb)	Recovery Method	Nw	qo_plateau (stb/d)
1025	GL	9	35000

Table D.2. Proxy model for validation case 1

Np (MMstb)	GOR (scf/stb)	WC (fraction)	qo_pot (stb/d)
0.00	456	0	59366
40.15	826	0	46552
80.41	878	0	41768
120.56	933	0	37914
160.71	1005	0	33784
200.86	1117	0	30152
241.12	1286	0	26135
281.27	1698	0	20280
321.42	2421	0	14481
361.57	0	0	0
401.83	0	0	0
441.98	0	0	0
482.13	0	0	0
492.17	0	0	0

Case 2:

Table D.3. Validation case 2 characteristics

IOIP (MMstb)	Recovery Method	Nw	qo_plateau (stb/d)
818	GL + WI	15	50000

Table D.4. Proxy model for validation case 2

Np (MMstb)	GOR (scf/stb)	WC (fraction)	qo_pot (stb/d)
0.00	513.81	0.00	87671
40.15	752.19	0.00	89648

80.41	752.18	0.00	89648
120.56	752.18	0.00	89648
160.71	752.18	0.00	89648
200.86	836.05	0.124	76095
241.12	1071.67	0.337	54759
281.27	1308.80	0.499	42848
321.42	1767.77	0.660	29667
361.57	2921.62	0.794	16772
401.83	5196.89	0.887	9058
441.98	10342.25	0.943	4493
482.13	21798.73	0.974	2106
522.28	52137.47	0.989	874

Case 3:

Table D.5. Validation case 3 characteristics

IOIP (MMstb)	Recovery Method	Nw	qo_plateau (stb/d)
1264	MPP+ WI	6	90000

Table D.6. Proxy model for validation case 3

Np (MMstb)	GOR (scf/stb)	WC (fraction)	qo_pot (stb/d)
0	0	0	119716
40.15	250.41	0	160146
80.41	250.41	0	160146
120.56	250.41	0	160146
160.71	250.41	0	160146
200.86	250.41	0	160146
241.12	250.41	0	160146
281.27	250.41	0	160146.
321.42	250.41	0.247	121169
361.57	250.41	0.335	106681
401.83	250.41	0.439	90018
441.98	250.41	0.546	72312
482.13	250.41	0.649	57612
522.28	250.41	0.743	42224
562.54	250.41	0.819	29587
602.69	250.41	0.877	20053
642.84	250.41	0.920	13029
682.99	250.41	0.949	8241
723.25	250.41	0.969	4999

763.40	250.41	0.982	2902
803.55	250.41	0.990	1636
843.70	250.41	0.994	850
883.96	250.41	0.997	411

Appendix E

MILP formulation

Mixed integer linear formulation of the optimization problem

Here, the formulation used to solve the optimization problem is presented

.

Table E.1. Set of time steps

Set	Description
$\mathcal{T}$	Set of all time steps

Table E.2. Optimization parameters

Parameter	Description
$q_{o,erosion}^{max}$	Maximum oil rate allow to avoid erosion (stb/d)
$q_{w,inj}^{max}$	Maximum water injection (stb/d)
$Nw_{drilled}^{min}$	Minimum number of well that can be drilled in a time step
$Nw_{drilled}^{max}$	Maximum number of wells that can be drilled in a time step
P_o	Oil Price (NOK/stb)
DR	Discount rate (%)
$Delta\_t$	Time step size (year)

Table E.3. Field variables

Variable	Description
q_o^j	Oil production rate (stb/d)
$q_{o,pot}^j$	Oil production potential rate (stb/d)
q_g^j	Gas production rate (MM scf/d)
q_w^j	Water production rate (stb/d)
$q_{w,inj}^j$	Water injection rate (stb/d)
Np^j	Cumulative oil production (stb)
Wp_{inj}^j	Cumulative water injection (stb)
Nw	Number of production wells in the field
$Nw_{drilled}^j$	Number of well drilled
$Nw_{d,p+i}^j$	Number of production and injection wells drilled
Nw^{field}	Maximum number of production and injection wells in the field
GOR^j	Gas oil rate (scf/stb)
WC^j	Water cut (-)
$q_o^{capacity}$	Oil rate capacity of processing facility (stb/d)

$q_g^{capacity}$	Gas rate capacity of processing facility (MM scf/d)
$q_w^{capacity}$	Water rate capacity of processing facility (stb/d)

Table E.4. Economic variables

Variable	Description
E_{cap}	Capital expenditures (MM NOK)
E_{op}	Operational expenditures (MM NOK)
E_{drill}^{j}	Drilling expenditures (MM NOK)
CF^{j}	Cash flow (MM NOK)
NPV^{j}	Net present value (MM NOK)

Table E.5. Set of breakpoints used in the MILP formulation

Set	Description
$\mathcal{V}_{Np}^{j}$	Set of cumulative oil production breakpoints for time step j
$\mathcal{N}_{Nw}^{j}$	Set of number of wells breakpoints for time step j
Q_{qo}^{j}	Set of oil rate breakpoints for time step j
$\mathcal{R}_{gor}^{j}$	Set of GOR breakpoint for time step j
$\mathcal{R}_{wc}^{j}$	Set of WC breakpoint for time step j

Table E. 6. Auxiliary variables used in the MILP formulation

Variable	Description
$\theta_{v.N}^{j}$	Weighting variable for breakpoint (v,N) , time step j
α_{v}^{j}	SOS2 variable for breakpoint v , time step j
β_{N}^{j}	SOS2 variable for breakpoint N , time step j
$\theta_{q,r_{gor}}^{j}$	Weighting variable for breakpoint (q, r_{gor}), time step j
α_{q}^{j}	SOS2 variable for breakpoint q , time step j
$\beta_{r_{gor}}^{j}$	SOS2 variable for breakpoint r_{gor}, time step j
$\theta_{q,r_{wc}}^{j}$	Weighting variable for breakpoint (q, r_{wc}) , time step j
$\beta_{r_{wc}}^{j}$	SOS2 variable for breakpoint r_{wc} , time step j
λ_{v}^{j}	Weighting variable for breakpoint v, time step j

Table E.7. Piecewise linear functions used in MILP

Function	Description
$\widehat{q_{o,pot}^{J}}$	PWL function given the oil production potential as function of cumulative oil produced and number of wells
$\widehat{GOR^{J}}$	PWL function given the GOR as function of cumulative oil produced and number of wells

$\widehat{WC^J}$	PWL function given the WC as function of cumulative oil production and number of wells
$\widehat{q_g^J}$	PWL function given the gas rate as function of oil rate and GOR
$\widehat{q_w^J}$	PWL function given the water rate as function of oil rate and WC
$\widehat{Wp_{inJ}^J}$	PWL function given the cumulative water injected as function of cumulative oil produced

$\forall j \in \mathcal{T}$:

$$\max_{\gamma} \quad NPV \tag{E.1}$$

by changing q_o^j and $Nw_{drilled}^j$. With γ the set of variables defined in Tables 3.9, 3.10 and 3.12. The problem is subjected to the following constraints:

$$NPV = \sum_{j \in \mathcal{T}} CF^j \tag{E.2}$$

$\forall j \in \mathcal{T}$:

$$CF^j = \frac{\left(Np^j \cdot P_o^j\right) - \left(E_{cap}^j + E_{op}^j + E_{drill}^j\right)}{\left(1+DR\right)^j} \tag{E.3}$$

E_{cap}^j, E_{op}^j and E_{drill}^j are estimated from equation (4.5) to (4.11). The cumulative oil produced, number of wells in the field and water injection rate are given by

$$Np^i = \sum_{j \in \mathcal{T}} Delta\_t \cdot q_o^{j-1} \tag{E.4}$$

$$Nw^j = \sum_{j \in \mathcal{T}} Nw_{drilled}^j \tag{E.5}$$

$$q_{w,inj}^j = \frac{Wp_{inj}^j - Wp_{inj}^{j-1}}{Delta\_t} \tag{E.6}$$

The optimization is subject to the operational constraints described in section 5.2:

$$q_o^j \le q_{o,pot}^j \tag{E.7}$$

$$Nw_{drilled}^{min} \le Nw_{drilled}^j \le Nw_{drilled}^{max} \tag{E.8}$$

$$q_{o,pot} = q_{o,pot}\left(Np, Nw\right) \tag{E.9}$$

$$q_o^j \le q_{o,erosion}^{max} \tag{E.10}$$

$$q_{w,inj}^j \le q_{w,inj}^{max} \tag{E.11}$$

$$q_o^{capacity} \ge q_o^j \tag{E.12}$$

$$q_g^{capacity} \ge q_g^j \tag{E.13}$$

$$q_w^{capacity} \ge q_w^j \tag{E.14}$$

$$Nw^{field} \ge Nw^j \tag{E.15}$$

The oil production potential, GOR and WC are given by

$$q_{o,pot}^j = \sum_{v \in \mathcal{V}_{Np}^j} \sum_{N \in \mathcal{N}_{Nw}^j} \theta_{vN}^j \cdot \widehat{q_{o,pot}^J}(v,N) \tag{E.16}$$

$$GOR^j = \sum_{v \in \mathcal{V}_{Np}^j} \sum_{N \in \mathcal{N}_{Nw}^j} \theta_{vN}^j \cdot \widehat{GOR^J}(v,N) \tag{E.17}$$

$$WC^j = \sum_{v \in \mathcal{V}_{Np}^j} \sum_{N \in \mathcal{N}_{Nw}^j} \theta_{vN}^j \cdot \widehat{WC^J}(v,N) \tag{E.18}$$

$$Np^j = \sum_{v \in \mathcal{V}_{Np}^j} \sum_{N \in \mathcal{N}_{Nw}^j} \theta_{vN}^j \cdot v \tag{E.19}$$

$$Nw^j = \sum_{v \in \mathcal{V}_{Np}^j} \sum_{N \in \mathcal{N}_{Nw}^j} \theta_{vN}^j \cdot N \tag{E.20}$$

$$\sum_{v \in \mathcal{V}_{Np}^j} \sum_{N \in \mathcal{N}_{Nw}^j} \theta_{vN}^j = 1 \tag{E.21}$$

$$\forall v \in \mathcal{V}_{Np}^j, \quad \forall N \in \mathcal{N}_{Nw}^j, \quad \theta_{vN}^j \ge 0 \tag{E.22}$$

$$\forall v \in \mathcal{V}_{Np}^j, \quad \alpha_v^j = \sum_{N \in \mathcal{N}_{Nw}^j} \theta_{vN}^j \tag{E.23}$$

$$\forall N \in \mathcal{N}_{Nw}^j, \quad \beta_N^j = \sum_{v \in \mathcal{V}_{Np}^j} \theta_{vN}^j \tag{E.24}$$

$$\left(\alpha_v^j\right)_{v \in \mathcal{V}_{Np}^j} \text{ is a SOS2} \tag{E.25}$$

$$\left(\beta_N^j\right)_{N \in \mathcal{N}_{Nw}^j} \text{ is a SOS2} \tag{E.26}$$

Since equations (5.15) and (5.16) are non-linear, they require some additional manipulation to be included in the MILP The gas rate is given by

$$q_g^j = \sum_{q \in Q_{qo}^j} \sum_{r_{gor} \in \mathcal{R}_{gor}^j} \theta_{qr_{gor}}^j \cdot \widehat{q_g^J}(q, r_{gor}) \tag{E.27}$$

$$q_o^j = \sum_{q \in Q_{qo}^j} \sum_{r_{gor} \in \mathcal{R}_{gor}^j} \theta_{qr_{gor}}^j \cdot q \tag{E.28}$$

$$GOR^j = \sum_{q \in Q_{qo}^j} \sum_{r_{gor} \in \mathcal{R}_{gor}^j} \theta_{qr_{gor}}^j \cdot r_{gor} \tag{E.29}$$

$$\sum_{q \in Q_{qo}^j} \sum_{r_{gor} \in \mathcal{R}_{gor}^j} \theta_{qr_{gor}}^j = 1 \tag{E.30}$$

$$\forall q \in Q_{qo}^j, \quad \forall r_{gor} \in \mathcal{R}_{gor}^j, \quad \theta_{qr_{gor}}^j \geq 0 \tag{E.31}$$

$$\forall q \in Q_{qo}^j, \quad \alpha_q^j = \sum_{r_{gor} \in \mathcal{R}_{gor}^j} \theta_{qr_{gor}}^j \tag{E.32}$$

$$\forall r_{gor} \in \mathcal{R}_{gor}^j, \quad \beta_{r_{gor}}^j = \sum_{q \in Q_{qo}^j} \theta_{qr_{gor}}^j \tag{E.33}$$

$$\left(\alpha_q^j\right)_{q \in Q_{qo}^j} \text{ is a SOS2} \tag{E.34}$$

$$\left(\beta_{r_{wc}}^j\right)_{r_{gor} \in \mathcal{R}_{gor}^j} \text{ is a SOS2} \tag{E.35}$$

The water rate is given by

$$q_w^j = \sum_{q \in Q_{qo}^j} \sum_{r_{wc} \in \mathcal{R}_{wc}^j} \theta_{qr_{wc}}^j \cdot \widehat{q_w^J}(q, r_{wc}) \tag{E.36}$$

$$q_o^j = \sum_{q \in Q_{qo}^j} \sum_{r_{wc} \in \mathcal{R}_{wc}^j} \theta_{qr_{wc}}^j \cdot q \tag{E.37}$$

$$WC^j = \sum_{q \in Q_{qo}^j} \sum_{r_{wc} \in \mathcal{R}_{wc}^j} \theta_{qr_{wc}}^j \cdot r_{wc} \tag{E.38}$$

$$\sum_{q \in Q_{qo}^j} \sum_{r_{wc} \in \mathcal{R}_{wc}^j} \theta_{qr_{wc}}^j = 1 \tag{E.39}$$

$$\forall q \in Q_{qo}^j, \quad \forall r_{wc} \in \mathcal{R}_{wc}^j, \quad \theta_{qr_{wc}}^j \geq 0 \tag{E.40}$$

$$\forall q \in Q_{qo}^j, \quad \alpha_q^j = \sum_{r_{wc} \in \mathcal{R}_{wc}^j} \theta_{qr_{wc}}^j \tag{E.41}$$

$$\forall r_{wc} \in \mathcal{R}_{wc}^j, \quad \beta_{r_{wc}}^j = \sum_{q \in Q_{qo}^j} \theta_{qr_{wc}}^j \tag{E.42}$$

$$\left(\alpha_q^j\right)_{q \in Q_{qo}^j} \text{ is a SOS2} \tag{E.43}$$

$$\left(\beta_{r_{wc}}^j\right)_{r_{wc} \in \mathcal{R}_{wc}^j} \text{ is a SOS2} \tag{E.44}$$

The cumulative water injection is given by

$$Wp_{inj}^j = \sum_{v \in \mathcal{V}_{Np}^j} \lambda_v^j \cdot \widehat{Wp_{inJ}^J}(v) \tag{E.45}$$

$$Np^j = \sum_{v \in \mathcal{V}_{Np}^j} \lambda_v^j \cdot v \tag{E.46}$$

$$\sum_{v \in \mathcal{V}_{Np}^j} \lambda_v^j = 1 \tag{E.47}$$

$$\forall v \in \mathcal{V}_{Np}^j, \quad \lambda_v^j \geq 0 \tag{E.48}$$

Appendix F

Proxy model for Study Case based on Wisting (used in chapter 7)

Gas Lifted wells

Table F.1. Potential oil rate for gas lifted wells concept

Oil Rate (stb/d)					
Np (MMSTB)	**Nw = 3**	**Nw = 6**	**Nw = 9**	**Nw = 12**	**Nw = 15**
0.00	20616	40476	59366	75751	87671
40.15	16897	33758	46552	56618	66156
80.41	15196	28701	41768	52221	59549
120.56	13546	25612	37914	46369	53894
160.71	11992	23062	33784	40642	47462
200.86	10575	20157	30152	35886	41545
241.12	9109	17720	26135	30620	36566
281.27	7729	14954	20280	25739	29440
321.42	0	0	14481	15680	19666

Table F.2. Gas oil ratio for gas lifted wells concept

GOR (scf/stb)					
Np (MMSTB)	**Nw = 3**	**Nw = 6**	**Nw = 9**	**Nw = 12**	**Nw = 15**
0.00	434	446	456	477	514
40.15	777	774	826	880	923
80.41	818	857	878	921	985
120.56	876	917	933	987	1052
160.71	960	987	1005	1087	1151
200.86	1078	1107	1117	1216	1303
241.12	1238	1274	1286	1442	1494
281.27	1512	1562	1698	1748	1895
321.42	0	0	2421	2854	2819

Table F.3. Water cut for gas lifted wells concept

WC (%)					
Np (MMSTB)	**Nw = 3**	**Nw = 6**	**Nw = 9**	**Nw = 12**	**Nw = 15**
0.00	0.0	0.0	0.0	0.0	0.0

40.15	0.0	0.0	0.0	0.0	0.0
80.41	0.0	0.0	0.0	0.0	0.0
120.56	0.0	0.0	0.0	0.0	0.0
160.71	0.0	0.0	0.0	0.0	0.0
200.86	0.0	0.0	0.0	0.0	0.0
241.12	0.0	0.0	0.0	0.0	0.0
281.27	0.0	0.0	0.0	0.0	0.0
321.42	0.0	0.0	0.0	0.0	0.0

Gas lifted wells + water injection

Table F.4. Potential oil rate for gas lifted wells + water injection concept

Oil Rate (stb/d)					
Np (MMSTB)	**Nw = 3**	**Nw = 6**	**Nw = 9**	**Nw = 12**	**Nw = 15**
0.00	20616	40476	59898	75750	87671
40.15	23134	42436	60199	78565	89648
80.41	23134	42436	60199	78565	89648
120.56	23134	42436	60199	78565	89648
160.71	23134	42436	60199	78565	89648
200.86	23134	42436	60199	78565	89648
241.12	23134	42436	60199	78565	89648
281.27	20554	39201	56271	72427	80088
321.42	15110	29164	42053	54167	59244
361.57	12897	23557	33932	42224	48918
401.83	9019	17811	25896	31290	36826
441.98	6847	13777	19773	23580	28264
482.13	4635	9014	12597	15466	17474
522.28	2895	5394	8070	9707	11006
562.54	1637	3218	4627	5825	6544
602.69	947	1818	2579	3066	3666
642.84	492	962	1371	1705	1987
682.99	245	471	668	863	991

Table F.5. Gas oil ratio for gas lifted wells + water injection concept

GOR (scf/stb)					
Np (MMSTB)	**Nw = 3**	**Nw = 6**	**Nw = 9**	**Nw = 12**	**Nw = 15**
0.00	434	446	452	477	514
40.15	638	673	700	713	752
80.41	638	673	700	713	752
120.56	638	673	700	713	752
160.71	638	673	700	713	752

200.86	638	673	700	713	752
241.12	638	673	700	713	752
281.27	691	708	735	747	810
321.42	845	868	893	920	1003
361.57	948	1015	1045	1103	1170
401.83	1243	1258	1292	1403	1464
441.98	1570	1549	1616	1791	1854
482.13	2188	2235	2385	2589	2843
522.28	3331	3582	3598	3976	4313
562.54	5778	5803	6067	6487	7142
602.69	9753	10161	10780	11907	12539
642.84	18504	18911	19851	21339	23090
682.99	37071	38324	40494	41922	45885

Table F.6. Water cut for gas lifted wells + water injection concept

WC (%)					
Np (MMSTB)	**Nw = 3**	**Nw = 6**	**Nw = 9**	**Nw = 12**	**Nw = 15**
0.00	0.0	0.0	0.0	0.0	0.0
40.15	0.0	0.0	0.0	0.0	0.0
80.41	0.0	0.0	0.0	0.0	0.0
120.56	0.0	0.0	0.0	0.0	0.0
160.71	0.0	0.0	0.0	0.0	0.0
200.86	0.0	0.0	0.0	0.0	0.0
241.12	7.7	7.7	7.7	7.7	7.7
281.27	29.1	29.1	29.1	29.1	29.1
321.42	41.2	41.2	41.2	41.2	41.2
361.57	54.5	54.5	54.5	54.5	54.5
401.83	67.1	67.1	67.1	67.1	67.1
441.98	78.0	78.0	78.0	78.0	78.0
482.13	86.0	86.0	86.0	86.0	86.0
522.28	91.7	91.7	91.7	91.7	91.7
562.54	95.3	95.3	95.3	95.3	95.3
602.69	97.5	97.5	97.5	97.5	97.5
642.84	98.7	98.7	98.7	98.7	98.7
682.99	99.4	99.4	99.4	99.4	99.4

Multiphase boosting + water injection

Table F.7. Potential oil rate for multiphase boosting + water injection concept

Oil Rate (stb/d)					
Np (MMSTB)	**Nw = 3**	**Nw = 6**	**Nw = 9**	**Nw = 12**	**Nw = 15**
0.00	60914	119716	177824	226610	275396
40.15	82264	160146	233029	292775	345613
80.41	82264	160146	233029	292775	345613
120.56	82264	160146	233029	292775	345613
160.71	82264	160146	233029	292775	345613
200.86	82264	160146	233029	292775	345613
241.12	75138	148748	213760	271283	321976
281.27	58061	113642	164698	209448	244735
321.42	48101	93660	135372	172673	203219
361.57	37224	72328	104230	133720	156636
401.83	27732	54059	78467	100072	119206
441.98	18337	36066	52648	67081	79646
482.13	11576	22778	33276	42120	50593
522.28	6835	13425	19534	25007	30309
562.54	3872	7632	11170	14332	16955
602.69	2061	4075	5908	7602	9050
642.84	1032	2032	2972	3804	5586
682.99	476	936	1372	1762	2123

Table F.8. Gas oil ratio for multiphase boosting + water injection concept

GOR ((scf/stb)					
Np (MMSTB)	**Nw = 3**	**Nw = 6**	**Nw = 9**	**Nw = 12**	**Nw = 15**
0.00	0	0	0	0	0
40.15	250	250	250	250	250
80.41	250	250	250	250	250
120.56	250	250	250	250	250
160.71	250	250	250	250	250
200.86	250	250	250	250	250
241.12	250	250	250	250	250
281.27	250	250	250	250	250
321.42	250	250	250	250	250
361.57	250	250	250	250	250
401.83	250	250	250	250	250
441.98	250	250	250	250	250
482.13	250	250	250	250	250

522.28	250	250	250	250	250
562.54	250	250	250	250	250
602.69	250	250	250	250	250
642.84	250	250	250	250	250
682.99	250	250	250	250	250

Table F. 9. Water cut for multiphase boosting + water injection concept

WC (%)					
Np (MMSTB)	**Nw = 3**	**Nw = 6**	**Nw = 9**	**Nw = 12**	**Nw = 15**
0.00	0.0	0.0	0.0	0.0	0.0
40.15	0.0	0.0	0.0	0.0	0.0
80.41	0.0	0.0	0.0	0.0	0.0
120.56	0.0	0.0	0.0	0.0	0.0
160.71	0.0	0.0	0.0	0.0	0.0
200.86	0.0	0.0	0.0	0.0	0.0
241.12	7.7	7.7	7.7	7.7	7.7
281.27	29.1	29.1	29.1	29.1	29.1
321.42	41.2	41.2	41.2	41.2	41.2
361.57	54.5	54.5	54.5	54.5	54.5
401.83	67.1	67.1	67.1	67.1	67.1
441.98	78.0	78.0	78.0	78.0	78.0
482.13	86.0	86.0	86.0	86.0	86.0
522.28	91.7	91.7	91.7	91.7	91.7
562.54	95.3	95.3	95.3	95.3	95.3
602.69	97.5	97.5	97.5	97.5	97.5
642.84	98.7	98.7	98.7	98.7	98.7
682.99	99.4	99.4	99.4	99.4	99.4

Appendix G

Water injection table used in optimization

Table G.1. Cumulative water injection table as function of cumulative oil production used in optimization routine

Np (MMstb)	Cum_Winj (MMstb)
0.00	0.00
40.15	43.5439
80.41	87.207
120.56	130.751
160.71	174.295
200.86	217.839
241.12	264.882
281.27	324.912
321.42	396.628
361.57	488.176
401.83	614.036
441.98	799.824
482.13	1090.96
522.28	1580.36
562.54	2441.17
602.69	4051.35
642.84	7250.61
682.99	14171.2

Appendix H

Result from optimization: Optimum production rate for study case

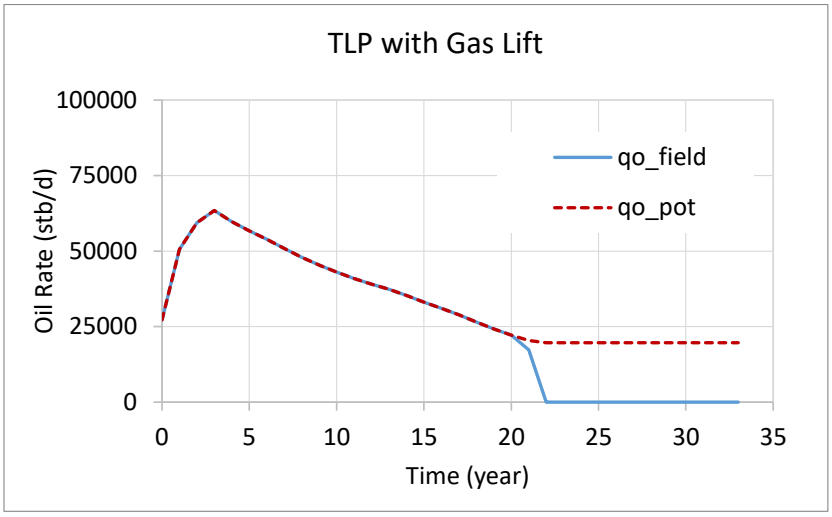

Figure H.1. Optimum oil production profile and oil production potential for strategy TLP with GL

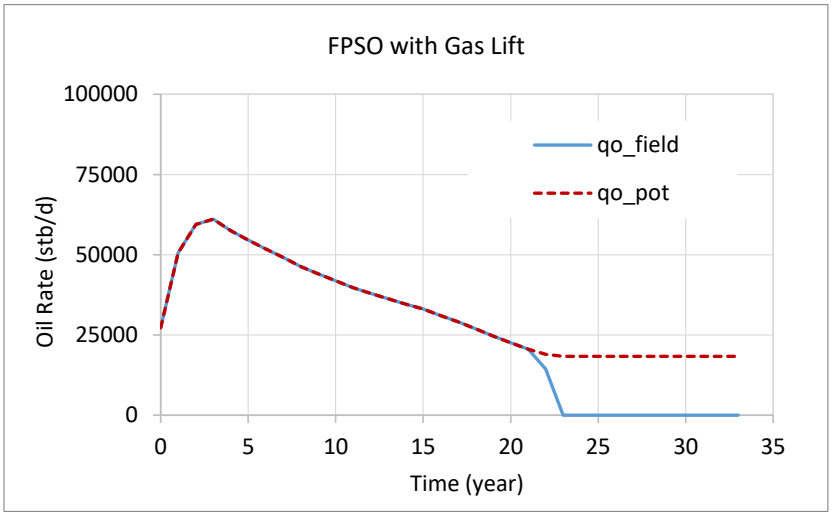

Figure H.2. Optimum oil production profile and oil production potential for strategy FPSO with GL

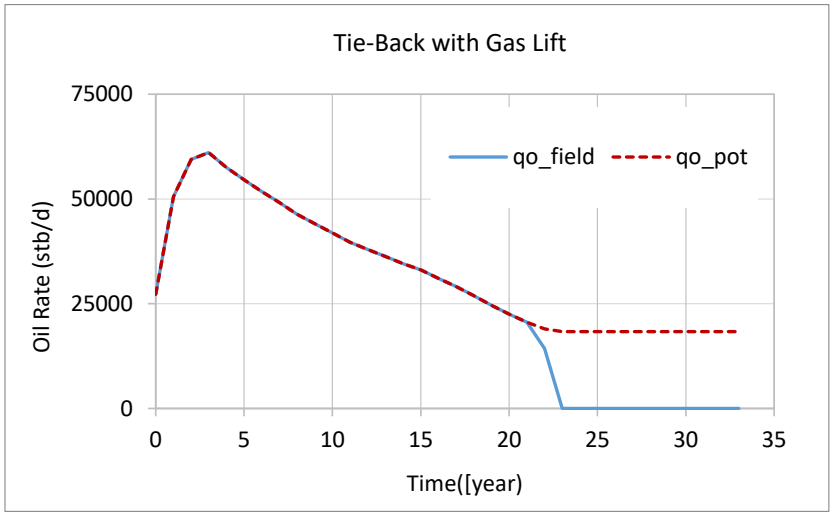

Figure H.3. Optimum oil production profile and oil production potential for strategy Tie-back with GL

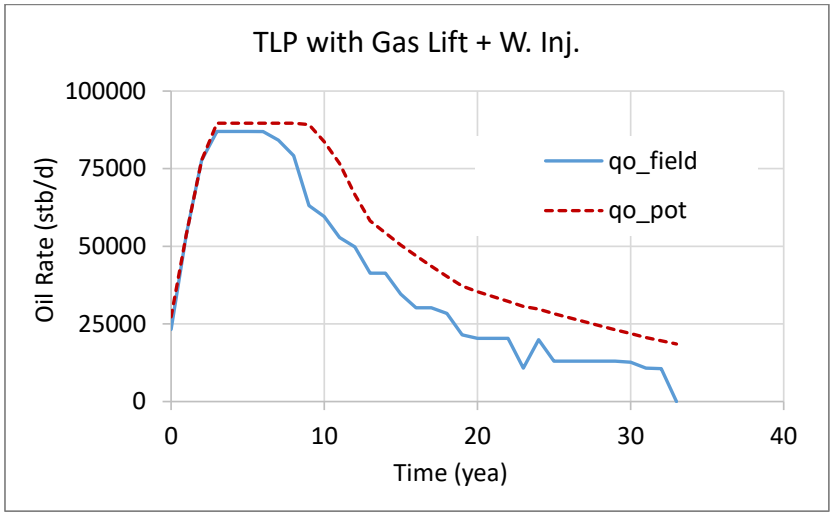

Figure H.4. Optimum oil production profile and oil production potential for strategy TLP with GL + WI

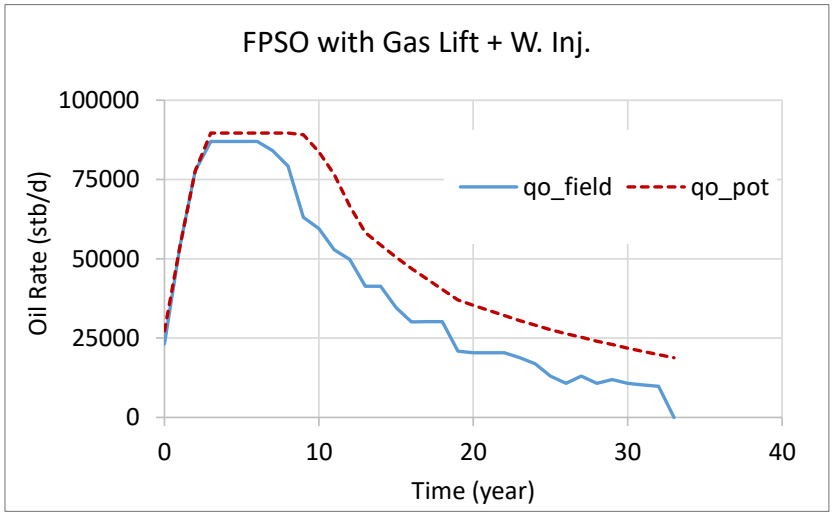

Figure H.5. Optimum oil production profile and oil production potential for strategy FPSO with GL + WI

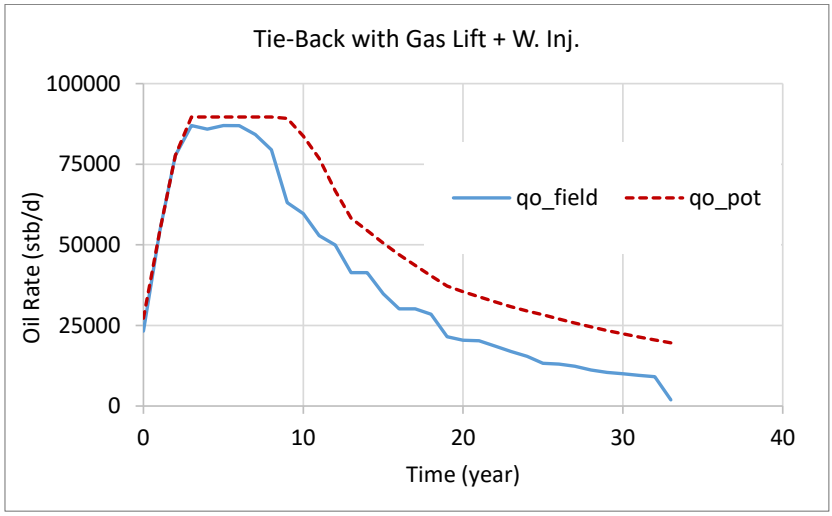

Figure H.6. Optimum oil production profile and oil production potential for strategy Tie-back with GL + WI injection

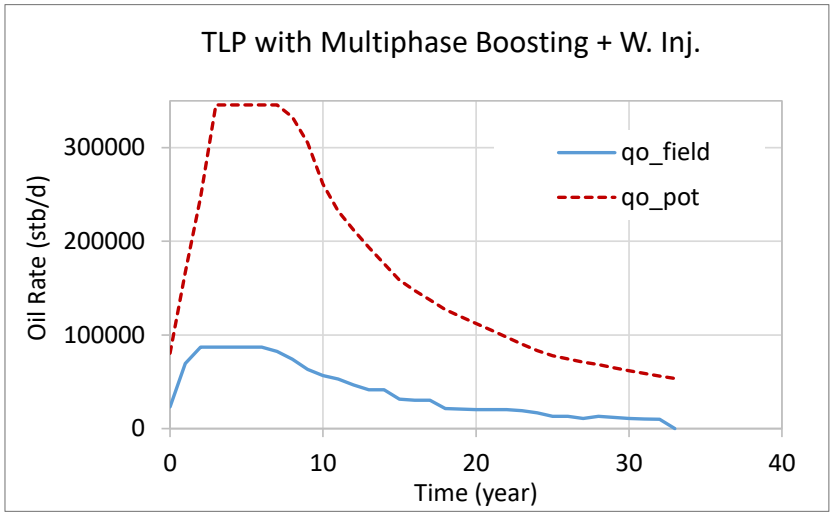

Figure H.7. Optimum oil production profile and oil production potential for strategy TLP with MPB + WI

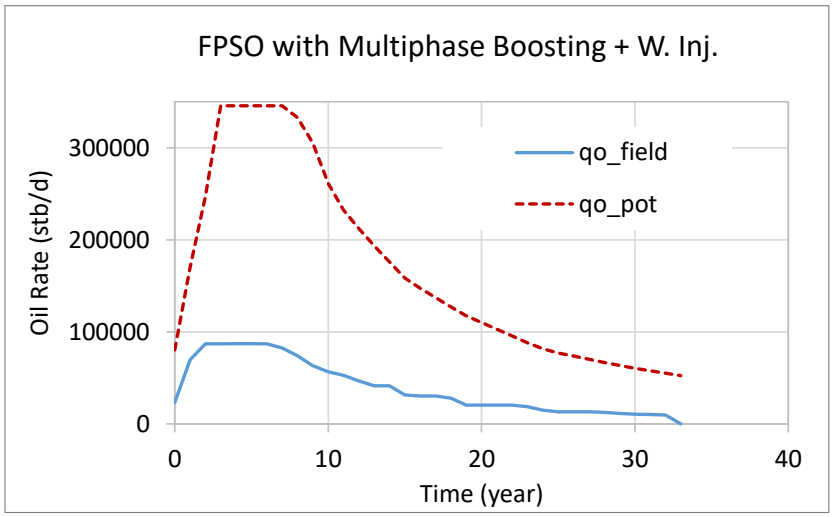

Figure H.8. Optimum oil production profile and oil production potential for strategy FPSO with MPB + WI

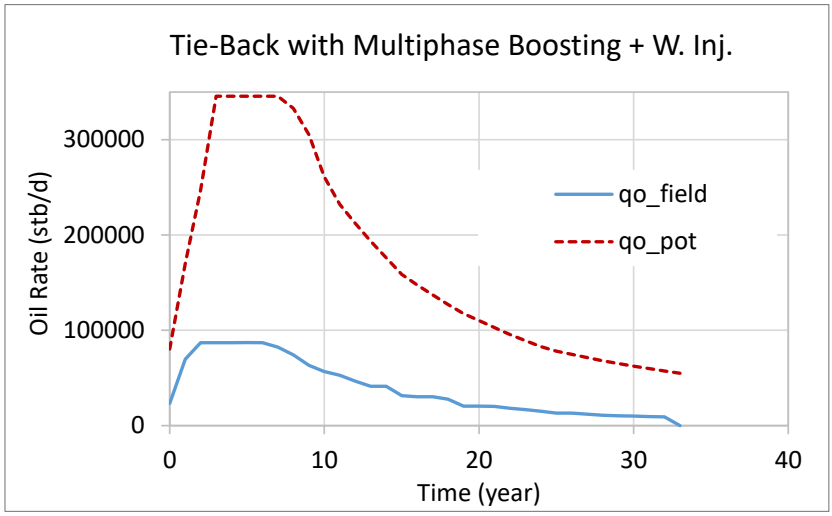

Figure H.9. Optimum oil production profile and oil production potential for strategy Tie-back with MPB + WI

Appendix I

AMPL's input files

Field-Opt.run

```
reset;
option presolve 0;
############################
### Solve Configuration  ###
############################

option solver "..\AMPLcml\cplex.exe";
option cplex_options 'mipdisplay 2 nodefile 3 sos 1 mipgap=5e-3 timelimit=6000 threads=16
parallelmode=0 scale=-1';
#mipgap=5e-18 mipemphasis 2
option presolve 0;
option show_stats 1;

option log_file 'LogFile.log';

# Include Variables, Parameters and Sets
include declaration.mod;

# include field data
include data.dat;

# Read tables
include read_table.run;

include preprocessing.run

model;
include optimization.mod;

# SOS2 constraints
include sos2.run;

# solve
solve;
display solve_message;

#display GOR_prod;
#display WC_prod;
#display qwater;
#display qgas;

# print results
include output.run;

#display{qo in qo_BP_g, R in GOR_BP_g} var_Omega_g[1,qo,R];

#display{t in TIMESTEPS, qo in qo_BP_g} var_alpha_g[t,qo];
#display{t in TIMESTEPS, GOR in GOR_BP_g} var_beta_g[t,GOR];
```

Declaration.mod

```
# Here are declared all variables, set and parameters;

# SETS
set TIMESTEPS;


## interpolation
set BP dimen 2;
set Np_BP := setof{(Np,Nw) in BP}(Np) ordered by [0, Infinity]; # set of breakpoints for the
cumulative oil production
set Nw_BP := setof{(Np,Nw) in BP}(Nw) ordered by [0, Infinity]; # set of breakpoints for the
number of wells

set Np_BP2 ordered by [0, Infinity]; # set of breakpoints for the the cumulative oil production
(water injection table)

# VARIABLES
## Decision variables
var var_qo_field{t in TIMESTEPS} >= 0;
var var_Nw_drilled{t in TIMESTEPS} integer >= 0, <= 4; # wells drilles in year t

## Hidden variables (mathematical variables)
var var_Np{t in TIMESTEPS} >= 0; # cumulative
var var_Np2{t in TIMESTEPS} >= 0; #cumulative, only to estimate qw_inject (same value as var_Np)
var var_Np_calc{t in TIMESTEPS} >= 0 ; #OIl produced during timestep t

var var_Nw{t in TIMESTEPS} integer >= 0; # number of wells producing
var var_qo_pot{t in TIMESTEPS} >= 0;
var var_qo_g{t in TIMESTEPS} >= 0;
var var_qo_w{t in TIMESTEPS} >= 0;
var var_qg{t in TIMESTEPS} >= 0;
var var_qw{t in TIMESTEPS} >= 0;
var var_qinj{t in TIMESTEPS} >= 0;

## SOS2 variables
var var_Gp{t in TIMESTEPS} >= 0;
var var_Wp{t in TIMESTEPS} >= 0;
var var_Omega{t in TIMESTEPS, Q in Np_BP, N in Nw_BP} >= 0;
var var_alpha{t in TIMESTEPS, Q in Np_BP} >= 0;
var var_beta{t in TIMESTEPS, N in Nw_BP} >= 0;

var var_cum_qwinj{t in TIMESTEPS} >= 0;
var var_Lamda{t in TIMESTEPS, Q in Np_BP2} >= 0;


### Economics
var var_CAPEX >= 0;
var var_OPEX >= 0;
var var_DRILLEX{t in TIMESTEPS} >= 0;
var var_NPV{t in TIMESTEPS};

var var_qo_max >= 0; # Maximum oil rate over the field life time
var var_qg_max >= 0; # Maximum gas rate over the field life time
var var_qw_max >= 0; # Maximum water rate over the field life time
var var_Nw_max integer >= 0; # Total number of wells
var var_NPV_project;

# Parameters
param TimeStepSize;
param LifeTime;


param qo_pot{Q in Np_BP, N in Nw_BP} >= 0;
param Gp_prod{Q in Np_BP, N in Nw_BP} >= 0;
param Wp_prod{Q in Np_BP, N in Nw_BP} >= 0;
param cum_qwinj{Q in Np_BP2} >= 0;

# economics
param a_capex;
param b_capex;
param c_capex;
param d_capex;
param e_capex;

param a_opex;
param b_opex;
param c_opex;
param d_opex;
param e_opex;

param a_drillex;
param b_drillex;

param fact_capex;
```

```
param fact_opex;
param fact_drillex;

param fact_qo_pot;

param OilPrice{t in TIMESTEPS};
param GasPrice{t in TIMESTEPS};
param interest_rate;

param Tax;
param MaxNw_year;
param MaxWinjWell;
```

Data.dat

```
data;

param TimeStepSize := 1;
param LifeTime := 33;


# economics

#############################################################################################
##Cost coefficients for scenario with TLP (capex, opex)
param a_capex := 0.007906;            #oil rate must be in STB/d
param b_capex := 29.814434;           #gas rate must be in 1e6 scf/d
param c_capex := 0.011468;            #water rate must be in STB/d
param d_capex := 307.534482;
param e_capex := 11702.41103;

param a_opex := 6.672171e-4;          #oil rate must be in STB/d
param b_opex := 0.892995;             #gas rate must be in scf/d
param c_opex := 2.177062e-4;          #water rate must be in STB/d
param d_opex := 14.012648;
param e_opex := 613.93221;

#############################################################################################
##Cost coefficients for scenario with FPSO (capex, opex)
#param a_capex := 0.012221;           #oil rate must be in STB/d
#param b_capex := 42.635030;          #gas rate must be in scf/d
#param c_capex := 0.017291;           #water rate must be in STB/d
#param d_capex := 307.873288;
#param e_capex := 15407.21085;

#param a_opex := 9.240968e-4;         #oil rate must be in STB/d
#param b_opex := 1.404980;            #gas rate must be in MMscf/d
#param c_opex := 3.627371e-4;         #water rate must be in STB/d
#param d_opex := 14.013987;
#param e_opex := 673.78145;

#############################################################################################
##Cost coefficients for scenario with Tie-Back (capex, opex)
#param a_capex := 0.036633;           #oil rate must be in STB/d
#param b_capex := 12.743544;          #gas rate must be in MMscf/d
#param c_capex := 0.047717;           #water rate must be in STB/d
#param d_capex := 369.288979;
#param e_capex := 21911.57716;

#param a_opex := 5.496545e-4;         #oil rate must be in STB/d
#param b_opex := 0.124479;            #gas rate must be in MMscf/d 1.0860e-7
#param c_opex := 1.824743e-4;         #water rate must be in STB/d
#param d_opex := 14.256659;
#param e_opex := 349.61604;
#############################################################################

##Cost coefficients for drillex
param a_drillex := 253.467588;
param b_drillex := 1.546141e-11 ;


param fact_capex := 1;
param fact_opex := 1;
param fact_drillex := 1;

param interest_rate := 0.08;
```

Optimization.mod

```
model;

maximize objective :
	var_NPV_project;


subject to NPV_project_Definition:
	var_NPV_project = sum{t in TIMESTEPS} var_NPV[t] ;

subject to dummy:
	var_NPV_project <= 1e15;

subject to NPV_definition_year_0:
	var_NPV[0] = - (var_CAPEX/4 + var_DRILLEX[0]);
subject to NPV_definition_year_1:
	var_NPV[1]  =  (((var_Np_calc[1]*OilPrice[1]*1e6   / 1e6)  -  var_CAPEX/4  -  var_OPEX  -
var_DRILLEX[1])/(1 + interest_rate)^1);
subject to NPV_definition_year_2:
	var_NPV[2]  =  (((var_Np_calc[2]*OilPrice[2]*1e6   / 1e6)  -  var_CAPEX/4  -  var_OPEX  -
var_DRILLEX[2])/(1 + interest_rate)^2);
subject to NPV_definition_year_3:
	var_NPV[3]  =  (((var_Np_calc[3]*OilPrice[3]*1e6   / 1e6)  -  var_CAPEX/4  -  var_OPEX  -
var_DRILLEX[3])/(1 + interest_rate)^3);

subject to NPV_definition_year {t in TIMESTEPS: t >= 4}:
	var_NPV[t]   =   (((var_Np_calc[t]*OilPrice[t])   -   var_OPEX   -   var_DRILLEX[t])/(1   +
interest_rate)^t);
## Np [1e6 STB], OilPrice [NOK/STB], Gp [1e6 scf], GasPrice [NOK/1e6 scf]


# Cost calculation
## Oil rate must be enter in STB/d.
## Gas rate must be enter in 1e6 scf/d.
## Water rate must be enter in STB/d.
subject to CAPEX:
	var_CAPEX = fact_capex * (a_capex * var_qo_max*1000 + b_capex * var_qg_max + c_capex *
var_qw_max*1000 + d_capex * var_Nw_max * 2 + e_capex);
# Unit: 1e6 NOK

subject to OPEX:
	var_OPEX = fact_opex * (a_opex * var_qo_max*1000 + b_opex * var_qg_max + c_opex *
var_qw_max*1000 + d_opex * var_Nw_max * 2 + e_opex);
# Unit: 1e6 NOK

subject to DRILLEX{t in TIMESTEPS}:
	var_DRILLEX[t] = fact_drillex * (a_drillex * var_Nw_drilled[t] * 2 + b_drillex);
# Unit: 1e6 NOK



## Oil rate constraints
subject to Maximum_Oil_Rate{t in TIMESTEPS}:
	var_qo_field[t] <= var_qo_pot[t];

subject to Maximum_Oil_Rate_Corrosion{t in TIMESTEPS}:
	var_qo_field[t] <= var_Nw[t] * 13000/1000;



## Cumulative oil production
subject to Cumulative_Np_def{t in TIMESTEPS}:
	var_Np[t] = sum{i in TIMESTEPS: i <= t} var_Np_calc[i];
# Units: 1e6 STB

subject to Cumulative_Np2_def{t in TIMESTEPS}:
	var_Np2[t] = sum{i in TIMESTEPS: i<=t} var_Np_calc[i];

subject to Np_calc_def{t in TIMESTEPS : t != 0}:
	var_Np_calc[t] = (TimeStepSize * 365 * (var_qo_field[t] + var_qo_field[t-1])/2) /1000;
# Units: 1e6 STB



## Number of wells
subject to Wells_producing_def{t in TIMESTEPS}:
	var_Nw[t] = sum{i in TIMESTEPS: i <= t} var_Nw_drilled[i];


## Water injection rate
subject to Field_Water_Injection_Rate_definition_year_0:
	var_qinj[0] = var_cum_qwinj[1]*1e6 / (TimeStepSize * 365);

subject to Field_Water_Injection_Rate_definition{t in TIMESTEPS: t != 0}:
	var_qinj[t] = (var_cum_qwinj[t] - var_cum_qwinj[t-1])*1e6 / (TimeStepSize * 365);
```

```
subject to Maximum_Water_Inj{t in TIMESTEPS}:
	var_qinj[t] <= var_Nw[t] * 6290;


## To use in SOS2 calculations
#subject to Produced_Water_Constraint{t in TIMESTEPS}:
	var_qw[t] <= 250000;

subject to Oil_Rate_Interpol_g{t in TIMESTEPS}:
	var_qo_g[t] = var_qo_field[t]*1000;

subject to Oil_Rate_Interpol_w{t in TIMESTEPS}:
	var_qo_w[t] = var_qo_field[t]*1000;

subject to GOR_Interpol_w{t in TIMESTEPS}:
	var_GOR2[t] = var_GOR[t];

subject to WC_Interpol_w{t in TIMESTEPS}:
	var_WC2[t] = var_WC[t];



## Maximum over the period of time
subject to MaximumOilRateDefinition{t in TIMESTEPS}:
	var_qo_max >= var_qo_field[t];

subject to MaximumGasRateDefinition{t in TIMESTEPS}:
	var_qg_max >= var_qg[t];

subject to MaximumWaterRateDefinition{t in TIMESTEPS}:
	var_qw_max >= var_qw[t];

subject to TotalWellsDefinition{t in TIMESTEPS}:
	var_Nw_max >= var_Nw[t];



## SOS2 modeling
###Potential oil rate, GOR and WC
subject to Potential_Oil_Rate_definition{t in TIMESTEPS}:
	var_qo_pot[t] = sum{Np in Np_BP, Nw in Nw_BP} var_Omega[t,Np,Nw] * (qo_pot[Np,Nw]/1000);
	# Units: 1e3 STB/d

subject to Potential_Gas_Rate_definition{t in TIMESTEPS}:
	var_GOR[t] = sum{Np in Np_BP, Nw in Nw_BP} var_Omega[t,Np,Nw] * GOR_prod[Np,Nw];
# Units: 1e6 scf/d

subject to Potential_Water_Rate_definition{t in TIMESTEPS}:
	var_WC[t] = sum{Np in Np_BP, Nw in Nw_BP} var_Omega[t,Np,Nw] * WC_prod[Np,Nw]*100;
# Units: 1e3 STB/d

subject to Cumulative_Prod_Constraint{t in TIMESTEPS}:
	var_Np[t] = sum{Np in Np_BP, Nw in Nw_BP} var_Omega[t,Np,Nw] * Np/1000000;
# Units: 1e6 STB

subject to Total_Number_Wells_Constraint{t in TIMESTEPS}:
	var_Nw[t] = sum{Np in Np_BP, Nw in Nw_BP} var_Omega[t,Np,Nw] * Nw;

subject to Convexity_Omega{t in TIMESTEPS}:
	sum{Np in Np_BP, Nw in Nw_BP} var_Omega[t,Np,Nw] = 1;

subject to Alpha_Definition {t in TIMESTEPS, Np in Np_BP}:
	var_alpha[t,Np] = sum{Nw in Nw_BP} var_Omega[t,Np,Nw];

subject to Beta_Definition{t in TIMESTEPS, Nw in Nw_BP}:
	var_beta[t,Nw] = sum{Np in Np_BP} var_Omega[t,Np,Nw];


###Gas Rate
subject to Gas_Rate_definition{t in TIMESTEPS}:
	var_qg[t] = sum{qo in qo_BP_g, R in GOR_BP_g} var_Omega_g[t,qo,R] * qgas[qo,R];

subject to Oil_Rate_Constraint_g{t in TIMESTEPS}:
	var_qo_g[t] = sum{qo in qo_BP_g, R in GOR_BP_g} var_Omega_g[t,qo,R] * qo;

subject to GOR_Constraint_g{t in TIMESTEPS}:
	var_GOR2[t] = sum{qo in qo_BP_g, R in GOR_BP_g} var_Omega_g[t,qo,R] * R;

subject to Convexity_Omega_g{t in TIMESTEPS}:
	sum{qo in qo_BP_g, R in GOR_BP_g} var_Omega_g[t,qo,R] = 1;

subject to Alpha_g_Definition{t in TIMESTEPS, qo in qo_BP_g}:
	var_alpha_g[t,qo] = sum{R in GOR_BP_g} var_Omega_g[t,qo,R];

subject to Beta_g_Definition{t in TIMESTEPS, R in GOR_BP_g}:
```

```
        var_beta_g[t,R] = sum{qo in qo_BP_g} var_Omega_g[t,qo,R];


##Water Rate
subject to Water_Rate_definition{t in TIMESTEPS}:
        var_qw[t]   =   sum{qoo   in   qo_BP_w,   WC   in   WC_BP_w}   var_Omega_w[t,qoo,WC]   *
qwater[qoo,WC]/1000;

subject to Oil_Rate_Constraint_w{t in TIMESTEPS}:
        var_qo_w[t] = sum{qoo in qo_BP_w, WC in WC_BP_w} var_Omega_w[t,qoo,WC] * qoo;

subject to GOR_Constraint_w{t in TIMESTEPS}:
        var_WC2[t] = sum{qoo in qo_BP_w, WC in WC_BP_w} var_Omega_w[t,qoo,WC] * WC;

subject to Convexity_Omega_w{t in TIMESTEPS}:
        sum{qoo in qo_BP_w, WC in WC_BP_w} var_Omega_w[t,qoo,WC] = 1;

subject to Alpha_w_Definition{t in TIMESTEPS, qoo in qo_BP_w}:
        var_alpha_w[t,qoo] = sum{WC in WC_BP_w} var_Omega_w[t,qoo,WC];

subject to Beta_w_Definition{t in TIMESTEPS, WC in WC_BP_w}:
        var_beta_w[t,WC] = sum{qoo in qo_BP_w} var_Omega_w[t,qoo,WC];




## SOS2 modeling in one dimension to get water injection rate
subject to Cumulative_Water_Injection_Rate_definition{t in TIMESTEPS}:
        var_cum_qwinj[t] = sum{Np2 in Np_BP2} var_Lamda[t,Np2] * cum_qwinj[Np2]/1000000;
# Units: Check

subject to Cumulative_Prod_Constraint_2{t in TIMESTEPS}:
        var_Np2[t] = sum{Np2 in Np_BP2} var_Lamda[t,Np2] * Np2/1000000;

subject to Convexity_Lamda{t in TIMESTEPS}:
        sum{Np2 in Np_BP2} var_Lamda[t,Np2] = 1;
```

read-table.run

```
# Read function B table

###Potencial rate table
table PotentialRate IN "Tables/pot.tab" : BP <- [Np, Nw], GOR_prod[Np,Nw] ~ GOR_produced,
WC_prod[Np,Nw] ~ WC_produced, qo_pot[Np,Nw] ~ qo_potential;
read table PotentialRate;

###Gas Rate Produced
table GasRate IN "Tables/GasRateProd.tab" : BP_g <- [qo, GOR], qgas[qo,GOR] ~ qg_field;
read table GasRate;

###Water Rate Produced
table WaterRate IN "Tables/WaterRateProd.tab" : BP_w <- [qo, WC], qwater[qo,WC] ~ qw_field;
read table WaterRate;

###Cumulative water injection rate table
table CumWaterInj IN "Tables/WaterInj.tab" : Np_BP2 <- [Np], cum_qwinj[Np] ~ cumulative_qw_inj;
read table CumWaterInj;

table OilGas_Price IN "Tables/OilGas_Price.tab" : [TIMESTEPS], OilPrice ~ Oil_price, GasPrice
~ Gas_price ;
read table OilGas_Price;
```

Preprocessing.run

```
let TIMESTEPS := {};
param param_t;
let param_t := 0;

repeat while param_t <= LifeTime {
        let TIMESTEPS := TIMESTEPS union {param_t};
        let param_t := param_t + TimeStepSize;
}


let var_Np_calc[0] := 0;
fix var_Np_calc[0];

#let var_Gp_calc[0] := 0;
#fix var_Gp_calc[0];
```

SOS2.run

```
param iter;
let iter := -1;

suffix sosno;
suffix ref;

for{t in TIMESTEPS} {
	if(card(Np_BP) > 2) then {
		let iter := iter-1;
		let {Np in Np_BP} var_alpha[t,Np].sosno := iter;
		let {Np in Np_BP} var_alpha[t,Np].ref   := ord(Np);
	}
	if(card(Nw_BP) > 2) then {
		let iter := iter-1;
		let {Nw in Nw_BP} var_beta[t,Nw].sosno := iter;
		let {Nw in Nw_BP} var_beta[t,Nw].ref   := ord(Nw);
	}
}

for{t in TIMESTEPS} {
	if(card(qo_BP_g) > 2) then {
		let iter := iter-1;
		let {qo in qo_BP_g} var_alpha_g[t,qo].sosno := iter;
		let {qo in qo_BP_g} var_alpha_g[t,qo].ref   := ord(qo);
	}
	if(card(GOR_BP_g) > 2) then {
		let iter := iter-1;
		let {GOR in GOR_BP_g} var_beta_g[t,GOR].sosno := iter;
		let {GOR in GOR_BP_g} var_beta_g[t,GOR].ref   := ord(GOR);
	}
}

for{t in TIMESTEPS} {
	if(card(qo_BP_w) > 2) then {
		let iter := iter-1;
		let {qo in qo_BP_w} var_alpha_w[t,qo].sosno := iter;
		let {qo in qo_BP_w} var_alpha_w[t,qo].ref   := ord(qo);
	}
	if(card(WC_BP_w) > 2) then {
		let iter := iter-1;
		let {WC in WC_BP_w} var_beta_w[t,WC].sosno := iter;
		let {WC in WC_BP_w} var_beta_w[t,WC].ref   := ord(WC);
	}
}

for{t in TIMESTEPS} {
	if(card(Np_BP2) > 2) then {
		let iter := iter-1;
		let {Np in Np_BP2} var_Lamda[t,Np].sosno := iter;
		let {Np in Np_BP2} var_Lamda[t,Np].ref   := ord(Np);
	}

}
```

Output.run

```
#############
## CONSOLE ##
#############
printf "\n" > output.out;
printf "***********\n"> output.out;
printf "* RESULTS *\n" > output.out;
printf "***********\n"> output.out;
printf "NPV_project : %g 10e6NOK\n", var_NPV_project*1000> output.out;
printf "\n" > output.out;
printf "Max_Oil Rate : %g STB/d\n", var_qo_max*1000> output.out;
printf "Max_Gas Rate : %g MMscf/d\n", var_qg_max> output.out;
printf "Max_Water Rate : %g STB/d\n", var_qw_max*1000> output.out;
printf "Max_Number_of_wells : %g wells\n", var_Nw_max> output.out;
printf "CAPEX : %g 10e6NOK\n", var_CAPEX> output.out;
printf "OPEX : %g 10e6NOK\n", var_OPEX> output.out;
#printf "Mipgap :      %g\n", var_NPV_project.relmipgap> output.out;
printf "\n" > output.out;
printf
"Time_Step\tNPV\tQo_field\tQo_BP\tQo_potential\tQg\tQw_prod\tCum_Qw_inj\tNp_annual\tCumulative
_Np\tNw_drilled\tTotal_Nw\tDRILLEX\tOilPrice\tGOR\tWC\tQw_inj\n" > output.out;
for{t in TIMESTEPS}{
        printf "%g\t", t> output.out;
        printf "%g\t", var_NPV[t]> output.out;
        printf "%g\t", var_qo_field[t]*1000> output.out;
        printf "%g\t", var_qo_w[t]>output.out;
        printf "%g\t", var_qo_pot[t]*1000> output.out;
        printf "%g\t", var_qg[t]> output.out;
        printf "%g\t", var_qw[t]*1000> output.out;
        printf "%g\t", var_cum_qwinj[t]*1e6> output.out;
        printf "%g\t", var_Np_calc[t]*1e6> output.out;
        printf "%g\t", var_Np[t]*1e6> output.out;
        printf "%g\t", var_Nw_drilled[t]> output.out;
        printf "%g\t", var_Nw[t]> output.out;
        printf "%g\t", var_DRILLEX[t]> output.out;
        printf "%g\t", OilPrice[t]> output.out;
        printf "%g\t", var_GOR[t]> output.out;
        printf "%g\t", var_WC[t]> output.out;
        printf "%g\n", var_qinj[t]> output.out;

}
```

ISBN 978-82-326-4486-5 (printed version)
ISBN 978-82-326-4487-2 (electronic version)
ISSN 1503-8181

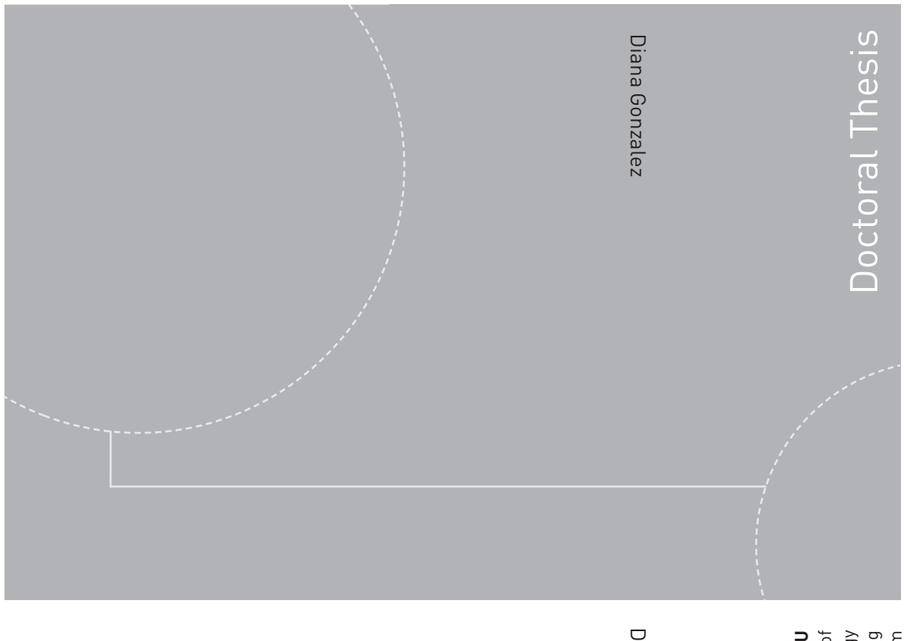

Doctoral theses at NTNU, 2020:67

Diana Gonzalez

Methodologies to determine cost-effective development strategies for offshore fields during early-phase studies using proxy models and optimization

NTNU
Norwegian University of
Science and Technology
Faculty of Engineering
Department of Geoscienceand Petroleum

NTNU
Norwegian University of
Science and Technology

Doctoral theses at NTNU, 2020:67

NTNU

NTNU
Norwegian University of
Science and Technology